

# UC Riverside

## UC Riverside Electronic Theses and Dissertations

### Title

Biophysical and Molecular Determinants of Acrosome Formation and Motility Regulation of Sperm From the Water Strider

### Permalink

<https://escholarship.org/uc/item/9sb5n2tz>

### Author

Miyata, Haruhiko

### Publication Date

2010

Peer reviewed|Thesis/dissertation

UNIVERSITY OF CALIFORNIA  
RIVERSIDE

Biophysical and Molecular Determinants of Acrosome Formation and Motility  
Regulation of Sperm From the Water Strider

A Dissertation submitted in partial satisfaction  
of the requirements for the degree of

Doctor of Philosophy

in

Evolution, Ecology and Organismal Biology

by

Haruhiko Miyata

March 2011

Dissertation Committee:

Dr. Richard A. Cardullo, Chairperson

Dr. Daphne J. Fairbairn

Dr. Morris F. Maduro

Copyright by  
Haruhiko Miyata  
2011

The Dissertation of Haruhiko Miyata is approved:

---

---

---

Committee Chairperson

University of California, Riverside

## ACKNOWLEDGEMENTS

This dissertation is the result of the cumulative efforts and contributions of many individuals. First, I would like to thank Dr. Richard Cardullo for providing the mentorship, support and resources necessary for this project. I appreciate Rich's guidance that gave me the latitude to choose a project of my liking. I also thank the former and current members of the Cardullo lab and the Fairbairn lab, especially, Dr. Juan Fraire-Zamora, Alex Cortez and Yuri Cheung for their camaraderie, assistance and thoughtful input. The members of the Fairbairn lab kindly provided water striders. Additionally, I'd like to thank Dr. Catherine Thaler. Cathy's assistance was invaluable and she proved to be an invaluable colleague and resource especially for the studies described in Chapter 3 of this dissertation. I would also like to thank the members of my dissertation committee, Drs. Daphne Fairbairn and Morris Maduro who, along with Rich, not only provided valuable input and advice but also provided their time. Gina Broitman-Maduro and Morris kindly provided expertise and equipment that assisted me in this dissertation. Additionally, I'd like to thank Dr. Leah Haimo for providing support and precious resources. The text of this dissertation, chapter 2 in full, is a reprint of the material as it appears in *Journal of Cellular Physiology*, 2010 September 20, Epub ahead of print. Rich and Daphne listed in that publication supervised the research which forms the basis for this dissertation. Drs. Naoki Noda and Rudolf Oldenbourg listed in that publication performed experiments on fluorescence polarization microscopy and provided comments on the manuscript.

## DEDICATION

This dissertation is dedicated to the first true love of my life, my wife, Joeun. Joeun provided copious amounts of encouragement, support and love throughout my life in the United States. There would be no dissertation without her. Joeun is, beyond doubt, my finest discovery in my life. In addition to Joeun, I would like to thank my father and mother in law. They encouraged and supported me to pursue my studies during graduate school. Lastly, and very importantly, I'd like to thank the support from my mom and the inspiration from my dad. I am forever indebted to them for their endless love.

ABSTRACT OF THE DISSERTATION

Biophysical and Molecular Determinants of Acrosome Formation and Motility  
Regulation of Sperm from the Water Strider

by

Haruhiko Miyata

Doctor of Philosophy, Graduate Program in Evolution, Ecology and Organismal Biology

University of California, Riverside, March 2011

Dr. Richard A. Cardullo, Chairperson

Sperm from a semi-aquatic insect, the water strider *Aquarius remigis*, are unusually long and possess a complex acrosome and flagellum. Like other animal systems, water strider sperm that emerge from the testis are incapable of fertilizing an egg and must undergo several highly regulated developmental steps in both the male and female reproductive tracts. However, in contrast to well-studied model animals such as mammals and echinoderms, little is known about these events in insects. In this dissertation, I describe the post-meiotic events in *Aquarius remigis* using biochemical and biophysical methodologies to follow the assembly, structure, and fate of the acrosome and the flagellum from spermatogenesis through fertilization and into early embryonic development. In contrast to other long insect sperm, half of the length of the *A. remigis*

sperm consists of an acrosomal matrix that emerges as a 300  $\mu\text{m}$  helical structure followed by a 2200  $\mu\text{m}$  linear region. This unusually long acrosome contains an intrinsically fluorescent molecule with properties consistent with those of Flavin Adenine Dinucleotide (FAD). Biophysical analyses showed that FAD is immobilized and oriented during acrosome formation and may be involved in the formation of disulfide bond formation during its assembly. Further, using the intrinsic fluorescence as a marker, I followed the fate of the acrosomal matrix through fertilization and observed it inside the fertilized egg where it remained structurally intact through gastrulation. The acrosomal matrix may play roles in sperm transport and fertilization. Similar to the proximal acrosomal process, the axoneme and its associated structures, appears helical. I describe a unique motility pattern in which the flagellum loops back upon itself and forms a coil. This structure can then twist and undergo forward progressive motility with the loop acting as the anterior end. *A. remigis* sperm are quiescent in the seminal vesicles, but sperm motility was initiated by specific proteases or phosphatase inhibitors. Further, a broad spectrum kinase inhibitor blocked sperm motility initiation by trypsin. These results suggest that quiescence is maintained by high levels of endogenous phosphatase activity and that activation of motility is regulated by protein phosphorylation through the action of one or more kinases.



## Table of Contents

	PAGE
<b>Chapter 1</b> LITERATURE REVIEW - COMPARATIVE STUDIES ON SPERM MORPHOGENESIS AND SPERM MATURATION IN MAMMALS, ECHINODERMS, AND INSECTS	1
References	19
Figure Legends	26
Figures and Tables	28
<b>Chapter 2</b> ASSEMBLY OF THE FLUORESCENT ACROSOMAL MATRIX AND ITS FATE IN FERTILIZATION IN THE WATER STRIDER, <i>AQUARIUS REMIGIS</i>	33
Abstract	34
Introduction	35
Materials and Methods	37
Results	41
Discussion	48
References	53
Figure Legends	57
Figures and Tables	61

<b>Chapter 3</b>	<b>THE UNIQUE STRUCTURE OF THE SPERM FLAGELLUM FROM THE WATER STRIDER, <i>AQUARIUS REMIGIS</i>, RESULTS IN COMPLEX MOTILITY BEHAVIOR THAT IS INITIATED BY A PROTEASE AND REGULATED BY PHOSPHORYATION</b>	<b>68</b>
	Abstract	69
	Introduction	70
	Materials and Methods	72
	Results	78
	Discussion	86
	References	91
	Figure Legends	96
	Figures and Tables	100
<b>Chapter 4</b>	<b>DICSUSSION - THE CONSEQUENCES OF MAKING A LONG SPERM: POTENTIAL ROLES FOR THE ACROSOMAL MATRIX, THE INITIATION OF SPERM MOTILITY, AND COMPARISONS WITH OTHER ANIMALS</b>	<b>112</b>
	References	130
	Figure Legends	135
	Figures and Tables	137

## List of Figures

	PAGE
<b>Chapter 1</b>	
Figure 1.1 Schematic illustration of the acrosome formation during guinea pig spermiogenesis	28
Figure 1.2 Schematic illustration of the acrosome reaction in sea urchin sperm	29
Figure 1.3 Beating patterns of mouse sperm	30
Figure 1.4 Schematic diagram of the gynatrial complex of female <i>A. remigis</i>	31
Figure 1.5 Transverse sections of <i>A. remigis</i> sperm	32
<b>Chapter 2</b>	
Figure 2.1 Morphology of mature <i>A. remigis</i> sperm	61
Figure 2.2 The periodic structure of the water strider sperm head is a helix	62
Figure 2.3 The fluorescent signal in the sperm head appears during spermatogenesis and is localized to the acrosome in spermatids	63
Figure 2.4 The fluorescent molecule becomes immobilized during spermiogenesis	64
Figure 2.5 The intrinsic fluorescence of mature sperm exhibits strong anisotropy	65
Figure 2.6 Properties of the fluorescent molecule in the matrix are similar to those of FAD	66
Figure 2.7 The fate of the fluorescent molecule associated with the acrosomal matrix during the fertilization process and early development	67

### Chapter 3

Figure 3.1	Morphology of the water strider sperm flagellum	100
Figure 3.2	Lag time in response to proteases	101
Figure 3.3	Water strider sperm waveforms	102
Figure 3.4	Sperm in the female reproductive tract exhibit the twisted axoneme morphology	103
Figure 3.5	Motility level in response to activators	104
Figure 3.6	Motility level in response to inhibitors	105
Figure 3.7	MPM-2 is localized in the axoneme and displays less phosphorylation in the presence of U0126	106
Figure 3.8	A PAR2-like protein is present in the tail	107
Figure 3.9	Consecutive images showing a possible model for the formation of the flagellar zippering motion in <i>A. remigis</i> sperm using a string	108
Figure 3.10	A micropyle of the <i>A. remigis</i> egg	109
Figure 3.11	A current model for the signaling pathways involved in motility activation of <i>A. remigis</i> sperm	110

### Chapter 4

Figure 4.1	Microtubules surround the acrosome during spermatogenesis but do not persist in the mature acrosome	137
Figure 4.2	The motility activation of the <i>C. quinquefasciatus</i> sperm is inhibited by both a protease inhibitor and the ERK kinase inhibitor U0126	138

## **List of Tables**

	<b>PAGE</b>
<b>Chapter 3</b>	
Table 3.1 Motility scale	111
<b>Chapter 4</b>	
Table 4.1 Summary of post-meiotic events in animal sperm	139

CHAPTER 1

LITERATURE REVIEW

COMPARATIVE STUDIES ON SPERM MORPHOGENESIS AND SPERM  
MATURATION IN MAMMALS, ECHINODERMS, AND INSECTS

## **Introduction**

Fertilization is a union of two gametes in organisms that reproduce sexually. In order to maintain ploidy through fertilization, germ cells must undergo meiosis. In a male, a round spermatid (haploid) is produced from a spermatocyte (diploid) through meiosis. However, the spermatid is still incapable of fertilizing an egg and must undergo several highly regulated developmental steps in both the male and female reproductive tracts culminating in the production of a mature sperm. Following meiosis, the spermatid differentiates into a highly specialized cell that in most described species possesses a flagellated motility apparatus and a sperm-specific organelle known as the acrosome that is located anterior to the haploid nucleus. During this process of spermiogenesis, the tail is elongated from a basal body that contains a cylindrical array of microtubules and associated proteins (the axoneme) and the acrosome is formed from a Golgi apparatus. Following spermiogenesis, both of these complex structures go through additional maturational steps. The tail does not beat when it is formed and its motility must be activated by various extracellular cues. Further, in most animals, the acrosome must undergo a regulated exocytotic event known as the acrosome reaction prior to fusion with the egg. Disruption in any of these events results in infertility.

Molecular mechanisms underlying the formation of the acrosome and the initiation and maintenance of sperm motility have been studied extensively in model animals such as mice and sea urchins (Yanagimachi, 1994; Ramalho-Santos *et al.*, 2002; Yoshinaga and Toshimori, 2003; Neill and Vacquier, 2004). These studies will be

reviewed in this chapter focusing on acrosome formation, the acrosome reaction, and motility regulation. In contrast, little is known about sperm maturational steps in insects. What is known to date concerning these events in insects will be reviewed comparing the similarities and differences between model animals and insects. Further, I will review fertilization in the water strider, *Aquarius remigis*, which is the basis for the studies encompassed in this dissertation. Key questions addressed in this dissertation will be mentioned at the end of the chapter.

## **Acrosome formation**

### ***General view (mammals)***

The acrosome is an organelle that is derived from the Golgi apparatus and is formed during spermiogenesis (Yoshinaga and Toshimori, 2003). The inability of the acrosome to form correctly leads to severe disorders in fertility (Holstein *et al.*, 1973). The cellular process of spermiogenesis can be divided into four phases in mammals (Figure 1.1). In the first phase known as the Golgi-phase, Golgi-derived proacrosomal granules fuse into a single acrosomal granule that is located proximal to the nucleus. In the subsequent cap-phase, a large acrosomal vesicle is formed by the fusion of many smaller vesicles into an acrosomal granule. These small vesicles are presumed to be derived from the Golgi apparatus. The acrosomal vesicle starts to elongate during the third phase known as the acrosomal-phase and reaches into its final form at the end of the last phase known as the maturation-phase (For a review see, Ramalho-Santos *et al.*, 2002). This dramatic change of the acrosomal morphology at both the acrosome-phase and the



maturation-phase is assisted by an ephemeral structure, the manchette, that consists of a parallel array of microtubules and intermediate filaments (Kierszenbaum and Tres, 2004).

In the cap-phase, the continuous supply of acrosomal proteins from the Golgi apparatus to the proacrosomal granule is achieved through Golgi-derived small vesicles (Ramalho-Santos *et al.*, 2002). The fusion of these small granules may be mediated by SNAREs (soluble NSF attachment protein receptors) that are involved in exocytotic vesicle fusion events in somatic cells since a number of well-characterized SNARE components, such as syntaxin and VAMP, are localized in acrosomal vesicles during mouse spermiogenesis (Ramalho-Santos *et al.*, 2001). Accordingly, when Golgi-associated PDZ- and coiled-coil motif-containing protein (GOPC) that interacts with syntaxin-6 has been disrupted, the acrosome is unable to form correctly (Yao *et al.*, 2002). These results suggest that molecular mechanisms underlying vesicle fusion in acrosome formation are similar to those of exocytotic vesicle fusion in somatic cells. Additional clues about the molecular mechanism of acrosome formation come from a specific knock-out experiment that is infertile because of the lack of an acrosome. In this study, sperm from mice in which the Asn-Pro-Phe (NPF) motif-containing protein Hrb has been disrupted do not possess an acrosome due to a defect in proacrosomal granule fusion (Kang-Decker *et al.*, 2001). Although this study suggests that Hrb is involved in the fusion of proacrosomal granules, the detailed mechanism is still unknown.

In addition to the transport of acrosomal molecules from the Golgi apparatus to the developing acrosome, a rearrangement of acrosomal molecules within the acrosomal

vesicle occurs during acrosome formation (Yoshinaga and Toshimori, 2003). For example, the acrosomal matrix protein, AM50, is first concentrated in the electron-lucent matrix of the acrosomal vesicle in the Golgi-phase and is then uniformly localized in the apical segment of the developing acrosome in the acrosome phase. AM50 is finally redistributed to the ventral matrix of the apical segment of the acrosome in guinea pig sperm (Westbrook-Case *et al.*, 1995). To date, it is unclear how these rearrangements are regulated. Since AM50 assembles into a disulfide cross-linked complex (Westbrook-Case *et al.*, 1995) and protein disulfide isomerase, which catalyzes the rearrangement of disulfide bonds, is expressed in the developing acrosome of rats (Ohtani *et al.*, 1993), rearrangement of disulfide bonds between acrosomal molecules may play a critical role in the organization of acrosomal proteins.

### ***Acrosome Formation in Insects***

The acrosome formation during spermiogenesis has been studied in many insect species using transmission electron microscopy. There are no outstanding differences between insects and model animals (mammals) in regard to the acrosome formation in the early stages of spermiogenesis although there is a remarkable diversity in the shaping of the acrosome at the later stages (Jamieson *et al.*, 1999). For example, in the water strider *Aquarius remigis*, numerous vesicles of the Golgi complex are fused into a large acrosomal vesicle that adheres to the nuclear envelope in the early stage of spermiogenesis (Pollister, 1930; Moriber, 1956). This process is similar to the Golgi-phase and cap-phase of mammals in that the vesicles from a Golgi apparatus join together

to form a large single vesicle next to the nucleus. Molecular mechanisms of this process in insects are still unclear. In the later stage of spermiogenesis of *A. remigis*, the acrosomal vesicle begins to elongate into its final shape. The elongating acrosome was reported to be surrounded by microtubules (Tandler and Moriber, 1966), which may be an analogous structure to the mammalian manchette.

### **Acrosome reaction**

#### ***General view (model animals)***

The sea urchin has long been a model organism for the study of fertilization since copious numbers of gametes are readily available for biochemical studies and its external fertilization makes it easy to observe fertilization events. When sea urchin sperm come in close proximity to eggs, they undergo the acrosome reaction, which is characterized by two major physiological events: exocytosis of the acrosomal vesicle and the extension of the acrosomal process (Figure 1.2) (For reviews see, Darszon *et al.*, 1999; Neill and Vacquier, 2004). In acrosomal exocytosis, the membrane of the acrosome fuses with the sperm's plasma membrane and the acrosomal contents are released into the extracellular environment. The acrosomal vesicle contains a trypsin-like protease, which may play a role in the fertilization process (Levine *et al.*, 1978), and bindin (Vacquier and Moy, 1977), which mediates a species-specific binding event between sperm and egg (Glabe and Lennarz, 1979). The acrosomal process is a thread-like structure at the tip of the head and it is formed by polymerization of actin monomers (Tilney *et al.*, 1978). These actin monomers (also known as globular- or G-actin) are stored in a cytoplasmic pool behind

the acrosome. The exposed membrane of the acrosomal process, which is covered with bindin, fuses with the egg plasma membrane (Barre *et al.*, 2003).

The acrosome reaction is induced by a fucose sulfate polymer (FSP) that is a component of the egg jelly (SeGall and Lennarz, 1979), a complex extracellular matrix that surrounds the egg. Binding of FSP to its complementary receptor, suREJ1, triggers both Na<sup>+</sup> influx and K<sup>+</sup> efflux, resulting in a membrane depolarization (Darszon *et al.*, 1999). Interestingly, suREJ1 is a homolog of the human polycystic kidney disease protein polycystin-1 that comprises a unique non-selective cation channel (Moy *et al.*, 1996). The binding of FSP also results in an increase in intracellular concentrations of Ca<sup>2+</sup> (Guerrero and Darszon, 1989) and inositol 1,4,5-triphosphate (IP3) (Domino and Garbers, 1988). These changes result in the opening of a Ca<sup>2+</sup> channel that is thought to be a store-operated channel (SOC) that is activated by calcium depletion of internal stores (Gonzalez-Martinez *et al.*, 2001). A large transient increase in Ca<sup>2+</sup> concentration by SOCs is sufficient to initiate the acrosome reaction (Hirohashi and Vacquier, 2003).

Analogous events occur in the sperm of mammals except that the egg-derived protein glycoprotein ZP3, a matrix protein embedded within the zona pellucida, and progesterone released from cumulus cells induce the acrosome reaction. As with sea urchin sperm, a number of proteases have been found in the acrosome such as the trypsin-like protease acrosin, collagenase-like peptidase, cathepsin D-like protease, and dipeptidyl peptidase 2 (for a review see, Honda *et al.*, 2002). Binding of ZP3 or progesterone to its complementary receptor on the sperm surface results in a change in

membrane potential, thereby increasing the intracellular concentration of  $\text{Ca}^{2+}$  and IP<sub>3</sub>, and the opening of SOCs, resulting in acrosomal exocytosis (for a review see, Patrat *et al.*, 2000). In mice, it has been shown that the acrosome is an internal calcium store and that release of  $\text{Ca}^{2+}$  from this store is sufficient to induce acrosomal exocytosis (Herrick *et al.*, 2005). If the sarcoendoplasmic reticulum  $\text{Ca}^{2+}$ -ATPase (SERCA), which pumps calcium from cytoplasm to an internal store, is inhibited, the acrosome reaction is induced, probably because  $\text{Ca}^{2+}$  leaks from the internal store to increase  $\text{Ca}^{2+}$  concentration in the cytosol (Meizel and Turner, 1993). These studies suggest that both sea urchin and mammalian sperm require an increase in intracellular calcium concentration to induce the acrosome reaction. Unlike sea urchin sperm, the formation of an acrosomal process does not occur in mammals. In contrast, the mammalian acrosome contains a triton X-100 (detergent)-insoluble structure known as the acrosomal matrix (for review see Buffone *et al.*, 2008). The acrosomal matrix regulates the distribution of acrosomal molecules within the acrosome and their subsequent release during the acrosome reaction. The fate of the acrosomal matrix during the fertilization process is still unknown.

### ***Insects***

A role for the acrosome in *Drosophila* sperm has been proposed to be different from that of echinoderms and mammals. The extremely long sperm of *D. melanogaster* is 1.9 mm in length and contains a 3.5  $\mu\text{m}$  long acrosome at the tip of the sperm head (Pitnick *et al.*, 1995; Perotti *et al.*, 2001). Despite the existence of an acrosome, it is unlikely that these sperm undergo an acrosome reaction since *Drosophila* sperm enters

the egg through a micropyle and there is no fusion involving egg and sperm membranes (Karr, 1991). For this reason, the role of the acrosome in *Drosophila* had been unclear. However, recently, Wilson and colleagues shed some light on the role of the acrosome in *D. melanogaster* (Wilson *et al.*, 2006). They showed that a protein known as Sneaky (Snky) is localized to the acrosome both before and following sperm entry into the egg, suggesting that the acrosomal membrane remains intact. The sperm of *snky* mutants are motile, are transferred to females in normal quantities, and successfully enter eggs through the micropyle. However, *snky* mutants result in male sterility, probably because the sperm that enter the eggs fail to undergo head decondensation, which is necessary for the formation of a functional haploid pronucleus. This suggests that the acrosome plays a role in head decondensation of the sperm after entry into the eggs (Wilson *et al.*, 2006). The Snky protein is predicted to be a transmembrane protein and BLAST searches have identified a series of Snky-related proteins present in both invertebrates and vertebrates (Wilson *et al.*, 2006). In addition to *snky*, the male sterile mutation, *misfire (mfr)*, of *D. melanogaster* displays a similar phenotype. The *mf* mutant sperm penetrates the egg but fails to form a pronucleus (Ohsako *et al.*, 2003). Although the Mfr protein may be related to the acrosome, the localization of this protein is still unknown.

As there are differences in the roles of the acrosome between sea urchin and *Drosophila*, physiological functions of the acrosome are not universal. There are also species that lack acrosomes, including *C. elegans* (Singson, 2001) and teleosts (Baccetti, 1985). In the bivalve molluscs, *Latunula* and *Lyonsia*, their acrosome begins to differentiate, but disappears in the later stage of spermiogenesis (Kubo, 1977; Kubo and

Ishikawa, 1978). Hence, the requirement for an acrosome during fertilization has been eliminated or bypassed in some lineages during the course of evolution (Wilson *et al.*, 2006).

## **Motility regulation**

### ***General view (Model animals)***

In most species, sperm are immotile after formation in the testis, presumably because they need to preserve their energy reserve and prevent production of reactive oxygen species (Aitken and Fisher, 2005). For example, sea urchin sperm are immotile in semen and begin their motility when they are spawned into seawater where sperm activation is regulated by changes in intracellular ion concentrations. In the semen, the intracellular pH ( $\text{pH}_i$ ) is kept at about 7.2 by high concentrations of  $\text{CO}_2$  (Johnson *et al.*, 1983). When sperm are spawned into seawater,  $\text{CO}_2$  tension decreases and the  $\text{pH}_i$  increases to 7.6 (Johnson *et al.*, 1983). This alkaline  $\text{pH}_i$  activates dynein ATPase, the motor protein of the axoneme that promotes microtubule sliding, thereby initiating sperm motility. Further, cellular respiration is elevated by high concentrations of ADP that are produced by the active dynein ATPase (Christen *et al.*, 1982). In addition to  $\text{pH}_i$ , external potassium concentration ( $[\text{K}^+]_o$ ) may also be involved in motility regulation since high  $[\text{K}^+]_o$  (100 mM) inhibits sperm motility (Darszon *et al.*, 1999).  $[\text{K}^+]_o$  of semen (19 mM) is higher than that of seawater (10 mM) (Johnson *et al.*, 1983) which may induce cellular hyperpolarization resulting in the activation of a cAMP signaling pathway (Neill and Vacquier, 2004).

Sperm motility of sea urchin sperm is activated further by a decapeptide known as speract that is released from the egg jelly in *Hemicentrotus pulcherrimus* (Suzuki 1995). Speract activates sperm motility by binding to a 77 kDa membrane receptor (Dangott and Garbers, 1984). Binding of speract to its receptor results in the activation of guanylate cyclase (GC) that is localized in the sperm membrane (Bentley *et al.*, 1988). A transient increase in cGMP caused by this active GC induces several physiological changes in  $\text{pH}_i$ , intracellular potassium concentration, membrane potential, intracellular  $\text{Ca}^{2+}$  concentration and cAMP level (for reviews, see Darszon *et al.*, 1999; Neill and Vacquier, 2004).

A similar mechanism is involved in the regulation of sperm motility in mammals. Mammalian sperm are immotile in the epididymis but their motility is initiated after ejaculation. The establishment of a low pH in the epididymal lumen is crucial to keep mammalian sperm immotile (Levine and Kelly, 1978; Acott and Carr, 1984; Carr *et al.*, 1985). A sub-population of epididymal epithelial cells, the clear cells, express high levels of the proton-pumping V-ATPase in their apical membrane and are important contributors to the establishment of a low pH in the epididymis (Shum *et al.*, 2009). Following ejaculation, elevation of intracellular pH is required to activate sperm motility, which may be mediated by a voltage-gated proton channel, Hv1 (Lishko *et al.*, 2010). Intracellular alkalization exerts its effects by stimulating sperm metabolism (Babcock *et al.*, 1983), hyperpolarizing membrane potential (Navarro *et al.*, 2007), and activating the axoneme (Giroux-Widemann *et al.*, 1991; Goltz *et al.*, 1988).



During the passage through the female reproductive tract, mammalian sperm motility is activated further. This activation process, known as hyperactivation, is characterized by a high amplitude and asymmetric beating pattern of the flagellum (Figure 1.3) (Yanagimachi, 1994). Hyperactivation can be induced by bicarbonate ( $\text{HCO}_3^-$ ) which directly activates soluble adenylyl cyclase (SACY) in the sperm (Chen *et al.*, 2000), resulting in the activation of a cAMP signaling pathway and downstream protein tyrosine phosphorylation (Visconti *et al.*, 1995). Further, increases in intracellular  $\text{Ca}^{2+}$  concentration through Catsper, a unique mammalian sperm voltage-gated calcium channel, are also involved in the induction of hyperactivation (Ren *et al.*, 2001). Catsper activity is potentiated by intracellular alkalization (Kirichok *et al.*, 2006).

### ***Insects***

Although a slightly basic pH seems to play a critical role in sperm motility regulation of model animals, insect sperm exhibit motility over a wide range of external pHs. For example, sperm from the sand fly, *Culicoides melleus*, are motile at pHs between 6.1 and 12.3 (Linley, 1979). Sperm from the saturniid moths, *Antheraea pernyi* (Guérin-Méneville) and *Hyalophora cecropia* (L.), exhibit their highest motility between pHs of 5.8 to 7.8 (Shepherd, 1974).

Clues about sperm motility regulation in insects come from studies in the silkworm *Bombyx Mori* (Order Lepidoptera) (Osanai and Kasuga, 1990; Aigaki *et al.*, 1994). They produce two types of sperm, eupyrene sperm and apyrene sperm, and both sperm are immotile in seminal vesicles. Eupyrene sperm possess nuclei and fertilize eggs

but apyrene sperm lack nuclei and are not able to fertilize eggs. When they are ejaculated into a spermatophore, apyrene sperm motility is initiated by initiatorin, a trypsin-like protease that is secreted from the prostatic gland. Initiatorin also degrades proteins in the spermatophore to supply an energy source for eupyrene sperm motility. Signaling pathways that mediate this trypsin motility initiation are largely unknown. Trypsin initiation of sperm motility is also reported in Orthopteran species that have only one type of sperm. In these species, sperm motility is not only initiated by trypsin but also enhanced by cAMP, suggesting that there is a two-step acquisition of motility (Osanaï and Baccetti, 1993). It is still unknown if a cAMP signaling pathway and protein phosphorylation are involved in this process, as seen in model animals.

Since trypsin initiation has been reported in Lepidoptera (holometabolism) and Orthoptera (hemimetabolism), this process may be well conserved among insect species. In addition to insects, sperm motility regulation by proteases has been reported in nematodes and fish. In nematodes, sperm initiate amoeboid crawling when they are incubated with pronase (Singson, 2001). In fish, intracellular proteasomes modulate the activity of outer arm dynein by regulating cAMP-dependent phosphorylation of the dynein light chain (Inaba *et al.*, 1998).

### **Fertilization in the water strider, *Aquarius remigis***

*A. remigis* is a common and abundant semi-aquatic water strider found throughout North America. It feeds on insects that are trapped on the water surface. During mating season, a female typically mates with males at least daily throughout her reproductive life.

A male initiates mating by attempting to mount a female and the female resists this attempt. It has been hypothesized that this pre-mating struggle occurs because carrying a male reduces mobility and thus increases the probability of predation (Fairbairn, 1993). Once a male succeeds in copulation, it continues for about 2-3 hours under laboratory conditions, which is substantially longer than other species (1-25 min) (Weigensberg and Fairbairn, 1994; Arnqvist, 1997). Ejaculation occurs at the end of the period and the male dismounts (Campbell and Fairbairn, 2001). A female receives and stores sperm in the gynatrial complex, which is composed of the gynatrial sac, vermiform appendix, fecundation canal, fecundation pump, and spermathecal tube (Figure 1.4). The sperm mass is deposited in the gynatrial sac and moves through the vermiform appendix to the spermathecal tube where sperm can be stored for at least 3 weeks (Rubenstein, 1989; Campbell and Fairbairn, 2001). Observations of sperm mass in the gynatrial sac suggest that this mass may prevent subsequent ejaculates from entering the fecundation canal and spermathecal tube. Some sperm move through the fecundation canal to the distal end and exit the fecundation canal to fertilize eggs. Since, the distal portion of the fecundation canal consists of a series of sclerotized S-curves, the long and rigid acrosome may play a role in passing through this region (Campbell and Fairbairn, 2001). If a female mates with two males subsequently, the last male to mate is able to fertilize 65% of the eggs that the female lays (Rubenstein, 1989). Further, Vermette and Fairbairn (2002) showed that in a lab simulation of natural mating conditions (4 males and 4 females over 4 days at natural densities), male paternity success was proportional to the number of successful matings he obtained. This suggests that there is competition between the sperm of

different males in the gynatrial complex (Rubenstein, 1989). Since a female mates repeatedly, the overall sperm competition can be very intense.

The sperm of *A. remigis* has an unusually long acrosome (~2.5  $\mu\text{m}$ ), which comprises approximately half of the total length of sperm. The remainder of the sperm consists of a 5  $\mu\text{m}$  long nucleus and a 2.5  $\mu\text{m}$  long tail (Tandler and Moriber, 1966). Surprisingly, the length of the *A. remigis* egg is considerably smaller with a diameter of about 1.0  $\mu\text{m}$  (Pollister, 1930). A previous ultrastructural study revealed that the tail region has some structures common to many insect sperm including a “9+9+2” microtubule-based axoneme and a mitochondrial sheath that surrounds the microtubules (Figure 1.5A) (Tandler and Moriber, 1966). These common structures suggest that the tail plays a role in the motility in *A. remigis*. This same study also showed that the head region contains an acrosome that is electron-dense and is filled with acrosomic tubules that are surrounded by “microtubules” (Figure 1.5B) (Tandler and Moriber, 1966). The acrosomic tubules are approximately 13 nm in diameter and exist throughout the length of the acrosome, whereas the “microtubules” that surround the acrosome measure about 22 nm in diameter, are composed of tubulins, and extend from a point near the insertion of the flagellum to the midpoint of the acrosome (Tandler and Moriber, 1966). These acrosomic tubules may be responsible for the relative rigidity of the acrosome (Tandler and Moriber, 1966).

Acrosomes that are filled with acrosomic tubules are also found in other Heteropterans including *Corixa sp.*, *Hydrometra sp.*, and *N. glauca* (Dallai and Afzelius,

1980; Afzelius *et al.*, 1976). While the acrosomes of *Hydrometra sp.* and *N. glauca* (1 mm) are long, the acrosome of *Corixa sp.* is substantially shorter than that of *Hydrometra sp.* (Dallai and Afzelius, 1980; Afzelius *et al.*, 1976). Although it is not known that sperm from *Hebrus ruficeps* and *H. pusillus* (Heteropterans) contain acrosomes that are filled with acrosomic tubules, their acrosomes are considerably shorter than that of *A. remigis* (*H. ruficeps*: sperm 2.1 mm, acrosome 51  $\mu\text{m}$ ; *H. pusillus*: sperm 0.84 mm, acrosome 26  $\mu\text{m}$ ) (Heming-Van Battum and Heming, 1989).

### **Questions to be addressed**

This dissertation addresses several questions pertaining to acrosome formation, the acrosome reaction, and motility regulation in the water strider, *A. remigis*. *A. remigis* will be used as an insect model because their mating behavior and sperm transfer in the female reproductive tract have been previously studied. Further, *A. remigis* possesses 4 large testes and 2 large seminal vesicles, which makes it easy to obtain a large amount of sperm for biochemical studies. The overall goal of this dissertation is to describe post-meiotic events in the *A. remigis* sperm and follow their life history from spermatogenesis to fertilization to thereby obtain insights into reproduction strategies in insects.

### ***Acrosome formation***

As mentioned previously, the *A. remigis* acrosome, at approximately 2.5 mm in length, is unusually long and therefore presents a good system to study its formation and function at both microscopical and biochemical levels. The acrosome is filled with a

tubular matrix, consisting of acrosomic tubules, which may be important for its rigidity. Although the formation of these tubular structures has been described using an electron microscope, no studies have been done to describe its formation in living cells. In the second chapter of this dissertation, the mechanism of this tubular structure formation will be explored using live imaging and biophysical methodologies. Further, nothing is known about the molecular component of the *A. remigis* acrosome. The description of a newly discovered and characterized intrinsic fluorescent molecule that is localized in the acrosome will be presented.

### ***Acrosome reaction***

Studies on the *Drosophila* acrosome suggest that an insect acrosome enters an egg without the necessity of an acrosome reaction. However, I hypothesized that this was unlikely in *A. remigis* since the unusually long acrosome of *A. remigis* sperm ( $\approx 2.5$  mm) is much longer than the diameter of the egg ( $\approx 1.0$  mm). The acrosomal matrix of the *A. remigis* sperm is intrinsically fluorescent, which I used as a marker for the acrosomal matrix both before and subsequent to fertilization. The fate of this long tubular matrix in fertilization will be described in the second chapter of this dissertation utilizing the fluorescent molecule that is associated with the matrix.

### ***Motility regulation***

The specific signaling pathways that lead to motility initiation in insect sperm are largely unknown. Since  $\text{Ca}^{2+}$ , cAMP, and protein phosphorylation are implicated in

sperm motility regulation in sea urchins and mice, these molecules may also be involved in sperm motility regulation in *A. remigis*. In the third chapter of this dissertation, signaling pathways that are involved in trypsin initiation of *A. remigis* sperm will be described.

## **Summary**

There are both similarities and differences in acrosome formation, the acrosome reaction, and motility regulation between model animals (echinoderms and mammals) and insects. In acrosome formation, development of acrosomal granules in the early stage of spermiogenesis seems to follow similar steps in both mammals and insects. However, the function of acrosome in echinoderms and mammals (acrosome reaction) is different from that suggested in *Drosophila melanogaster*. Further, a slightly basic pH that is involved in motility regulation in echinoderms and mammals may not play a critical role in motility regulation in insects although it is possible that downstream signaling pathways are similar. As it is reviewed in this chapter, little is known about these processes in insect in contrast to mammals and echinoderms. Understanding these processes in insects may shed light on adaptive significance of insect sperm morphology that is remarkably diverse.

## CHAPTER 1: REFERENCES

- Acott T.S. and Carr D.W. (1984): Inhibition of bovine spermatozoa by caudal epididymal fluid: II. Interaction of pH and a quiescence factor. *Biol Reprod.* 30, 926-35.
- Afzelius B.A., Baccetti B. and Dallai R. (1976): The giant spermatozoon of *Notonecta*. *J Submicr Cytol.* 8, 149-61.
- Aigaki T., Kasuga H., Nagaoka S. and Osanai M. (1994): Purification and partial amino acid sequence of initiatorin, a prostatic endopeptidase of the silkworm, *Bombyx mori*. *Insect Biochem Molec Biol.* 24, 969-75.
- Aitoken J. and Fisher H. (2005): Reactive oxygen species generation and human spermatozoa: The balance of benefit and risk. *Bioessays.* 16, 259-67.
- Arnqvist G. (1997): The evolution of water strider mating systems: causes and consequences of sexual conflicts. In: Choe J.C. and Crespi B.J., editors. *The evolution of mating systems in insects and arachnids.* Cambridge University Press. pp.146-163.
- Babcock D.F., Rufo Jr G.A. and Lardy H.A. (1983): Potassium-dependent increases in cytosolic pH stimulate metabolism and motility of mammalian sperm. *Proc Natl Acad Sci USA.* 80, 1327-31.
- Bacetti B. (1985): Evolution of the sperm cell. In: Metz C.B. and Monroy A., editors. *Biology of fertilization Vol 2.* Academic Press, Inc. pp.3-47.
- Barre P., Zschornig O., Arnold K. and Huster D. (2003): Structural and dynamical changes of the bindin B18 peptide upon binding to lipid membranes. A solid-state NMR study. *Biochemistry.* 42, 8377-86.
- Bentley J.K., Khatra A.S. and Garbers D.L. (1988): Receptor-mediated activation of detergent-solubilized guanylate cyclase. *Biol Reprod.* 39, 639-47.
- Buffone M.G., Foster J.A. and Gerton G.L. (2008): The role of the acrosomal matrix in fertilization. *Int J Dev Biol.* 52, 511-22.
- Campbell V. and Fairbairn D.J. (2001): Prolonged copulation and the internal dynamics of sperm transfer in the water strider *Aquarius remigis*. *Can J Zool.* 79, 1801-12.
- Carr D.W., Usselman M.C. and Acott T.S. (1985): Effects of pH, lactate, and viscoelastic drag on sperm motility: a species comparison. *Biol Reprod.* 33, 588-95.



- Chen Y., Cann M.J., Litvin T.N., Iourgenko V., Sinclair M.L., Levin L.R. and Buck J. (2000): Soluble adenylyl cyclase as an evolutionarily conserved bicarbonate sensor. *Science*. 289, 625-8.
- Christen R., Schackmann R.W. and Shapiro B.M. (1982): Elevation of the intracellular pH activates respiration and motility of sperm of the sea urchin, *Strongylocentrotus purpuratus*. *J Biol Chem*. 257, 14881-90.
- Dallai R. and Afzelius B.A. (1980): Characteristics of the sperm structure in heteroptera (Hemiptera, insecta). *J Morphol*. 164, 301-9.
- Dangott L.J. and Garbers D.L. (1984): Identification and partial characterization of the receptor for speract. *J Biol Chem*. 259, 13712-6.
- Darszon A., Labarca P., Nishigaki T. and Espinosa F. (1999): Ion channels in sperm physiology. *Physiol Rev*. 79, 481-510.
- Domino S.E. and Garbers D.L. (1988): The fucose-sulfate glycoconjugate that induces an acrosome reaction in spermatozoa stimulates inositol 1,4,5-trisphosphate accumulation. *J Biol Chem*. 263, 690-5.
- Fairbairn D.J. (1993): Costs of loading associated with mate-carrying in the waterstrider, *Aquarius remigis*. *Behav Ecol*. 4, 224-31.
- Giroux-Widemann V., Jouannet P., Pignot-Paintrand I. and Feneux D. (1991): Effects of pH on the reactivation of human spermatozoa demembrated with Triton X-100. *Mol Reprod Dev*. 29, 157-62.
- Glabe C.G. and Lennarz W.J. (1979): Species-specific sperm adhesion in sea urchins. A quantitative investigation of bindin-mediated egg agglutination. *J Cell Biol*. 83, 595-604.
- Goltz J.S., Gardner T.K., Kanous K.S. and Lindemann C.B. (1988): The interaction of pH and cyclic adenosine 3',5'-monophosphate on activation of motility in Triton X-100 extracted bull sperm. *Biol Reprod*. 39, 1129-36.
- Gonzalez-Martinez M.T., Galindo B.E., de De La Torre L., Zapata O., Rodriguez E., Florman H.M. and Darszon A. (2001): A sustained increase in intracellular  $Ca^{2+}$  is required for the acrosome reaction in sea urchin sperm. *Dev Biol*. 236, 220-9.
- Guerrero A. and Darszon A. (1989): Evidence for the activation of two different  $Ca^{2+}$  channels during the egg jelly-induced acrosome reaction of sea urchin sperm. *J Biol Chem*. 264, 19593-9.

- Heming-Van Battum K.E. and Heming B.S. (1989): Structure, function, and evolutionary significance of the reproductive system in males of *Hebrus ruficeps* and *H. pusillus* (Heteroptera, Gerromorpha, Hebridae). *J Morphol.* 202, 281-323.
- Herrick S.B., Schweissinger D.L. Kim S.W., Bayan K.R., Mann S. and Cardullo R.A. (2005): The acrosomal vesicle of mouse sperm is a calcium store. *J Cell Physiol.* 202, 663-71.
- Hirohashi N. and Vacquier V.D. (2003): Store-operated calcium channels trigger exocytosis of the sea urchin sperm acrosomal vesicle. *Biochem Biophys Res Commun.* 304, 285-92.
- Holstein A.F., Schirren C. and Schirren C.G. (1973): Human spermatids and spermatozoa lacking acrosomes. *J Reprod Fert.* 35, 489-91.
- Honda A., Siruntawineti J. and Baba T. (2002): Role of acrosomal matrix proteases in sperm-zona pellucida interactions. *Hum Reprod Update.* 8, 405-12.
- Inaba K., Morisawa S. and Morisawa M. (1998): Proteasomes regulate the motility of salmonid fish sperm through modulation of cAMP-dependent phosphorylation of an outer arm dynein light chain. *J Cell Sci.* 111, 1105-15.
- Jamieson B.G.M., Dallai R. and Afzerius B.A. (1999): *Insects: Their Spermatozoa and Phylogeny*, USA: Science Publishers, 1-23.
- Johnson C.H., Clapper D.L., Winkler M.M., Lee H.C. and Epel D. (1983): A volatile inhibitor immobilizes sea urchin sperm in semen by depressing the intracellular pH. *Dev Biol* 98, 493–501.
- Kang-Decker N., Mantchev G.T., Juneja S.C., McNiven M.A. and van Deursen J.M.A. (2001): Lack of acrosome formation in Hrb-deficient mice. *Science.* 294, 1531-3.
- Karr T.L. (1991): Intracellular sperm/egg interactions in *Drosophila*: A tree-dimensional structural analysis of a paternal product in the developing egg. *Mech Dev.* 34, 101-11.
- Kierszenbaum A.L. and Tres L.L. (2004): The acrosome-acroplaxome-manchette complex and the shaping of the spermatid head. *Arch Histol Cytol.* 67, 271-84.
- Kirichok Y., Navarro B. and Clapham D.E. (2006): Whole-cell patch-clamp measurements of spermatozoa reveal an alkaline-activated Ca<sup>2+</sup> channel. *Nature.* 439, 737-40.

- Kubo M. (1977): The formation of a temporary acrosome in the spermatozoon of *Laternula limicola* (Bivalvia, Mollusca). *J Ultrastruct Res* 61, 140-8.
- Kubo M. and Ishikawa M. (1988): Organizing process of the temporary-acrosome in spermatogenesis of the Bivalve *Lyonsia ventricosa*. *J Submicr Cytol.* 10, 411-21.
- Levine A.E., Walsh K.A. and Fodor E.J.B. (1978): Evidence of an acrosin-like enzyme in sea urchin sperm. *Dev Biol.* 63, 299-306.
- Levine N and Kelly H. (1978): Measurement of pH in the rat epididymis *in vivo*. *J Reprod Fertil.* 52, 333-5.
- Linley J.R. (1979): Activity and motility of spermatozoa of *Culicoides melleus* (Diptera: Ceratopogonidae). *Entomol Exp Appl.* 26, 85-96.
- Lishko P.V., Botchkina I.L., Fedorenko A. and Kirichok Y. (2010): Acid extrusion from human spermatozoa is mediated by flagellar voltage-gated proton channel. *Cell.* 140, 327-37.
- Meizel S. and Turner K.O. (1993): Initiation of the human sperm acrosome reaction by thapsigargin. *J Exp Zool.* 267, 350-5.
- Moriber L.G. (1956): A cytochemical study of hemipteran spermatogenesis. *J Morphol.* 99, 271-327.
- Moy G.W., Mendoza L.M., Schulz J.R., Swanson W.J., Glabe C.G. and Vacquier V.D. (1996): The sea urchin sperm receptor for egg jelly is a modular protein with extensive homology to the human polycystic kidney disease protein, PKD1. *J. Cell Biol.* 133, 809-17.
- Navarro B., Kirichok Y. and Clapham D.E. (2007): KSper, a pH-sensitive K<sup>+</sup> current that controls sperm membrane potential. *Proc Natl Acad Sci U S A.* 104, 7688-92.
- Neill A.T. and Vacquier V.D. (2004): Ligands and receptors mediating signal transduction in sea urchin spermatozoa. *Reproduction.* 127, 141-9.
- Ohsako T., Hirai K. and Yamamoto M.T. (2003): The *Drosophila misfire* gene has an essential role in sperm activation during fertilization. *Genes Genet Syst.* 78, 253-66.
- Ohtani H., Wakui H., Ishino T., Komatsuda A. and Miura A.B. (1993): An isoform of protein disulfide isomerase is expressed in the developing acrosome of spermatids during rat spermiogenesis and is transported into the nucleus of mature spermatids and epididymal spermatozoa. *Histochemistry.* 100, 423-9.

- Osanai M. and Baccetti B. (1993): Two-step acquisition of motility by insect spermatozoa. *Experientia*. 49, 593-5.
- Osanai M. and Kasuga H. (1990): Role of endopeptidase in motility induction in apyrene silkworm spermatozoa; micropore formation in the flagellar membrane. *Experientia*. 46, 261-4.
- Patrat C., Serres C. and Jouannet P. (2000): The acrosome reaction in human spermatozoa. *Bio Cell*. 92, 255-66.
- Perotti M.E., Cattaneo F., Pasini M.E., Verni F. and Hackstein J. H. (2001): Male sterile mutant *casanova* gives clues to mechanisms of sperm-egg interactions in *Drosophila melanogaster*. *Mol Reprod Dev*. 60, 248-59.
- Pitnick S., Markow T.A. and Spicer G.S. (1995): Delayed male maturity is a cost of producing large sperm in *Drosophila*. *Proc Natl Acad Sci U S A*. 92, 10614-8.
- Pollister A.W. (1930): Cytoplasmic phenomena in the spermatogenesis of *Gerris*. *J Morphol*. 49, 455-507.
- Ramalho-Santos J., Moreno R.D., Wessel G.M., Chan E.K.L and Schatten G. (2001): Membrane trafficking machinery components associated with the mammalian acrosome during spermiogenesis. *Exp. Cell Res*. 267, 45-60.
- Ramalho-Santos J., Schatten G. and Moreno R. D. (2002): Control of membrane fusion during spermiogenesis and the acrosome reaction. *Biol Reprod*. 67, 1043-51.
- Ren D., Navarro B., Perez G., Jackson A.C., Hsu S., Shi Q., Tilly J.L. and Clapham D.E. (2001): A sperm ion channel required for sperm motility and male fertility. *Nature*. 413, 603-9.
- Rubenstein D.I. (1989): sperm competition in the water strider, *Gerris remigis*. *Anim Behav*. 38, 631-6.
- SeGall G.K and Lennarz W.J. (1979): Chemical characterization of the component of the jelly coat from sea urchin eggs responsible for induction of the acrosome reaction. *Dev. Biol*. 71, 38-48.
- Shepherd J.D. (1974): Activation of saturniid moth sperm by a secretion of the male reproductive tract. *J Insect Physiol*. 20, 2107-22.

- Shum W.W.C., Da Silva N., Brown D. and Breton S. (2009): Regulation of luminal acidification in the male reproductive tract *via* cell-cell crosstalk. *J Exp Biol.* 212, 1753-61.
- Singson A. (2001): Every sperm is sacred: fertilization in *Caenorhabditis elegans*. *Dev Biol.* 230, 101-9.
- Suzuki N. (1995): Structure, function and biosynthesis of sperm-activating peptides and fucose sulfate glycoconjugate in the extracellular coat of sea urchin eggs. *Zoolog Sci.* 12, 13-27.
- Tandler B. and Moriber L.G. (1966): Microtubular structures associated with the acrosome during spermiogenesis in the Water-strider, *Gerris remigis* (Say). *J Ultrastruct Res.* 14, 391-404.
- Tilney L.G., Kiehart D.P., Sardet C. and Tilney M. (1978): Polymerization of actin. IV. Role of  $\text{Ca}^{++}$  and  $\text{H}^+$  in the assembly of actin and in membrane fusion in the acrosomal reaction of echinoderm sperm. *J Cell Biol.* 77, 536-50.
- Vacquier V.D. and Moy G.W. (1977): Isolation of bindin: the protein responsible for adhesion of sperm to sea urchin eggs. *Proc Natl Acad Sci U S A.* 74, 2456-60.
- Vermette R. and Fairbairn D.J. (2007): How well do mating frequency and duration predict paternity success in the polygynandrous water strider *Aquarius remigis*? *Evolution.* 56, 1808-20.
- Visconti P.E., Bailey J.L., Moore G.D., Pan D., Olds-Clarke P. and Kopf G.S. (1995): Capacitation of mouse spermatozoa I. Correlation between the capacitation state and protein tyrosine phosphorylation. *Development.* 121, 1129-37.
- Weigensberg I. and Fairbairn D.J. (1994): Conflicts of interest between the sexes: a study of mating interactions in a semiaquatic bug. *Anim Behav.* 48, 893-901.
- Westbrook-Case V.A., Winfrey V.P. and Olson G.E. (1995): Sorting of the domain-specific acrosomal matrix protein AM50 during spermiogenesis in the guinea pig. *Dev Biol.* 167, 338-49.
- Wilson K.L., Fitch K.R., Bafus B.T. and Wakimoto B.T. (2006): Sperm plasma membrane breakdown during *Drosophila* fertilization requires Sneaky, an acrosomal membrane protein. *Development.* 133, 4871-9.

Wolf D.E., Hagopian S.S. and Ishijima S. (1986): Changes in sperm plasma membrane lipid diffusibility after hyperactivation during in vitro capacitation in the mouse. *J Cell Biol.* 102,1372-7.

Yanagimachi R. (1994): In: Knobil, E., Neill, J.D. (Eds.), *The Physiology of Reproduction*. Raven Press, New York, 2nd Ed., pp. 189-317.

Yao R., Ito C., Natsume Y., Sugitani Y., Yamanaka H., Keretake S., Yanagida K., Sato A., Toshimori K., Noda T. (2002): Lack of acrosome formation in mice lacking a golgi protein, GOPC. *Proc Natl Acad Sci U S A.* 99, 11211-16.

Yoshinaga K. and Toshimori K. (2003): Organization and modifications of sperm acrosomal molecules during spermatogenesis and epididymal maturation. *Microsc Rec Tech.* 61, 39-45.

## FIGURE LEGENDS

**Figure 1.1** Schematic illustration of the acrosome formation during guinea pig spermiogenesis. A developing acrosome is shown in blue. There are four phases in spermiogenesis (Golgi phase, cap phase, acrosomal phase and maturation phase). ER, Endoplasmic reticulum; G, Golgi apparatus; N, Nucleus. (modified from Yoshinaga and Toshimori, 2003).

**Figure 1.2** Schematic illustration of the acrosome reaction in sea urchin sperm. (a) Intact acrosome. (b) Induction of acrosome reaction. (c) Formation of acrosomal process. (d) Membrane fusion. M, mitochondrion; N, nucleus. (from, Neill and Vacquier, 2004).

**Figure 1.3** Beating patterns of mouse sperm. Sperm are collected from the cauda epididymis. Fresh sperm (a) have low amplitude symmetric beats, whereas hyperactivated sperm (b) exhibit larger amplitude lower frequency beats. Successive frames are separated by 1/60 s. (from Wolf *et al.*, 1986).

**Figure 1.4** Schematic diagram of the gynatrial complex of female *A. remigis*. Df, distal portion of the fecundation canal; fb, fertilization chamber; fp, fecundation pubp; gg, gynatrial gland; gs, gynatrial sac; pf proximal portion of the fecundation canal; st, spermathecal tube; va, vermiform appendix. Scale bar = 500  $\mu\text{m}$  (from Campbell and Fairbairn, 2001).

**Figure 1.5** Transverse sections of *A. remigis* sperm. **A.** Tail region. The tail contains 2 mitochondrial derivatives and a 9+9+2 axoneme. **B.** Acrosome region. The acrosome is filled with a tubular matrix. AT, acrosomic tubules; L acrosomal lumen; MD, Mitochondrial derivative; SM sleeve membrane. Arrow indicates a single cytoplasmic microtubule. Scale bar = 0.5  $\mu\text{m}$ . (from Tandler and Moriber, 1966).



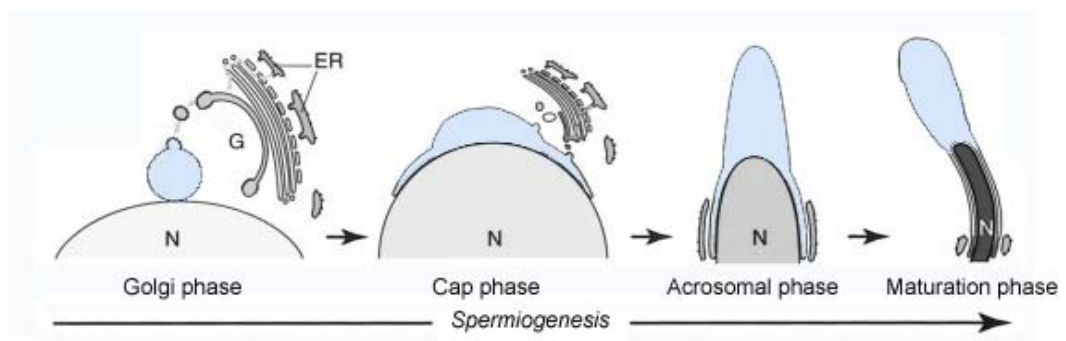


Figure 1.1 Schematic illustration of the acrosome formation during guinea pig spermiogenesis.

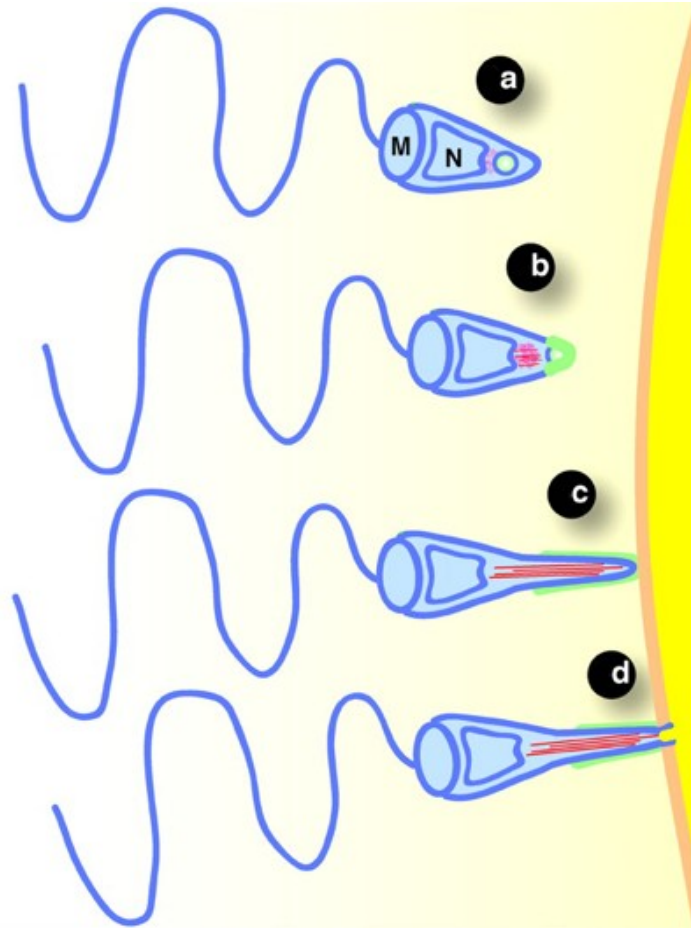


Figure 1.2 Schematic illustration of the acrosome reaction in sea urchin sperm.

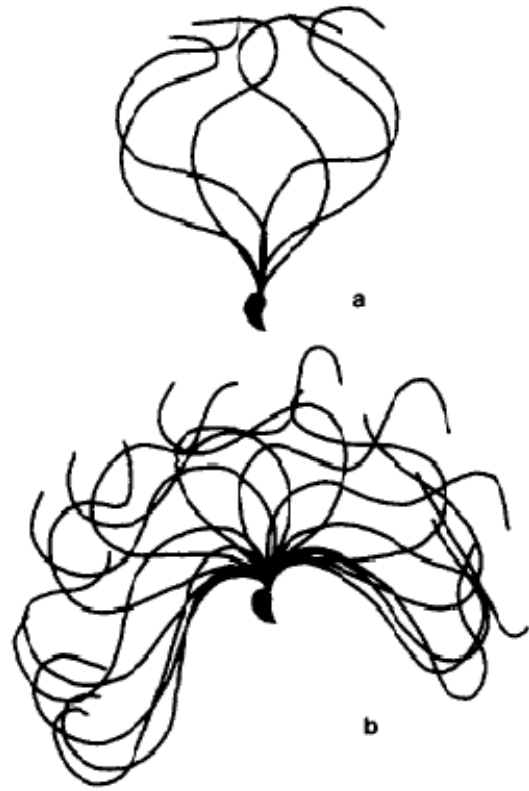


Figure 1.3 Beating patterns of mouse sperm.

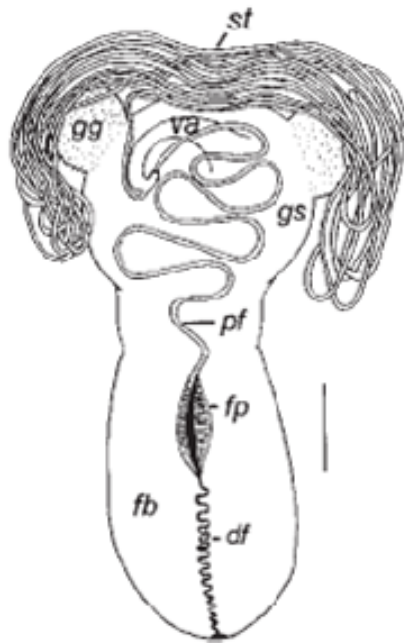
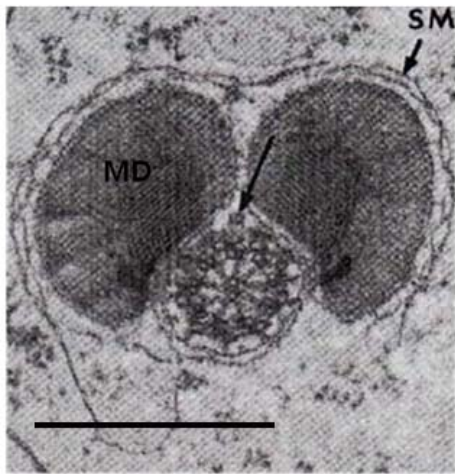


Figure 1.4 Schematic diagram of the gynatrial complex of female *A. remigis*.

**A**



**B**

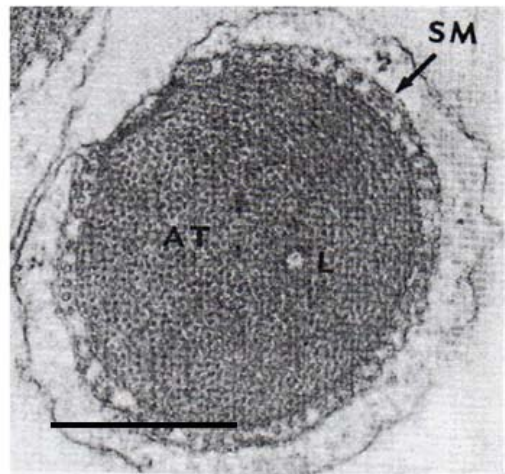


Figure 1.5 Transverse sections of *A. remigis* sperm.

CHAPTER 2

ASSEMBLY OF THE FLUORESCENT ACROSOMAL MATRIX AND ITS FATE IN  
FERTILIZATION IN THE WATER STRIDER, *AQUARIUS REMIGIS*

## ABSTRACT

Animal sperm show remarkable diversity in both morphology and molecular composition. Here we describe the novel morphology and molecular structure in the sperm of a semi-aquatic insect, the water strider, *Aquarius remigis*. Our deconvolution fluorescence microscopy reveals that the *A. remigis* mature acrosome contains two distinct domains: a proximal 300  $\mu\text{m}$  long helix with a 7  $\mu\text{m}$  repeat and a much longer distal linear extension (2200  $\mu\text{m}$ ). Further, the sperm possesses an intrinsically fluorescent molecule with properties consistent with those of Flavin Adenine Dinucleotide (FAD) which appears first in the acrosomal vesicle of round spermatids and persists in the acrosome throughout spermiogenesis. Fluorescence recovery after photobleaching reveals that the fluorescent molecule exhibits unrestricted mobility in the acrosomal vesicle of round spermatids, but is completely immobile in the acrosome of mature sperm. Fluorescence polarization microscopy shows a net alignment of the fluorescent molecules in the acrosome of the mature sperm but not in the acrosomal vesicle of round spermatids. These results suggest that acrosomal molecules are rearranged in the elongating acrosome and FAD is incorporated into the acrosomal matrix during its formation. Further, we followed the fate of the acrosomal matrix in fertilization utilizing the intrinsic fluorescence. The fluorescent acrosomal matrix was observed inside the fertilized egg and remained structurally intact even after gastrulation started. This observation suggests that FAD is not released from the acrosomal matrix during the fertilization process or early development and supports an idea that FAD is involved in the formation of the

acrosomal matrix. The intrinsic fluorescence of the *A. remigis* acrosome will be a useful marker for following spermatogenesis and fertilization.

## **INTRODUCTION**

Most animal sperm are highly differentiated cells that possess a flagellated motility apparatus (the tail) that is separated from a head region containing a haploid nucleus and a specialized organelle known as the acrosome. In the most studied systems, the acrosome is known as a secretory vesicle that undergoes a requisite exocytotic event (the acrosome reaction) prior to sperm-egg fusion. During the acrosome reaction, the acrosome releases hydrolytic enzymes and other components that facilitate sperm binding and penetration through the outer vestments of the egg (Yanagimachi, 1994; Neill and Vacquier, 2004).

In contrast to well-studied systems such as mice and sea urchins, little is known about the role of acrosomes in insect sperm. Insect eggs are encased in a shell that permits sperm entry only through a specialized structure known as the micropyle (Margaritis, 1985, Triplehorn and Johnson, 2005). It is unclear whether the acrosome plays a role in enabling sperm passage through the micropyle. However, Wilson *et al.* (2006) suggested a different function for the acrosome in the fruit fly, *Drosophila melanogaster* (Order Diptera). Rather than undergoing an exocytotic event, the acrosome in these sperm remains intact after entry through the micropyle and may facilitate sperm plasma membrane breakdown inside the egg. The acrosome is released into the egg cytoplasm after this event and persists in the cytoplasm at least as late as prometaphase of



the first embryonic cycle (Wilson *et al.*, 2006). Although the function of the released acrosome in the egg cytoplasm is still unknown, this study suggests that the functions of the acrosome are not the same across all species.

Sperm from the semi-aquatic insect, the water strider, *Aquarius remigis* (Hemiptera; Gerridae) have a markedly different morphology than most sperm. These giant sperm ( $\approx 5$  mm long) (Pollister, 1930) are substantially longer than the eggs they fertilize (egg lengths range from  $\approx 1.3$  to 1.5 mm, and widths from  $\approx 0.5$  to 0.6 mm; Fairbairn unpublished data). Unlike most sperm, including those of *D. melanogaster*, where the length of the tail far exceeds the head length, *A. remigis* sperm heads and tails are nearly equal in length. A 5  $\mu\text{m}$ -long nucleus is located proximal to the tail and the remainder of the head, which is more than 2500  $\mu\text{m}$  in length, contains an acrosome (Tandler and Moriber, 1966). A previous ultrastructural study using transmission electron microscopy revealed that the acrosome is filled with a tubular structure that runs parallel to the long axis of the acrosome and is likely responsible for its rigidity (Tandler and Moriber, 1966). However, the process and the molecular components that lead to the assembly of this long tubular acrosomal matrix are largely unknown. Further, the role of this unusually long acrosome in the fertilization process is enigmatic, particularly as its length exceeds that of the egg by at least 1000  $\mu\text{m}$ .

In the present study, we report that the acrosome of *A. remigis* sperm possesses an intrinsically fluorescent molecule with properties consistent with those of Flavin Adenine Dinucleotide (FAD). Fluorescence recovery after photobleaching (FRAP)

showed that the fluorescent molecule became immobilized during spermiogenesis. We also demonstrate that the fluorescent molecule exhibits a static, partial alignment in the acrosome of mature sperm using fluorescence polarization microscopy (FPM). These results suggest that FAD assembles into the acrosomal matrix during spermiogenesis in a fashion that results in a net alignment of FAD. The function of FAD in the acrosomal matrix will be discussed. Further, the intrinsic fluorescence of the *A. remigis* acrosome would serve as a useful biomarker for elucidating reproductive strategies in water striders. Utilizing this intrinsic fluorescence we followed the fate of the acrosomal matrix during the fertilization process and early development.

## **MATERIALS AND METHODS**

### **Sample preparations**

*A. remigis* is a common and abundant semi-aquatic water strider found throughout North America (Preziosi and Fairbairn, 1992). Sexually mature *A. remigis* males were obtained from a laboratory culture where they had been mating ad libitum. Females mate with many males and are able to store sperm for at least 3 weeks in the spermathecal tubes (Rubenstein, 1989, Campbell and Fairbairn, 2001). Males were anaesthetized with chloroform and testes and seminal vesicles were dissected under a dissecting microscope and transferred into phosphate-buffered saline (PBS: 7.7 mM Na<sub>2</sub>HPO<sub>4</sub>, 2.7 mM NaH<sub>2</sub>PO<sub>4</sub> and 150 mM NaCl, pH 7.2). Mature sperm were obtained by teasing the seminal vesicles in PBS. To observe sperm bundles and spermatids, the testes were

transferred to a drop of PBS on a glass slide and squashed with a cover slip. Laid eggs were collected from a culture tank.

### **Microscopy and image processing**

Cells were observed under differential interference contrast (DIC) or epifluorescence optics using an Olympus BX-71 microscope or a Zeiss Axiovert 10 microscope. A GFP filter set (model 41012, Chroma Technology) was used for intrinsic fluorescence. Three-dimensional images were generated using a deconvolution microscope system (DeltaVision, Applied Precision) that consisted of an Olympus IX-71 microscope with a 250 W Xenon lamp and a GFP filter set. To determine an intrinsic fluorescence emission spectrum, a Leica TCS-SP2 confocal microscope was used in lambda scan mode with an excitation wavelength of 351 nm or 458 nm and a detection bandwidth of 10 nm. DIC and epifluorescence micrographs were processed for contrast enhancement using Image J (National Institutes of Health) and Adobe Photoshop 6.0.

### **Fluorescence Recovery After Photobleaching (FRAP)**

FRAP analysis was performed on a Leica-SP2 confocal microscope equipped with a 63x/1.20 water immersion objective lens. Photobleaching of the intrinsic fluorescence was carried out using the 351 nm, 364 nm, 442 nm, 458 nm, 476 nm and 488 nm laser lines at full power for 20 iterations. Images were obtained with an excitation wavelength of 476 nm at 10% laser power, a detection bandwidth of 500 nm to 550 nm and a temporal resolution between frames of 823 msec. The collected images were analyzed with Leica Confocal Software (LCS, 2.61.1537) in combination with Microsoft

Excel 2004 with double normalization performed as described by Phair *et al.* (2004). For the normalization of mature sperm bundles, the acrosome region in the image was used instead of the entire acrosome. The mobile fraction  $M_f$  was calculated using the equation:  $M_f = (F_\infty - F_0)/(F_i - F_0)$  where  $F_\infty$  is the fluorescence in the bleached region after full recovery,  $F_i$  is the average fluorescence before bleaching and  $F_0$  is the fluorescence immediately following the bleach. To obtain  $F_\infty$  for round acrosomes, fluorescence recovery curves were fitted to a single exponential function using nonlinear regression (Prism 5, GraphPad).

### **Fluorescence Polarization Microscopy (FPM)**

We analyzed the polarization of the acrosomal fluorescence using a liquid crystal universal compensator that is usually employed to measure the birefringent fine structure in living cells and other transparent objects (LC-PolScope, CRI, Woburn MA, [Oldenbourg and Mei, 1995; Shribak and Oldenbourg, 2003]). For measuring the fluorescence anisotropy, the LC compensator was placed into the analyzer slot of a Zeiss Axiovert 200M microscope stand and operated as a fast switching polarization analyzer. Using epi-illumination, acrosomes were illuminated by unpolarized light (450 nm – 490 nm) and the polarization of the emitted fluorescence (510 nm – 550 nm) was analyzed sequentially using four LC compensator settings representing linear polarization states with azimuthal angles of 0°, 45°, 90° and 135°. In addition, a fifth LC compensator setting returned to the angle of 0° for assessing the effect of photobleaching. For each setting a fluorescence image was automatically recorded (exposure time 1 sec) in quick

succession (total recording time 5.1 sec) using custom software. The first four intensity images were used to calculate the fluorescence anisotropy in each pixel after correcting for photobleaching based on the intensity reduction between the first and the fifth image. The fluorescence anisotropy coefficient was calculated using image arithmetic and the following formula: Anisotropy Coefficient (AC) =  $((I_0 - I_{90})^2 + (I_{45} - I_{135})^2)^{1/2} / (I_0 + I_{90} + I_{45} + I_{135})$ . The anisotropy coefficient is related to the polarization ratio =  $I_{\max}/I_{\min}$ , in which  $I_{\max}$  is the maximum fluorescence intensity observed for a specific azimuth angle  $\Theta_{\max}$ . The minimum intensity  $I_{\min}$  is necessarily observed for an azimuth of  $\Theta_{\max} + 90^\circ$ . The following relationship holds: polarization ratio =  $I_{\max}/I_{\min} = (1+2 \cdot AC)/(1-2 \cdot AC)$ . The polarization ratio is 1 for randomly oriented fluorophores and increases with increasing mutual alignment. The azimuth angle associated with the fluorescence maximum is computed using:  $\Theta_{\max} = \text{atan2}((I_0 - I_{90}), (I_{45} - I_{135}))/2$ . The  $\text{atan2}(x,y)$  function is the same as  $\arctan(y/x)$ , except that the signs of the numerator and denominator are used to determine the quadrant of the angle. More details on the fluorescence polarization measurements will be presented in a forthcoming publication.

### **Tricine-SDS-PAGE and fluorescence spectrophotometry**

Tricine-SDS-PAGE was performed as described by Schägger and von Jagow (1987) using 16.5 % polyacrylamide gel. Fluorescent signals on the gel were detected with ImageMaster VDS-CL (Amersham Bioscience) using a 321-nm ultraviolet transilluminator and a 520-nm bandpass filter (full width at half maximum: 50 nm).

Excitation and emission spectra of a liquid sample were obtained using a Hitachi F-2000 fluorescence spectrophotometer.

## **RESULTS**

### **Morphology of mature *A. remigis* sperm**

A schematic drawing of *A. remigis* sperm is shown in Figure 2.1A based on our observations using both DIC and epifluorescence optics. As reported previously (Pollister, 1930), these sperm are extremely long cells with a well-defined head, nucleus, and tail that were readily observed in DIC. A periodic, wavelike, structure was found proximal to the nucleus that extends for approximately 300  $\mu\text{m}$  and then tapers to a thinner, linear structure for the remainder of the sperm head (Figure 2.1A). Using a GFP filter set we observed an intense fluorescent signal that was restricted to the periodic and linear regions of the sperm head anterior to the nucleus with no signal observed in the tail (Figure 2.1B). When filter sets for DAPI (model 31000, Chroma Technology) or TRITC (model 31002, Chroma Technology) were used, no fluorescent signals were detected in the periodic and linear regions of the sperm head suggesting that the intrinsic fluorescence has a defined excitation and emission spectrum.

The intrinsic fluorescent signal enabled us to investigate the three-dimensional structure of the head. To create a three-dimensional image, sperm were observed using a deconvolution microscope system with a GFP filter set. The periodic wavelike fluorescent structure was detected in both the X-Z projected plane and the Y-Z projected plane, indicating that this region of the head is helical (Figure 2.2A and 2.2B). This

helical structure was confirmed when sperm were observed in Z-sections down the shaft (Figure 2.2C). The fluorescent signal rotated around a central axis with a pitch of approximately 7  $\mu\text{m}$  in the Z-axis, consistent with the images in the X-Z and Y-Z projected planes.

### **The intrinsically fluorescent signal in *A. remigis* sperm first appears during spermatogenesis in the developing acrosome**

Localization of the intrinsic fluorescence anterior to the nucleus in *A. remigis* sperm suggested that the fluorescence is in the acrosome. To see when the fluorescent signal in *A. remigis* sperm first appears, and to see if its appearance coincides with the formation of the acrosome, we used cells from the testis and observed cells in various stages of spermatogenesis using both DIC and epifluorescence optics. As with other spermatogenic cells, the acrosome of *A. remigis* sperm first appears following meiosis in round spermatids. In *A. remigis* spermatids, the nascent acrosome appears as a spherical organelle that consists of two distinct regions (Figure 2.3A). This observation is consistent with a previous ultrastructural study that identified two distinct acrosomal regions with different electron densities: a "core" that is proximal to the nucleus and is less electron-dense than a more distal region described as the "sheath" (Tandler and Moriber, 1966). When we observed the intrinsic fluorescence that was restricted to the acrosome of spermatids, the fluorescence intensity in the core was higher than the sheath (Figure 2.3A).

The fluorescent signal was also detected in the developing acrosome of condensing spermatids (Figure 2.3B). In this stage, the acrosome begins to elongate and is bounded by two basal bodies that surround an acrosome that is proximal to the nucleus (Figure 2.3B) (Pollister, 1930; Tandler and Moriber, 1966). The intrinsic fluorescent signal, however, was not observed in these basal bodies and was only detected in the acrosome (Figure 2.3B).

Mature sperm in the testis were observed in bundles with their long heads and tails precisely aligned (Figure 2.3C). Consistent with mature sperm from seminal vesicles, the fluorescent signal in testicular sperm was restricted to the linear and helical regions of the head (Figure 2.3C). Taken together these results suggest that the fluorescent molecule is restricted to the acrosome of *A. remigis* sperm.

### **The fluorescent molecule becomes immobilized during spermiogenesis**

Since the acrosome of *A. remigis* is filled with a tubular acrosomal matrix (Tandler and Moriber, 1966), we hypothesized that the fluorescent molecule may be associated with this structure. This is supported by the fact that we detected no fluorescent signals in the basal bodies of the condensing spermatid (Figure 2.3B) where the tubular structure is absent (Tandler and Moriber, 1966). In order to test this hypothesis, we determined the mobile fraction ( $M_f$ ) of the fluorescent molecule using Fluorescence Recovery After Photobleaching (FRAP) in sperm bundles. If the fluorescent molecule is tightly associated with the acrosomal matrix, we argued that the fluorescence intensity should not recover and the mobile fraction should be low. Indeed, the mobile fraction of the



fluorescent molecule associated with the acrosomes in mature sperm bundles was low ( $M_f = 7.23 \pm 2.07\%$ ,  $n = 5$ , Figure 2.4A). In contrast, the fluorescent molecule was found to freely move in both sheath and core regions of round spermatids (Sheath;  $M_f = 96.84 \pm 5.99\%$ ,  $n = 9$ , Figure 2.4A, Core;  $M_f = 96.53 \pm 6.78\%$ ,  $n = 8$ ). Since the tubular acrosomal matrix first appears when the round acrosome begins to elongate (Tandler and Moriber, 1966), these results suggest a model in which the fluorescent molecule is incorporated into the acrosomal matrix during its formation.

To test this model further, we isolated the acrosomal matrix as a heat/detergent resistant fraction by boiling the mature sperm in PBS containing 2% SDS. There were no tails and nuclei observed after this treatment under DIC optics. However, the acrosomal matrix was insoluble under this harsh condition and retained an intense intrinsic fluorescence (Figure 2.4B). In contrast, when 100 mM DTT or 1%  $\beta$ -mercaptoethanol was added under this condition, the acrosomal matrix dissolved completely. This result supports a model in which the acrosomal matrix includes the fluorescent moiety and suggests that the matrix is stabilized by disulfide bonds.

### **The fluorescent molecules are aligned in the acrosome of mature sperm**

In order to investigate further the assembly of the fluorescent molecule we observed both the round acrosomes of spermatids and the extended acrosome of mature sperm using Fluorescence Polarization Microscopy (FPM) that can analyze the orientation distribution of fluorophores (Axelrod, 1979; Inoue *et al.*, 2002; Vrabioiu and Mitchinson, 2006). We applied a liquid crystal compensator for rapidly and sensitively

measuring the static fluorescence anisotropy in every resolved image point. The LC-compensator was used as a tunable linear polarization analyzer to determine the azimuth angle and the ratio of highest to lowest polarized fluorescence (see Materials and Methods). The fluorescence signal throughout the acrosomes of mature sperm exhibited a high polarization ratio of 3.6 with an azimuth angle nearly perpendicular to the long axis of the acrosome (i.e. the maximum intensity was observed when the linear analyzer was oriented nearly perpendicular to the extended acrosome, Figure 2.5B and 2.5C). Our measurements gave nearly identical results using live sperm ( $I_{\max}/I_{\min} = 3.64 \pm 0.43$ , mean  $\pm$  SD,  $n = 7$ ) and sperm that were fixed with 4% formaldehyde in PBS for 10 minutes ( $I_{\max}/I_{\min} = 3.63 \pm 0.57$ , mean  $\pm$  SD,  $n = 8$ ). In contrast, the fluorescence signal of round acrosomes of either live or fixed spermatids exhibited no anisotropy. These results indicate that the fluorescent molecules are incorporated into the acrosomal matrix during spermiogenesis in a fashion that results in a net alignment of the emission transition dipole moment of the fluorescent molecules.

### **Properties of the fluorescent molecule are similar to those of Flavin Adenine Dinucleotide (FAD)**

The FRAP and FPM analyses suggest that the fluorescent molecule is incorporated into a rigid acrosomal structure. In order to determine the fluorescence characteristics of the matrix, we obtained the emission spectrum of the fluorescent signal from *A. remigis* sperm *in vivo* using a confocal microscope. Sperm bundles from the testes were used instead of a single sperm in order to maximize the overall fluorescent

signal. A maximum emission wavelength of 515 nm was detected using an excitation wavelength of 351 nm (Figure 2.6A). Although keratin, collagen, and elastin have all been reported to form tubular matrices in cells or connective tissues that display intrinsic fluorescence (Fujimoto, 1977; Wu *et al.*, 2004; Pena *et al.*, 2005; Wu and Qu, 2006), the emission spectrum of these molecules is not similar to that of the fluorescence in *A. remigis* sperm. Rather, the spectrum of *A. remigis* sperm is similar to that of flavin or a flavin-containing molecule (Weber, 1950; Kleiner *et al.*, 1999). The flavin molecule has two absorption maxima at 375 nm and 455 nm (Weber, 1950). When an excitation wavelength of 458 nm was used instead of 351 nm, a similar spectrum was obtained. To test if the emission spectrum is similar to that of flavin or a flavin-containing molecule, we determined the emission spectrum of flavin adenine dinucleotide (FAD), a common flavin-containing molecule, using an excitation wavelength of 351 nm. As reported previously, a maximum emission wavelength of about 530 nm was detected for FAD (Figure 2.6A). This emission spectrum is similar to that of the fluorescent molecule in the matrix although the spectrum of FAD is red-shifted about 15 nm. This difference could be due to differences in microenvironments of flavin in the matrix.

In cells, flavin is a component of FAD, riboflavin and flavin mononucleotide (FMN). To further investigate the fluorescent molecule in the matrix, the acrosomal matrix that was isolated from the *A. remigis* sperm as a SDS-insoluble fraction was subjected to tricine-SDS-PAGE and fluorescent signals were examined on the gel. The mass-to-charge ratio of the fluorescent molecule from the matrix was similar to that of FAD but not riboflavin or FMN (Figure 2.6B). After the gel was stained with coomassie

blue, there was a major protein band with a molecular weight of approximately 75 kDa, but there was no protein band observed in the same region as the fluorescent signal (Figure 2.6B).

We also investigated the excitation and emission spectra of the isolated acrosomal matrix that was solubilized by the addition of  $\beta$ -mercaptoethanol. Consistent with the excitation spectrum *in vivo* (Figure 2.6A), a maximum emission wavelength of 520 nm was detected using an excitation wavelength of 370 nm (Figure 2.6C). There were 2 excitation peaks detected at 370 nm and 440 nm (Figure 2.6D). These emission and excitation spectra were matched with those of FAD. Further, the fluorescent intensity of FAD but not riboflavin or FMN increases dramatically when pH is low (Bessey *et al.*, 1949). When the spectra were investigated at pH 7.1, the fluorescence intensities decreased about 10-fold as compared to those of pH 2.5. Taken together, these results strongly suggest that the fluorescent molecule in the acrosomal matrix is FAD.

### **The fate of FAD that is associated with the acrosomal matrix in the fertilization process and early development**

In well-studied systems such as mice and sea urchins, the acrosomal contents are released prior to sperm-egg fusion and facilitate sperm binding and penetration through the outer vestments of the egg (Yanagimachi, 1994; Neill and Vacquier, 2004). In order to examine if it is also the case for FAD from the *A. remigis* sperm acrosome, we followed its fate during the fertilization process and early development utilizing its intrinsic fluorescence. Both helical and thinner linear regions of the fluorescent matrix

were observed inside the fertilized egg (Figure 2.7A), indicating that the long acrosomal matrix enters the egg during the fertilization process. The single fluorescent acrosomal matrix was often found near the micropyle of the fertilized egg. Further, the fluorescent matrix remained structurally intact even after gastrulation had started (Figure 2.7B). The fertilized egg that contained the acrosomal matrix inside developed normally into a nymph. These results suggest that FAD is not released from the acrosomal matrix during the fertilization process or early development and is likely an important component of the acrosomal matrix.

## DISCUSSION

Our characterization of the *A. remigis* acrosome reveals a unique fluorescent molecule that becomes immobilized and oriented during spermiogenesis. To our knowledge, a bright fluorescence in the acrosome has not been previously reported in any other animal species. Acrosomes that are filled with tubular structures are also found in other Heteropteran species including *Corixa sp.*, *Hydrometra sp.*, and *Notonecta glauca* although their lengths vary substantially (Afzelius *et al.*, 1976; Dallai and Afzelius, 1980). Comparison among the sperm of these species may shed light on the evolution of the intrinsic fluorescence in the acrosome.

The apparent continuous filamentous structure of *A. remigis* sperm previously made it difficult to distinguish head and tail regions using brightfield microscopic methods. However, previous ultrastructural work using transmission electron microscopy revealed that the tail contains both two mitochondrial derivatives and a “9+9+2”

microtubule-containing axoneme (Tandler and Moriber, 1966), which are commonly observed in insect sperm (Jamieson *et al.*, 1999) and a head that contains an unusually long acrosome. Using the intrinsic fluorescence of the acrosome we confirmed that the acrosome is unusually long, is formed subsequent to meiosis, and is derived from a spherical organelle adjacent to the nucleus of spermatids.

Our deconvolution microscope identified two distinct domains of the 2500  $\mu\text{m}$  acrosome that contains a 300  $\mu\text{m}$  long helix with a 7  $\mu\text{m}$  repeat followed by a much longer linear extension. As far as we know, this long helical structure in the acrosome has not been reported previously. Since this structure enters an egg through a micropyle, the helical structure may facilitate its penetration through the micropyle.

Our results of FRAP and FPM suggest that the fluorescent molecule is incorporated into a tubular acrosomal matrix, and thus may play a functional role to form the tubular structure in the acrosome. The phenomenon of cellular intrinsic fluorescence has been reported previously in other cell types (Aubin, 1979; Benson *et al.*, 1979; Anderson *et al.*, 1998) with three major sources of intrinsic fluorescence in animal cells routinely identified: NADH, lipofuscin, and flavin. These are obvious candidates for the intrinsic fluorescence in the acrosome of *A. remigis*. Although the emission spectrum can be influenced by intracellular and environmental conditions to some degree, only flavin appears to be a viable candidate. The intrinsic fluorescence in *A. remigis* acrosome has an emission peak at 515 nm *in vivo*, while NADH has an emission peak at approximately 440 nm (Avi-Dor *et al.*, 1962). Lipofuscin, a pigment that is composed of a complex

mixture of lipids, metals, and organic molecules that result from oxidative degradation in lysosomes or mitochondria, has a broad emission spectrum with a peak at approximately 630 nm (Delori *et al.*, 1995; Brunk and Terman, 2002; Haralampus-Grynawski *et al.*, 2003). The most likely candidate here is flavin with an emission peak of approximately 520 nm that is excited by both ultraviolet and blue light (Weber, 1950; Kleiner *et al.*, 1999). This idea is further supported by the results of tricine-SDS-PAGE and *in vitro* fluorescence spectrophotometry. These results also suggest that the flavin-containing molecule is FAD but not riboflavin or FMN.

FAD exists in cells in isolation or as a prosthetic group of flavoproteins that are capable of catalyzing various oxidation-reduction reactions (Massey, 2000; Joosten and Berkel, 2007). Tricine-SDS-PAGE of the acrosomal matrix indicates that there are several proteins that form the acrosomal matrix. It is likely that FAD is associated with one of these proteins. If the fluorescence in the acrosome is due to FAD, it is unclear why the acrosome possesses a significant amount of FAD that is associated with the acrosomal matrix, which renders the matrix strongly fluorescent. Considering the redox ability of FAD, it is possible that this molecule may facilitate the formation of the acrosomal matrix through oxidation-reduction reactions. Since the acrosomal matrix is stabilized by disulfide bonds, there should be a molecule that accepts electrons caused by the disulfide bond formation in the acrosome. In other organelles such as endoplasmic reticulum and mitochondria, FAD is known to accept electrons caused by the disulfide bond formation (Riemer *et al.*, 2009).

Acrosomal proteins of mammalian species are also stabilized by disulfide bonds (Mate *et al.*, 1994; Westbrook-Case *et al.*, 1995, Kim *et al.*, 2001). Further, protein disulfide isomerase, which catalyzes the rearrangement of disulfide bonds, is expressed in the developing acrosome of rats (Ohtani *et al.*, 1993). It would be interesting to determine if the acrosome of these species also contains FAD. Although it is not reported that the acrosome of these species exhibits a flavin-like intense intrinsic fluorescence, it may contain less FAD than the *A. remigis* acrosome considering its much smaller size.

The functions of FAD in the acrosomal matrix remains to be determined, but this intrinsic fluorescence can be used as a marker for the *A. remigis* acrosome to follow its fate subsequent to fertilization. Using this intrinsic fluorescence, we observed that the unusually long acrosomal matrix remained associated with the sperm during the fertilization process. This observation suggests that this long acrosome may play a structural role during the passage of the sperm through the female reproductive tract. A part of the *A. remigis* female reproductive tract is narrow ( $\approx 12 \mu\text{m}$  in diameter) and tightly wound (Campbell and Fairbairn, 2001). It seems difficult for the long, relatively rigid acrosome to pass through this tightly winding region of the female reproductive tract. This structure may be stretched and straightened by females to ensure that the sperm with the long acrosomal matrix can move through this region. In model species such as mice and *Drosophila*, their acrosome is very small compared to that of *A. remigis* and is not known to play a structural role during the passage of a female reproductive tract. Our observation also suggests that it is unlikely that the long acrosomal matrix contributes to physiological processes within the fertilized egg during the early development because



the acrosomal matrix remained structurally intact even after gastrulation had started. The acrosomal matrix may not be used by the embryo and may be expelled into a midgut as it is suggested for the fate of mitochondrial derivatives in *Drosophila* (Pitnick and Karr, 1998). Alternatively, it is possible that the matrix is degraded and used as nutrition by the embryo.

In summary, our study describes a novel phenomenon in which the *A. remigis* acrosome possesses an intrinsically fluorescent molecule with properties similar to those of FAD that becomes immobilized and aligned during the acrosome formation. Further, utilizing the intrinsic fluorescence, we observed that the fluorescent acrosomal matrix remained structurally intact in the embryo during the early development. Further detailed investigations on the fluorescent molecule of the *A. remigis* sperm will provide an insight into the mechanisms of the acrosomal matrix formation.

## CHAPTER 2: REFERENCES

- Afzelius B.A., Baccetti B. and Dallai R. (1976): The giant spermatozoon of *Notonecta*. J Submicrosc Cytol. 8, 149-61.
- Anderson H., Baechi T., Hoechl M. and Richter C. (1998): Autofluorescence of living cells. J Microsc. 191, 1-7.
- Aubin J.E. (1979): Autofluorescence of viable cultured mammalian cells. J Histochem Cytochem. 27, 36-43.
- Avi-Dor Y., Olson J.M., Doherty M.D. and Kaplan N.O. (1962): Fluorescence of pyridine nucleotides in mitochondria. J Biol Chem. 237, 2377-83.
- Axelrod D. (1979): Carbocyanine dye orientation in red cell membrane studied by microscopic fluorescence polarization. Biophys J. 26, 557-73.
- Benson R.C., Meyer R.A., Zaruba M.E. and McKhann G.M. (1979): Cellular autofluorescence -- Is it due to flavins? J Histochem Cytochem. 27, 44-8.
- Brunk U.T. and Terman A. (2002): Lipofuscin: mechanisms of age-related accumulation and influence on cell function. Free Radic Biol Med. 33, 611-9.
- Bessey O.A., Lowry O.H. and Love R.H. (1949): The fluorometric measurement of the nucleotides of riboflavin and their concentration in tissues. J Biol Chem. 180, 755-69.
- Campbell V. and Fairbairn D.J. (2001): Prolonged copulation and the internal dynamics of sperm transfer in the water strider *Aquarius remigis*. Can J Zool. 79, 1801-12.
- Dallai R. and Afzelius B.A. (1980): Characteristics of the sperm structure in Heteroptera (Hemiptera, Insecta). J Morphol. 164, 301-9.
- Delori F.C., Dorey C.K., Staurenghi G., Arend O., Goger D.G. and Weiter J.J. (1995): In vivo fluorescence of the ocular fundus exhibits retinal pigment epithelium lipofuscin characteristics. Invest Ophthalmol Vis Sci. 36, 718-29.
- Fujimoto D. (1977): Isolation and characterization of a fluorescent material in bovine achilles tendon collagen. Biochem Biophys Res Commun. 76, 1124-9.
- Haralampus-Grynaviski N.M., Lamb L.E., Clancy C.M.R., Skumatz C., Burke J.M., Sarna T. and Simon J.D. (2003): Spectroscopic and morphological studies of human retinal lipofuscin granules. Proc Natl Acad Sci USA. 100, 3179-84.

- Inoue S., Shimomura O., Goda M., Shribak M. and Tran P.T. (2002): Fluorescence polarization of green fluorescence protein. *Proc Natl Acad Sci USA*. 99, 4272–7.
- Jamieson B.G.M., Dallai R. and Afzerius B.A. (1999): *Insects: Their spermatozoa and phylogeny*. USA: Science Publishers. p 1-23.
- Joosten V. and van Berkel W.J. (2007): Flavoenzymes. *Curr Opin Chem Biol*. 11, 195-202.
- Kim K., Cha M.C. and Gerton G.L. (2001): Mouse sperm protein sp56 is a component of the acrosomal matrix. *Biol Reprod*. 64, 36-43.
- Kleiner O., Butenandt J., Carell T. and Batschauer A. (1999): Class II DNA photolyase from *Arabidopsis thaliana* contains FAD as a cofactor. *Eur J Biochem*. 264, 161-7.
- Margaritis L.H. (1985): Structure and physiology of the insect eggshell. In: Kerkut GA, Gilbert LI, Editors. *Comprehensive insect physiology, biochemistry and pharmacology*, Vol. 1. Elmsford NY:Pergamon. p 153-230.
- Massey V. (2000): The chemical and biological versatility of riboflavin. *Biochem Soc Trans*. 28, 283-96.
- Mate K., Kosower N.S., White I.G. and Rodger J.C. (1994): Fluorescent localization of thiols and disulfides in marsupial spermatozoa by bromobimane labelling. *Mol Reprod Dev*. 37, 318–25.
- Neill A.T. and Vacquier V.D. (2004): Ligands and receptors mediating signal transduction in sea urchin spermatozoa. *Reproduction*. 127, 141-9.
- Ohtani H., Wakui H., Ishino T., Komatsuda A. and Miura A.B. (1993): An isoform of protein disulfide isomerase is expressed in the developing acrosome of spermatids during rat spermiogenesis and is transported into the nucleus of mature spermatids and epididymal spermatozoa. *Histochemistry*. 100, 423-9.
- Oldenbourg R. and Mei G. (1995): New polarized light microscope with precision universal compensator. *J Microsc*. 180, 140-7.
- Pena A.M., Strupler M., Boulesteix T., Godeau G. and Schanne-Klein M.C. (2005): Spectroscopic analysis of keratin endogenous signal for skin multiphoton microscopy. *Opt Express*. 13, 6268-74.
- Phair R.D., Gorski S.A. and Misteli T. (2004): Measurement of dynamic protein binding to chromatin *in vivo*, using photobleaching microscopy. *Methods Enzymol*. 375, 393–414.

- Pitnick S. and Karr T.L. (1998): Paternal products and by-products in *Drosophila* development. Proc R Soc Lond B. 265, 821-6.
- Pollister A.W. (1930): Cytoplasmic phenomena in the spermatogenesis of *Gerris*. J Morphol. 49, 455-507.
- Preziosi R.F. and Fairbairn D.J. (1992): Genetic population structure and levels of gene flow in the stream-dwelling waterstrider, *Aquarius* (= *Gerris*) *remigis* (Hemiptera: Gerridae). Evolution. 44, 430-40.
- Riemer J., Bulleid N. and Herrmann J.M. (2009): Disulfide formation in the ER and mitochondria: two solutions to a common process. Science. 324, 1284-7.
- Rubenstein D.I. (1987): Sperm competition in the water strider, *Gerris remigis*. Anim Behav. 38, 631-6.
- Schäagger H. and von Jagow G. (1987): Tricine-sodium dodecyl sulfate-polyacrylamide gel electrophoresis for the separation of proteins in the range from 1 to 100 kDa, Anal Biochem. 166, 368-79.
- Shribak M. and Oldenbourg R. (2003): Techniques for fast and sensitive measurements of two-dimensional birefringence distributions. Appl Opt. 42, 3009-17.
- Tandler B. and Moriber L.G. (1966): Microtubular structures associated with the acrosome during spermiogenesis in the Water-strider, *Gerris remigis* (Say). J Ultrastruct Res. 14, 391-404.
- Triplehorn C.A. and Johnson N.F. (2005): Borror and DeLong's introduction to the study of insects. Belmont CA:Thompson Brooks/Cole. p 864.
- Vrabioiu A.M. and Mitchison T.J. (2006): Structural insights into yeast septin organization from polarized fluorescence microscopy. Nature. 443, 466-9.
- Weber G. (1950): Fluorescence of riboflavin and flavin-adenine dinucleotide. Biochem J. 47, 114-21.
- Westbrook-Case V.A., Winfrey V.P. and Olson G.E. (1995): Sorting of the domain-specific acrosomal matrix protein AM50 during spermiogenesis in the guinea pig. Dev Biol. 167, 338-49.
- Wilson K.L., Fitch K.R., Bafus B.T. and Wakimoto B.T. (2006): Sperm plasma membrane breakdown during *Drosophila* fertilization requires Sneaky, an acrosomal membrane protein. Development. 133, 4871-9.

Wu Y. and Qu J.Y. (2006): Autofluorescence spectroscopy of epithelial tissues. *J Biomed Opt.* 11, 054023.

Wu Y., Xi P., Qu J.Y., Cheung T.H. and Yu M.Y. (2004): Depth-resolved fluorescence spectroscopy reveals layered structure of tissue. *Opt Express.* 12, 3218-23.

Yanagimachi R. (1994): Mammalian fertilization. In: Knobil E and Neill JD, editors. *The physiology of reproduction.* New York: Raven Press. p 189-317.

## FIGURE LEGENDS

**Figure 2.1** Morphology of mature *A. remigis* sperm. **(A)** A schematic drawing showing the major features of water strider sperm. The sperm contains a 2500  $\mu\text{m}$  linear tail structure and a complex head region separated by a 5  $\mu\text{m}$  nucleus. The head region consists of a 300  $\mu\text{m}$  periodic structure followed by a 2200  $\mu\text{m}$  thinner, linear apical region. Both of these structures in the head region contain a fluorescent molecule. **(B)** Panels on the left are DIC images with corresponding fluorescence images in the right panels using a GFP filter set. Top. The region of the head proximal to the nucleus contains a regularly periodic fluorescent structure that extends for 300  $\mu\text{m}$ . Bottom. The head region consists of both the 300  $\mu\text{m}$  periodic structure and a thinner linear region. The contrast of the fluorescence image is enhanced to show the presence of fluorescence in the thinner linear region.  $h_p$ , periodic region of the head;  $h_l$ , linear region of the head;  $n$ , nucleus;  $t$ , tail. Scale bars = 10  $\mu\text{m}$ .

**Figure 2.2** The periodic structure of the water strider sperm head is a helix. **(A)** A schematic drawing showing the water strider acrosome. The periodic structure is helical with a pitch of approximately 7  $\mu\text{m}$ . **(B)** Images of the periodic structure from a sperm head in the X-Z projected plane (left panel) and Y-Z projected plane (right panel). Scale bar = 5  $\mu\text{m}$ . **(C)** Z-sections down the shaft of the periodic structure reveal that it rotates about a central axis to form a helix. The panels from left to right are successive images moving toward the nucleus. Scale bar = 1  $\mu\text{m}$ .

**Figure 2.3** The fluorescent signal in the sperm head appears during spermatogenesis and is localized to the acrosome in spermatids. Panels on the left are DIC images with corresponding fluorescence images (a GFP filter set) on the right. **(A)** A mid-stage spermatid shows that the fluorescent signal originates in the spherical acrosome. **(B)** A condensing spermatid with associated fluorescence in the elongating acrosome. **(C)** Top. The periodic structure is bundled together with adjacent sperm when they are stored in the testis. Bottom. Bundled sperm showing both the periodic and linear regions of the sperm head.  $a_c$ , core region of the acrosomal vesicle;  $a_s$ , sheath region of the acrosomal vesicle;  $ba$ , basal body of the acrosome;  $h_p$ , periodic region of the head;  $h_l$ , linear region of the head;  $n$ , nucleus;  $t$ , tail. Scale bars = 10  $\mu\text{m}$ .

**Figure 2.4** The fluorescent molecule becomes immobilized during spermiogenesis. **(A)** FRAP analysis was performed on the acrosome of a round spermatid (RS) and a mature sperm bundle (MS). Panels on the left are images before photobleaching with corresponding images just after photobleaching in the middle and plots of fluorescence recovery on the right. Red rectangles in the pre-bleach images show the areas of photobleaching. Scale bars = 10  $\mu\text{m}$ . **(B)** An isolated acrosomal matrix still exhibits a bright fluorescence. A panel on the left is a DIC image with a corresponding fluorescence image (a GFP filter set) on the right. Scale bar = 5  $\mu\text{m}$ .

**Figure 2.5** The intrinsic fluorescence of mature sperm exhibits strong anisotropy. Fluorescence polarization microscopy was performed on the acrosome of fixed mature sperm. **(A)** A DIC image of the acrosome. Scale bar = 5  $\mu\text{m}$ . **(B)** An image showing

fluorescence polarization ratios for each pixel as indicated in the grayscale bar. High polarization ratios were observed in the acrosome. A white square shows the area magnified for C. (C) A magnified image showing azimuth angles with red lines. The azimuth angle is nearly perpendicular to the long axis of the acrosome.

**Figure 2.6** Properties of the fluorescent molecule in the matrix are similar to those of FAD. (A) A sperm bundle from the testis (white circle) and 1 mM FAD (black circle) were imaged with a confocal microscope using an excitation wavelength of 351 nm. An emission spectrum was collected from 410 nm to 650 nm with a maximum wavelength of 515 nm for the fluorescent signal of the acrosome and 530 nm for FAD. (B) An isolated acrosomal matrix, riboflavin, FMN and FAD were subjected to tricine-SDS-PAGE and the fluorescent signals were detected. The gel was also stained for proteins. Mr, molecular weight. (C, D) Emission (C) and Excitation (D) spectra of the acrosomal matrix that was solubilized by the addition of  $\beta$ -mercaptoethanol were determined at pH 2.5 (red line) and pH 7.1 (blue line) using a fluorescence spectrophotometer. The spectra were matched with those of FAD at pH 2.5 (green line).

**Figure 2.7** The fate of the fluorescent molecule associated with the acrosomal matrix during the fertilization process and early development. Helical regions of the acrosome were observed in a fertilized egg (A) and an embryo that underwent gastrulation (B). Panels on the left are bright field images with fluorescence images (a GFP filter set) on the right. Black squares show the area magnified for the fluorescence images. An



arrowhead indicates the region where invagination occurred. Scale bars for bright field images = 100  $\mu\text{m}$  and fluorescence images = 10  $\mu\text{m}$ .

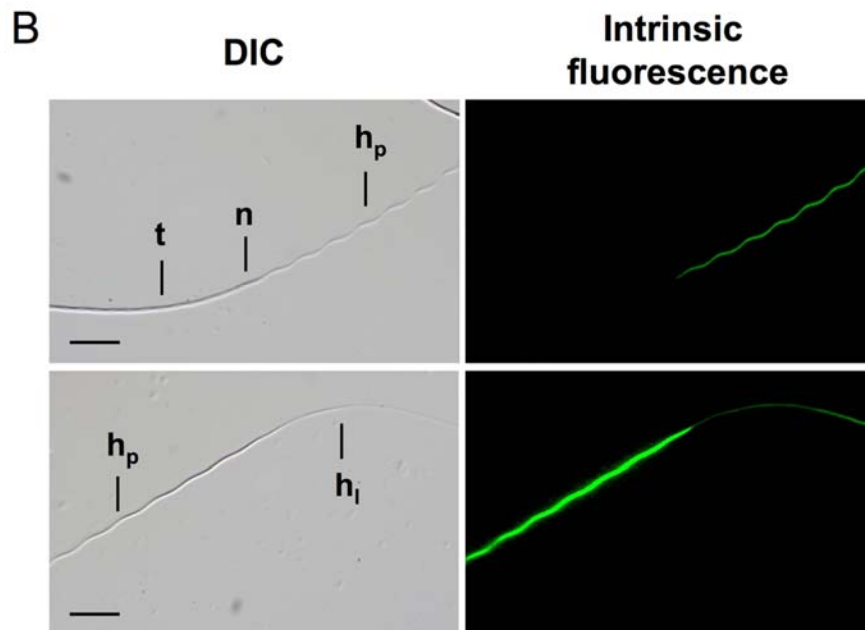
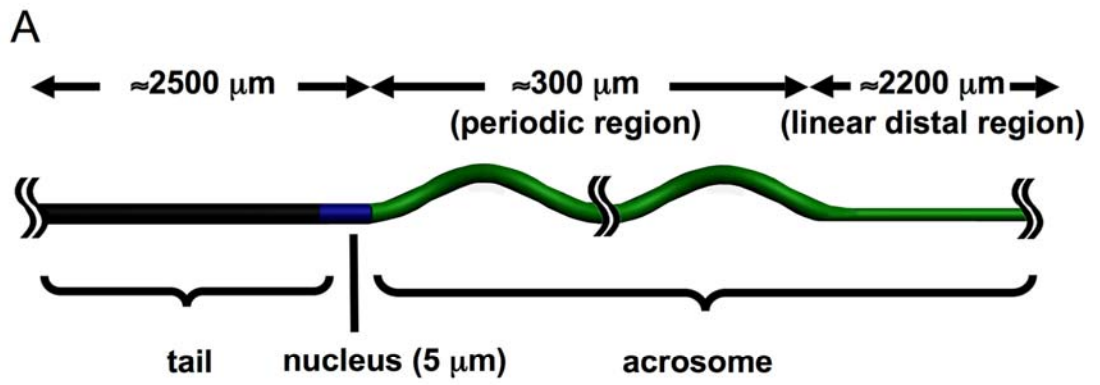


Figure 2.1 Morphology of mature *A. remigis* sperm.

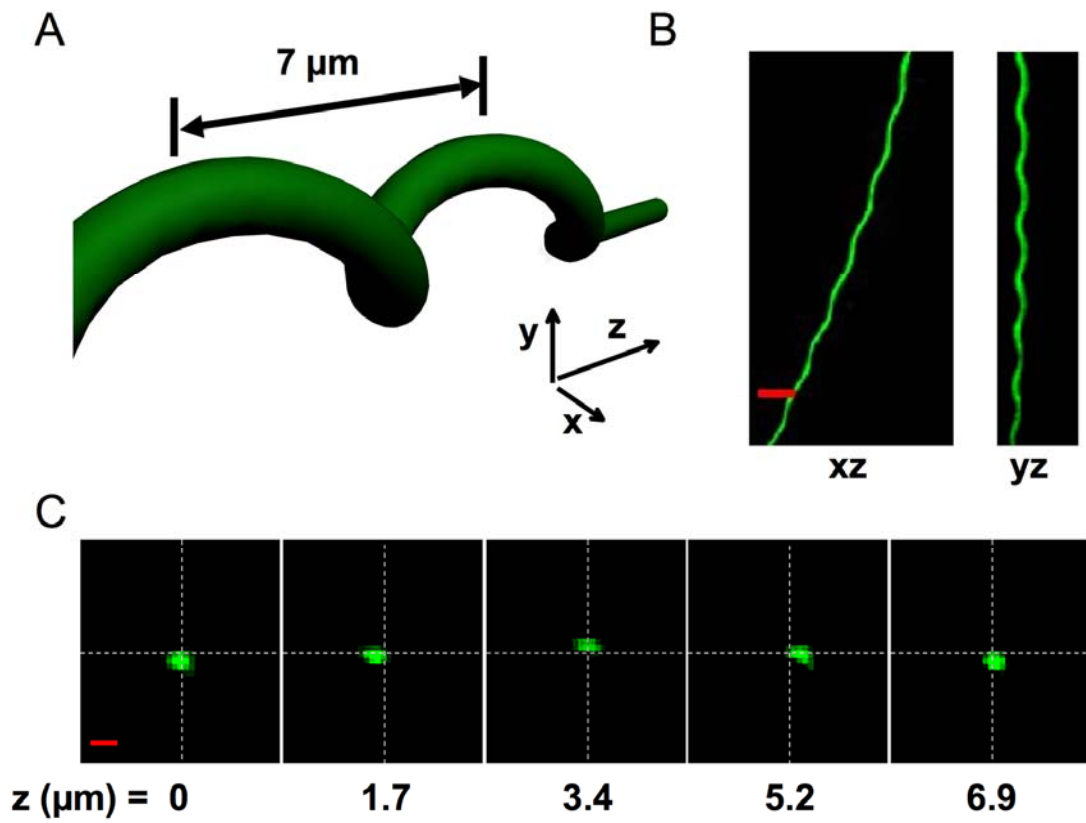


Figure 2.2 The periodic structure of the water strider sperm head is a helix.

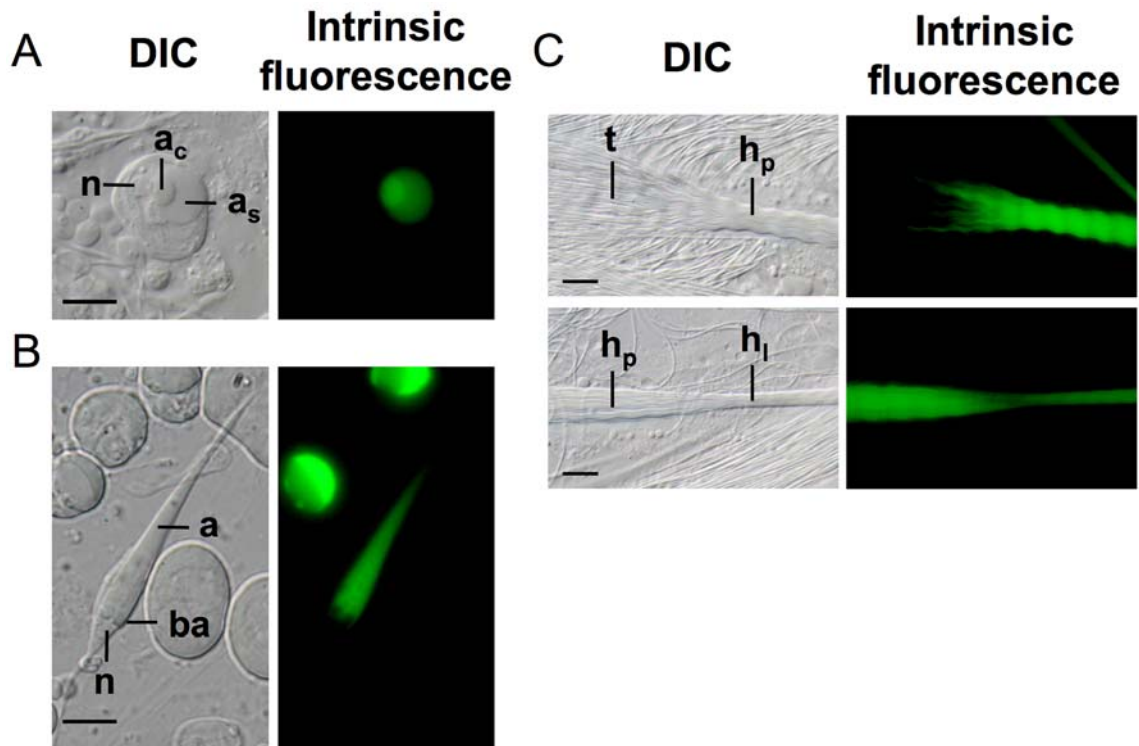


Figure 2.3 The fluorescent signal in the sperm head appears during spermatogenesis and is localized to the acrosome in spermatids.

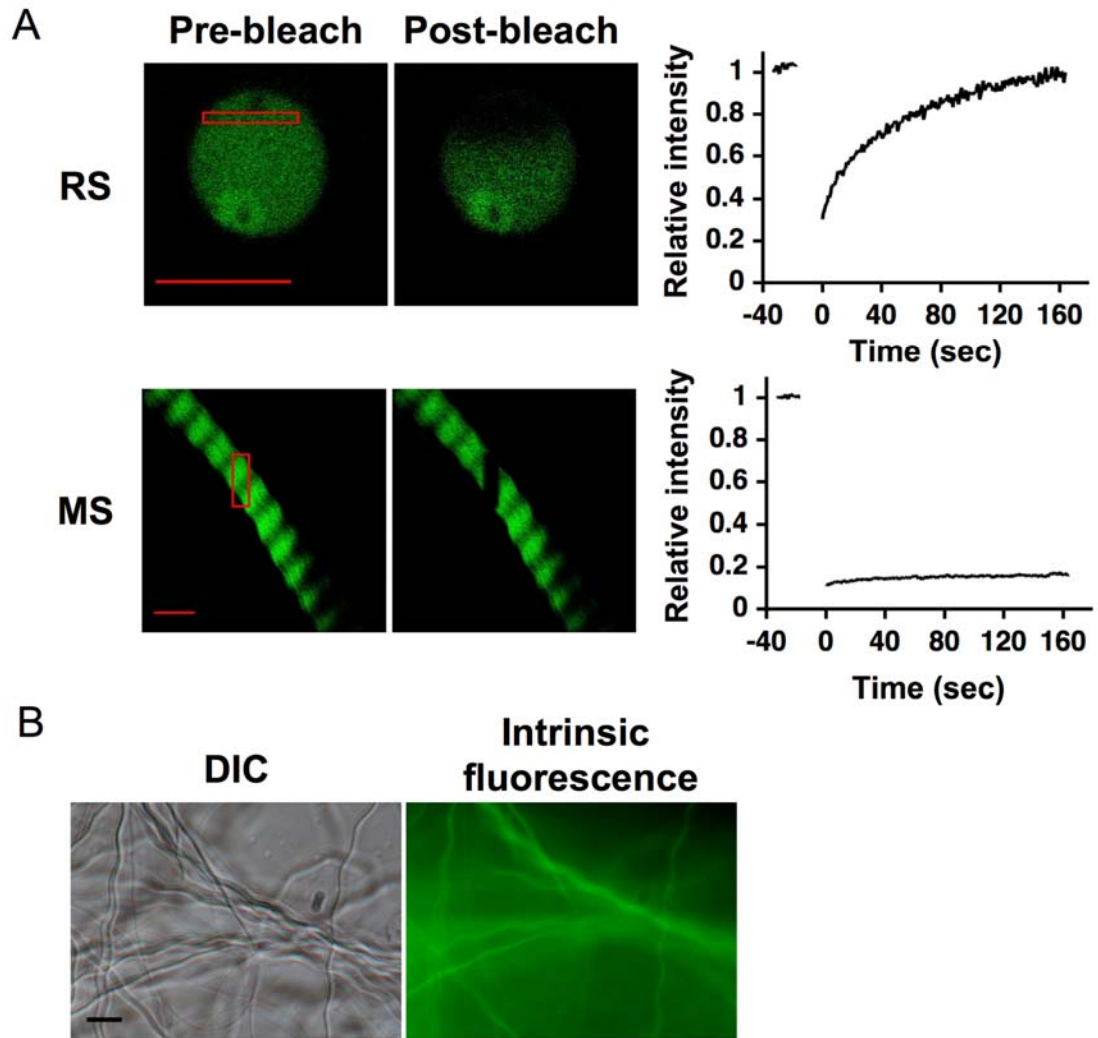


Figure 2.4 The fluorescent molecule becomes immobilized during spermiogenesis.

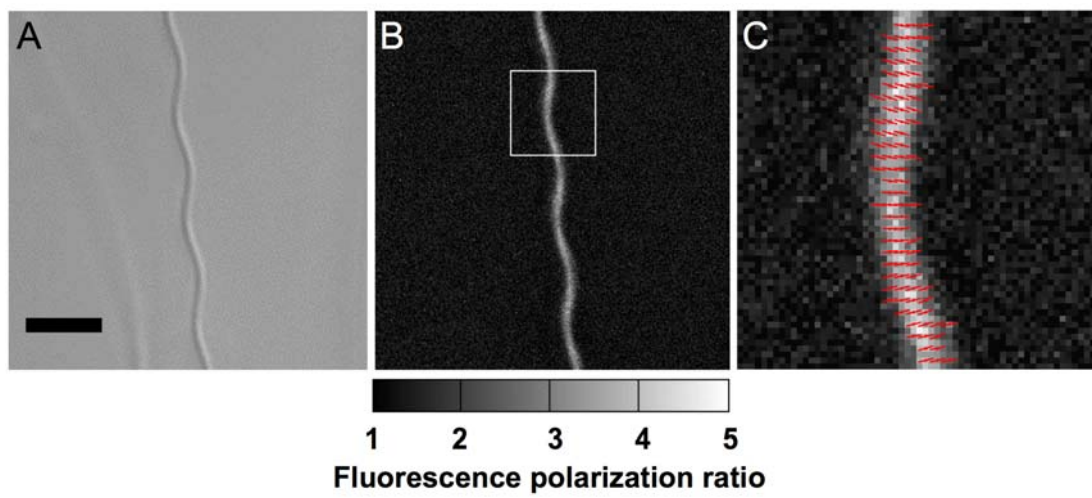


Figure 2.5 The intrinsic fluorescence of mature sperm exhibits strong anisotropy.

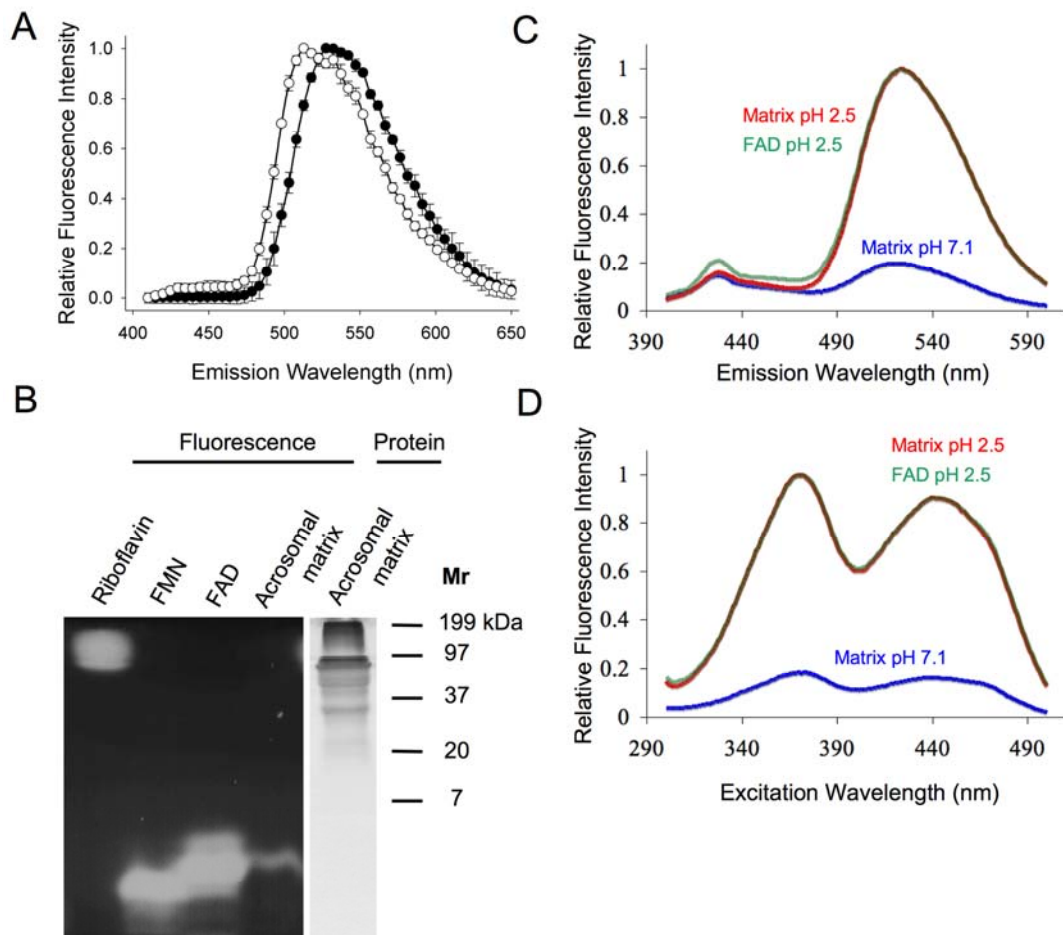


Figure 2.6 Properties of the fluorescent molecule in the matrix are similar to those of FAD.

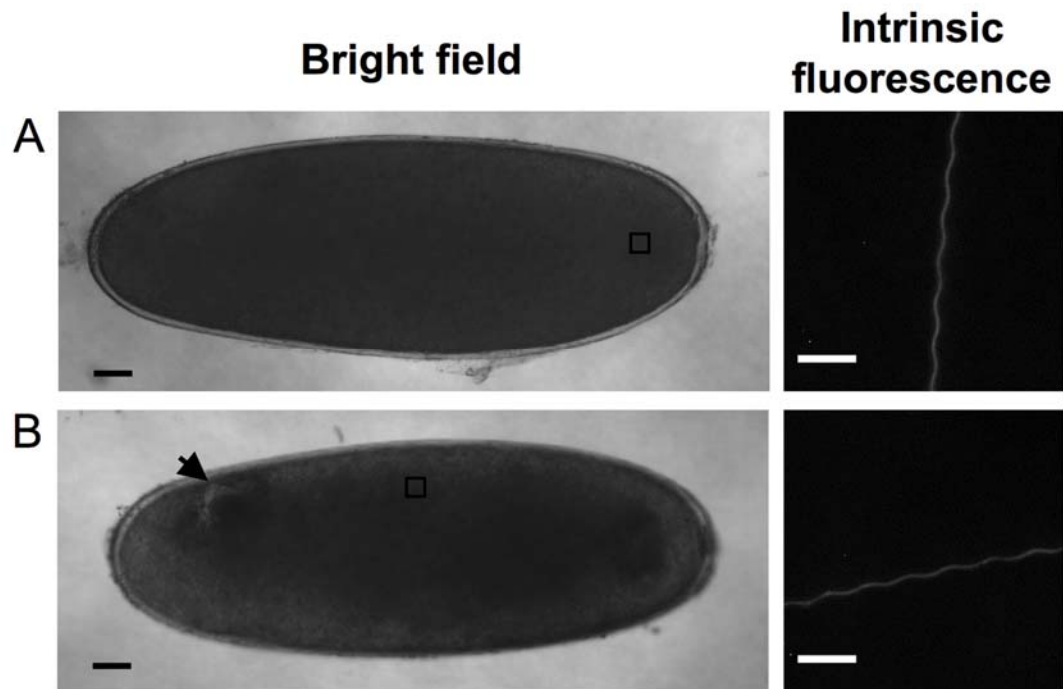


Figure 2.7 The fate of the fluorescent molecule associated with the acrosomal matrix during the fertilization process and early development.



## CHAPTER 3

THE UNIQUE STRUCTURE OF THE SPERM FLAGELLUM FROM THE WATER  
STRIDER, *AQUARIUS REMIGIS*, RESULTS IN COMPLEX MOTILITY BEHAVIOR  
THAT IS INITIATED BY A PROTEASE AND REGULATED BY  
PHOSPHORYATION

## ABSTRACT

*Aquarius remigis* (Order Hemiptera) is a common and abundant semi-aquatic water strider found throughout North America. The *A. remigis* sperm possesses an unusually long and rigid acrosome ( $\approx 2.5$   $\mu\text{m}$ ), which comprises about half of the total length of sperm and therefore may affect sperm motility. However, little is known about *A. remigis* sperm motility. Here, we describe a novel flagellar motility exhibited by the *A. remigis* sperm *in vitro*. The flagellum loops back upon itself and forms a coil, and this structure can then zipper and undergo forward progressive motility with the loop acting as the anterior end. In addition, a sperm flagellum fixed in this zippered configuration has been observed in the female spermathecal tube, as well as fertilized eggs, suggesting that this unusual motility may also occur *in vivo*. *A. remigis* sperm are quiescent in the seminal vesicles, but sperm motility can be initiated by trypsin or a phosphatase inhibitor such as calyculin A or okadaic acid. Further, the broad spectrum kinase inhibitor staurosporine blocks the sperm motility initiation by trypsin. These results suggest that quiescence is maintained by high levels of endogenous phosphatase activity and that protein phosphorylation by one or more kinases is required to activate sperm motility. A kinase that is involved in regulating sperm motility is sensitive to the mitogen-activated protein kinase kinase inhibitor U0126 and its target may be a 46 kDa protein that is localized to the axoneme. Moreover, we observed a protease-activated receptor 2 (PAR2)-like protein in the tail. It is suggested that activation of this receptor may initiate a signaling cascade in the cell in response to trypsin.

## INTRODUCTION

Sperm motility and other behaviors are generally initiated and maintained by a variety of extracellular cues (Yoshida *et al.*, 2008). In well-studied systems such as sea urchins and mice, protein phosphorylation of key intracellular proteins is an important mechanism that activates sperm in response to chemical cues (Visconti and Kopf, 1998; Darszon *et al.*, 1999; Urner and Sakkas, 2003; Neill and Vacquier, 2004). In these species, changes in protein phosphorylation are regulated by various kinases and phosphatases that are activated by second messengers, including  $\text{Ca}^{2+}$ , cAMP and/or cGMP (Visconti and Kopf, 1998; Darszon *et al.*, 1999; Urner and Sakkas, 2003; Neill and Vacquier, 2004). Although these signaling pathways have been extensively studied in model animal systems, little is known about the molecular mechanisms that regulate motility in insect sperm.

Activation of sperm motility in insects has been studied mainly in the silkworm *Bombyx mori* (Order Lepidoptera). These Saturniid moths produce both eupyrene and apyrene sperm, and both are immotile in the seminal vesicles. When the sperm are ejaculated into a spermatophore, apyrene sperm motility is initiated by initiatorin, a trypsin-like protease that is secreted from the prostatic gland (Aigaki *et al.*, 1987; Aigaki *et al.*, 1994). Initiatorin activates apyrene sperm motility by catalyzing the hydrolysis of glycoproteins in the sperm membrane and forming micropores through which macromolecules can enter the cell (Osanai and Kasuga, 1990). The activator of apyrene sperm may be cAMP which can enter the sperm through these micropores (Osanai *et al.*,

1989; Osanai and Kasuga, 1990). However, little is known about the signaling pathways downstream of cAMP mobilization. Initiatorin also facilitates dissociation of eupyrene sperm bundles (Katsuno, 1977; Osanai *et al.*, 1986) and degrades proteins in the spermatophore to supply an energy source that supports flagellar motility (Kasuga *et al.*, 1987; Osanai *et al.*, 1987). Activation of sperm motility by a trypsin-like protease has also been reported in the moth *Manduca sexta* (Order Lepidoptera) (Friedländer *et al.*, 2001).

Trypsin initiation of sperm motility has been reported in some Orthopteran species that have only one type of sperm (Osanai and Baccetti, 1993). Similar to Lepidopterans, motility in Orthopteran species is initiated by trypsin and enhanced by cAMP (Osanai and Baccetti, 1993). Since sperm motility activation by a trypsin-like protease has been observed in both holometabola (Lepidoptera) and hemimetabola (Orthoptera), this mechanism may represent a common and evolutionary conserved mechanism in insects (Osanai and Baccetti, 1993). However, since both Lepidopterans and Orthopterans form a spermatophore where trypsin activation occurs, whether this mechanism is used by insects that do not form a spermatophore is unclear (Osanai and Baccetti, 1993).

*Aquarius remigis* (Order Hemiptera) is a common and abundant semi-aquatic water strider found throughout North America (Preziosi and Fairbairn, 1992) and mating behavior and sperm transfer into the female reproductive tract have been studied previously (Pollister, 1930; Rubenstein, 1989; Weigensberg and Fairbairn, 1994;

Arnqvist, 1997; Campbell and Fairbairn, 2001). Females mate with many males and are able to store sperm in the spermathecal tubes for at least 3 weeks prior to fertilization (Rubenstein, 1989, Campbell and Fairbairn, 2001). Males do not form a spermatophore and produce only one type of sperm, which is extremely long ( $\approx 5$  mm) (Pollister, 1930). Further, the *A. remigis* sperm has an unusually long acrosome (2.5 mm), which comprises approximately half of the total length of the sperm (Tandler and Moriber, 1966, Miyata *et al.*, 2010). This unusually long and rigid acrosome may affect sperm motility. However, the characteristics and regulation of sperm motility in *A. remigis* have not been examined previously. In the present study, we report that *A. remigis* sperm are activated by proteases such as trypsin and papain, and exhibit a unique motility behavior that, to the best of our knowledge, has not been reported previously in other insects. A molecular mechanism underlying this unique motility will be discussed. Further, we have investigated the signaling events that are involved in the regulation of the water strider sperm motility.

## **MATERIALS AND METHODS**

### **Chemicals**

H-8, H-89, Staurosporine, U-126 and 8-bromo-cAMP were purchased from BioMol (Plymouth Meeting, PA). BAPTA-AM, A23187, bisindolylmaleimide I (BIM), KN-62, thapsigargin, 8-bromo-cGMP, calyculin A, and okadaic acid were obtained from Alexis Biochemicals (Plymouth Meeting, PA). Go 6983 was purchased from Tocris Bioscience (Ellisville, MO). Trypsin, papain, thrombin and PNGaseF were purchased

from Sigma-Aldrich (St. Louis, MO). All other reagents were obtained from Sigma-Aldrich or Fisher Scientific (Pittsburgh, PA).

## **Animals**

Sexually mature *A. remigis* males were housed at room temperature in tanks partially filled with water. Styrofoam cups were provided for shelter, and animals were fed daily, ad libitum, with frozen crickets. Tanks were cleaned weekly.

## **Sperm collection**

Adult males were euthanized with chloroform and the seminal vesicles were dissected out and held in insect Ringer's (110 mM NaCl, 5 mM KCl, 0.5 mM CaCl<sub>2</sub>, 1.2 mM MgCl<sub>2</sub>, 1.2 mM MgSO<sub>4</sub>, 1.2 mM NaHCO<sub>3</sub>, 2 mM KH<sub>2</sub>PO<sub>4</sub>, 1 mM glucose, 20mM Hepes, pH 7.4) or Phosphate Buffered Saline (PBS, 10 mM Na<sub>2</sub>HPO<sub>4</sub>, 2 mM NaH<sub>2</sub>PO<sub>4</sub>, 135 mM NaCl, pH 7.2) until use for motility assays and/or Western blot samples. Mature sperm were obtained by teasing away the seminal vesicle tissue in PBS.

## **Sperm Fixation and Processing for Fluorescent Labeling**

### Staining of mitochondria

Mature sperm that were activated with 20 µg/mL trypsin were stained with 500 nM Mitotracker Red CMXRos (Molecular Probes, Eugene, OR) in PBS for 45 min at room temperature. Sperm were washed in PBS 3 times for 5 min each, mounted on a

slide, and viewed using a Zeiss Axiovert 10 microscope (Carl Zeiss, Inc., Thornwood, NY).

#### Staining of filamentous actin

Mature sperm were fixed with 4% formaldehyde in PBS for 10 min, permeabilized with 1 % Triton X-100 for 5 min and blocked with 5% BSA for 1 h. Sperm were incubated with tetramethylrhodamine B isothiocyanate conjugated phalloidin (Phalloidin-TRITC, Sigma-Aldrich, 1:200 dilution), washed in PBS 3 times for 5 min each, mounted on a slide, and viewed using a Zeiss Axiovert 10 microscope.

#### Indirect immunofluorescence localization of tubulin, actin and MPM-2 epitopes

The sperm were rinsed 3 times in PBS, and fixed according to Pisano *et al.* (1993) with minor modifications. Briefly, mature sperm were placed in a drop of PBS on a glass slide and covered with a cover slip. The slide was then frozen on an aluminum block on dry ice and, after removal of the cover slip with a razor blade, was immersed in methanol for 5 min at -20 °C, followed by immersion in acetone for 2 min at -20 °C. The slide was dried for 1 min at room temperature, immersed in PBS containing 1% Triton X-100 and 0.5% acetic acid for 10 min at room temperature, and finally washed 3 times in PBS for 5 min each time.

Slides with fixed sperm were immersed in a blocking solution (5% goat serum, 1% BSA, 0.1% Triton X-100, 0.05% Tween-20 and 0.05% sodium azide) for 1 h at room temperature. The slide was then incubated with a solution containing 1% BSA and a

primary antibody specific for tubulin (E7, supernatant, 1:5 dilution, Developmental Studies Hybridoma Bank at the University of Iowa, Iowa City, IA or Sigma-Aldrich T3526, 1:200 dilution), actin (1:40 dilution, Sigma-Aldrich A2066) and/or MPM-2 (Millipore, Billerica, MA, 10 µg/mL) for 1 h at room temperature. After washing 3 times in PBS for 5 min each, the samples were incubated with an Alexa Fluor 488-conjugated secondary antibody and/or an Alexa Fluor 594-conjugated secondary antibody (10 µg/mL, Molecular Probes) for 1 h at room temperature and washed 3 times in PBS for 5 min each. Samples were mounted with one drop of Vectashield mounting medium (Vector Laboratories, Burlingame, CA). Imaging of the sample was performed using a Zeiss Axiovert 10 microscope or an Olympus IX-71 microscope equipped with deconvolution software (DeltaVision, Applied Precision, Issaquah, WA).

#### Indirect immunofluorescence localization of PAR2

Mature sperm were fixed with 1% formaldehyde in PBS for 10 min and blocked with 5% BSA for 1 h. The sperm were then incubated with a solution containing 1% BSA and a primary antibody specific for PAR2 (SAM-11, Santa Cruz Biotechnology, Santa Cruz, CA, 20 µg/mL) for 1 h at room temperature. After washing 3 times in PBS for 5 min each, the sperm were incubated with an Alexa Fluor 594-conjugated secondary antibody (10 µg/mL, Molecular Probes) for 1 h at room temperature and washed 3 times in PBS for 5 min each. Samples were mounted with one drop of Vectashield mounting medium containing DAPI (Vector Laboratories). Imaging of the sample was performed using a Leica SP2 confocal microscope.



## **Motility Assays**

Non-motile sperm were teased away from the seminal vesicle tissue and incubated in PBS. Sperm were observed at 100x magnification using a Nikon Labphot microscope with phase contrast or dark-field optics and images recorded using Scion image with a DAGE-MTI CCD100 camera (DAGE-MTI, Michigan City, IN), or with Simple PCI (Hamamatsu, Corp., Bridgewater, NJ) using a Hamamatsu CCD camera. Sperm were treated with various reagents to activate or inhibit motility and the extent of motility was quantified using a rank scale (Table 3.1).

### Activators of Motility

Trypsin (20  $\mu\text{g}/\text{mL}$ ) was used as the control activator of motility and normally produced full motility (3 on the rank scale, Table 3.1) with a lag time of approximately 2 min. Non-motile sperm freshly dissected from a seminal vesicle were incubated with various concentrations of compounds being tested for their ability to activate motility, as indicated in the Results, and observed for 5-10 min. The extent of motility and the time to reach the greatest extent of motility (lag time) were recorded. At the end of the observation period, sperm were treated with trypsin to verify that the sperm were capable of fully activated motility.

### Inhibitors of Motility

Two approaches were used to examine the effects of potential inhibitors of motility on seminal vesicle sperm. In the first approach, non-motile sperm were pre-

incubated with an inhibitor for 10 or 30 min, as indicated. The sperm were then incubated with trypsin, in the continued presence of the inhibitor, and motility was observed for 5-10 min. The extent of motility was recorded. In the second approach, non-motile sperm were activated with trypsin and, after motility was fully activated (5 min), the inhibitor was added, in the continued presence of trypsin. Motility was observed and the length of time for 50% of the sperm to become immotile (half-time of inhibition) was recorded. Sperm treated with trypsin alone remained fully motile for at least 45 min.

### **Western Blots**

Samples were separated on SDS-PAGE gels (Figure 3.1, 15%; Figure 3.7, 10%) and blotted onto nitrocellulose. Blots were blocked with Blotto (5% non-fat dried milk, 0.1% Tween-20, in TBS). A monoclonal anti-tubulin (E7, 1:500 dilution, Developmental Studies or Sigma-Aldrich T5201, 1:200 dilution), a polyclonal anti-actin (Sigma-Aldrich A2066, 1:200 dilution), anti-MPM-2 (Millipore, 5 µg/mL) or anti-ERK1/2 (Cell Signaling Technology, Danvers, MA, 1:1,000 dilution) were used with horseradish peroxidase labeled goat anti-mouse (Bio-Rad Laboratories, Hercules, CA, 170-6616, 1:10,000 dilution) and goat anti-rabbit (Santa Cruz Biotechnology, 0.4 µg/mL) as the secondary antibodies. Signals were detected with ECL (Figure 3.1, Pierce West Femto, Thermo Scientific, Rockford, IL; Figure 3.7, Amersham ECL Plus, GE Healthcare, Piscataway, NJ).

## **Statistical Analysis**

At least three independent experiments were performed for all motility assays. The numbers of experiments are indicated in the Figure Legends. Significant differences were determined using KaleidaGraph (Synergy Software, Reading, PA). Specific tests are indicated in the Figure Legends.  $P < 0.05$  was considered significant (student's t-test).

## **RESULTS**

### **Sperm Tail Morphology**

Like many insect sperm, *A. remigis* are extremely long, approximately 5 mm. However, in contrast to other extremely long insect sperm, half of the length of the water strider sperm consists of the head (containing the acrosome and nucleus) and the remaining half consists of the flagellum (Tandler and Moriber, 1966, Miyata *et al.*, 2010). Previous ultrastructural studies using transmission electron microscopy revealed that the flagellum contains two mitochondrial derivatives and a “9+9+2” axoneme (Tandler and Moriber, 1966), which are commonly observed in insect sperm (Jamieson *et al.*, 1999; Werner and Simmons, 2008). To confirm that these structures could be observed in the flagellum using fluorescence microscopy, we stained tubulin and mitochondria using anti-tubulin and Mitotracker Red CMXRos, respectively. Rather than exhibiting the typical linear morphology, the *A. remigis* axoneme appears to follow a helical twist (Figure 3.1A) and the two mitochondrial derivatives exhibit a similar pattern (Figure 3.1B). Sperm motility exhibited by this *A. remigis* flagellum is described below. In

addition, actin was detected in the flagellum and appears to follow the helical twist of the axoneme, but with a half-phase offset (Figure 3.1C). The flagellum could not be stained with a phalloidin-TRITC conjugate (data not shown), suggesting that actin may exist in its monomeric form. Alternatively, it is possible that the sperm possess actin filaments, but their phalloidin-binding site is masked by other proteins such as cofilin and nebulin (Nishida *et al.*, 1987; Ao and Lehrer, 1995). The antibodies used to stain tubulin and actin recognized these proteins on Western blots of whole sperm (Figure 3.1D).

### **Seminal Vesicle Sperm are Quiescent Unless Exposed to a Specific Protease**

Mature sperm removed from the seminal vesicles of males are quiescent and do not become spontaneously motile in buffer (either insect Ringer's or PBS). However, as reported previously for some Lepidopteran and Orthopteran species (Osanai and Baccetti, 1993; Friedländer *et al.*, 2001), sperm motility can be activated by incubating the sperm in 20 µg/mL trypsin (a serine protease) in PBS (Figure 3.2). Within approximately 2 min following trypsin addition, sperm were fully active and usually remain activated for at least 45 min. Sperm motility could also be activated by the addition of 200 µg/mL papain (a cysteine protease) to the sperm suspension in PBS (Figure 3.2). In contrast, thrombin (5 - 1000 U/mL, data not shown) did not activate sperm motility, suggesting that proteolysis at specific sites is required for sperm motility activation.

Some previous studies of insect sperm have suggested that trypsin is required to release sperm from an extracellular matrix or glycocalyx that restricts motility (Osanai and Kasuga, 1990; Friedländer *et al.*, 2001). Although no visible matrix was detected in

sperm isolated from the seminal vesicles of water strider sperm, we tested this hypothesis by treating sperm with PNGase F to disrupt a glycocalyx should one be present. Sperm treated with PNGase F (500 U/mL) showed no activation of motility over a 10 min observation period (Figure 3.2). Sperm were subsequently treated with trypsin to ensure that the sperm were capable of motility. Sperm were fully activated by this addition of trypsin (Figure 3.2).

### ***A. remigis* Sperm Exhibits a Novel Motility**

When *A. remigis* sperm are activated with trypsin, the sperm flagellum generates a waveform typical of many insect sperm (Figure 3.3A). This waveform appeared helical since the darkfield images show periodic dark areas that indicate that some parts of the flagellum are farther from the plane focus than others, which would not be seen in a planar wave. Further, segments of the flagellum can generate a localized waveform, while adjacent regions are quiescent. In addition to these typical waveforms, an unusual configuration can be generated in which the flagellum loops back upon itself and forms a coil with an open loop at one end (Figure 3.3B1-3). This structure can then zipper (spin) and undergo forward progressive motility with the loop acting as the anterior end (Figure 3.3C1-3). Further, the zippered part of the flagellum can be loosened and return to a waveform pattern. This unusual motion was observed much more often than the typical waveform, suggesting that the zippering motion (which we have named flagellar zippering) is not an artifact. The twist frequency of this zippering motion is highly variable. Some slow-twisting flagella exhibit a twist frequency of approximately 3 Hz,

but, in other cases, the twist frequency was much faster, making it difficult to reliably and quantitatively analyze the zippering motility with a camera that captures 30 frames per second. A detailed analysis of the flagellar motility parameters will be the subject of a future study.

To investigate whether flagellar zippering occurs *in vivo*, we observed sperm in a female spermathecal tube where sperm are stored prior to fertilization (Campbell and Fairbairn, 2001). Motile sperm were not observed in this structure presumably because we did not dissect females immediately after copulation. However, sperm fixed in a zippered configuration were observed in the spermathecal tube (Figure 3.4A), suggesting that this zippering motion occurs *in vivo*. Further, a sperm tail with this configuration was observed inside a fertilized egg that was squashed for observation (Figure 3.4B). This observation suggests that the fertilizing sperm also exhibits the zippering motion.

### **Effect of Activators on *A. remigis* Sperm Motility**

Since flagellar motility is often regulated by cyclic nucleotides (cAMP and cGMP),  $\text{Ca}^{2+}$ , and downstream protein phosphorylation (Visconti and Kopf, 1998; Darszon *et al.*, 1999; Urner and Sakkas, 2003; Neill and Vacquier, 2004), we tested whether reagents that activate these signaling events initiate sperm motility in the absence of trypsin and whether the sperm still exhibit the unusual zippering motion. Neither 8-bromo-cAMP nor 8-bromo-cGMP initiated full sperm motility although a fraction of sperm exhibited a twitching motion (Figure 3.5A). In contrast, treatment with 10  $\mu\text{M}$  A23187 and 100  $\mu\text{M}$   $\text{Ca}^{2+}$ , or with 20  $\mu\text{M}$  thapsigargin, partially activated sperm motility

(Figure 3.5A). The responses to these reagents were bimodal, in that some samples responded with vigorous motility (fully active for several minutes), including the zippering motion, while other samples responded very weakly or not at all. There were no statistically significant differences for A23187 and thapsigargin compared to PBS because of this bimodality.

Among the compounds that we tested, we found that two phosphatase inhibitors, calyculin A and okadaic acid, were able to initiate sperm motility. The extent of motility in response to calyculin A or okadaic acid was similar to treatment with trypsin (Figure 3.5A), although the time interval required to attain the greatest extent of motility (lag time) was much longer (Figure 3.5B). These results suggested that quiescence is maintained by high levels of endogenous phosphatase activity and that protein phosphorylation by one or more kinases is required to activate sperm motility. Further, the lack of full, sustained activation by  $\text{Ca}^{2+}$  may reflect the endogenous high levels of phosphatase activity that keep the sperm quiescent. The sperm activated by the phosphatases exhibited the same zippering motion as the sperm activated by trypsin (data not shown).

### **Effect of Inhibitors on *A. remigis* Sperm Motility**

Since our data have implicated  $\text{Ca}^{2+}$  and protein phosphorylation in the regulation of sperm motility, we tested reagents that inhibit protein phosphorylation or block elevation of intracellular free  $\text{Ca}^{2+}$ . To examine the requirement for  $\text{Ca}^{2+}$ , sperm were pre-incubated in 1, 5, 10, or 20  $\mu\text{M}$  BAPTA-AM for 30 min and then incubated with 20

$\mu\text{g/mL}$  trypsin to stimulate motility. Sperm treated with 1 or 5  $\mu\text{M}$  BAPTA-AM were capable of substantial motility, although the level was less than that of control sperm. However, motility of sperm treated with 10 or 20  $\mu\text{M}$  BAPTA-AM was significantly reduced (Figure 3.6A). These results suggest that  $\text{Ca}^{2+}$  is involved in the motility regulation. In various other species,  $\text{Ca}^{2+}$  is implicated in changes of the flagellar waveform (Brokaw, 1979; Ho *et al.*, 2002; Yoshida *et al.*, 2003). However, *A. remigis* sperm exhibited both the helical waveform and the zippering motion in the presence of various concentrations of BAPTA-AM.

Further, the broad spectrum kinase inhibitor staurosporine blocked motility of trypsin stimulated seminal vesicle sperm. When sperm were pre-incubated with 1, 5, 10, or 20  $\mu\text{M}$  staurosporine for 10 min and then stimulated to initiate motility by the addition of 20  $\mu\text{g/mL}$  trypsin, the overall level of motility was reduced (Figure 3.6B). Sperm treated with 20  $\mu\text{M}$  staurosporine were completely immotile. In addition, when sperm motility was activated with trypsin for 5 min and sperm were then incubated with buffer containing various concentrations of staurosporine in the continued presence of trypsin, motility was rapidly inhibited. In sperm treated with 1, 5, 10, or 20  $\mu\text{M}$  staurosporine, motility was reduced by 50% by 7.9, 5.8, 5.0, and 5.9 min, respectively, (Figure 3.6C). Control sperm remained motile for at least 45 min. These results suggest that protein phosphorylation is important for the initiation and/or the maintenance of sperm motility. There were no significant differences observed in terms of the zippering motion in response to staurosporine.



Our results suggest that one or more kinases activate sperm motility. In order to identify kinases involved in sperm motility, we tested various kinase inhibitors (protein kinase A (PKA) inhibitors: H8 or H89; protein kinase C (PKC) inhibitors: bisindolylmaleimide I (BIM) or Go 6983; a Ca<sup>2+</sup>/calmodulin-dependent protein (CaM) kinase inhibitor: KN-62) (Figure 3.6D). However, none of these inhibitors blocked motility activation by trypsin. In contrast to these inhibitors, we found that the MEK1/2 (MAP kinase kinase) inhibitor U0126 significantly blocked sperm motility (Figure 3.6D).

### **Phosphorylation of a 46 kDa Protein in the Axoneme is Reduced in the Presence of U0126**

MEK1/2 is a component of the MAP kinase signaling pathway and phosphorylates ERK1/2 (MAP kinase) and U0126 blocks the MEK1/2-directed phosphorylation of ERK1/2 (English *et al.*, 1999). ERK1/2 is a proline-directed protein kinase that phosphorylates serine or threonine residues adjacent to a proline (English *et al.*, 1999). To investigate whether ERK1/2 is involved in motility activation, we examined *A. remigis* sperm proteins that cross react with the MPM-2 antibody, which recognizes many (but not all) phosphorylated proline-directed phosphorylation sites (Wu *et al.*, 2010). One MPM-2 epitope was detected in sperm at a molecular mass of 46 kDa as determined by Western blot (Figure 3.7A). This 46 kDa protein is localized to the axoneme (Figure 3.7B), suggesting that the protein may play a role in motility regulation. Further, phosphorylation of the 46 kDa protein was inhibited by U0126 (Figure 3.7C), indicating that the 46 kDa protein functions downstream of MEK1/2. However,

phosphorylation of the 46 kDa protein did not increase in response to trypsin (Figure 3.7C). Considering that a phosphatase inhibitor is sufficient to activate motility, these results suggest that the 46 kDa protein may be constitutively phosphorylated to initiate motility, but that initiation is blocked by high levels of phosphatase activity. ERK1/2 was not detected in the mature sperm by Western blot although it was detected in a whole testis sample (Figure 3.7D). It is possible that the sperm protein is below the detection limits or that, alternatively, an ERK-like protein that cannot be detected by this anti-ERK1/2 antibody may be involved in motility activation.

#### **A PAR2-like Protein is Localized in the Tail**

Since our results show that protein phosphorylation is involved in trypsin activation of motility, we hypothesized that a protease activated receptor (PAR) may mediate activation of motility because this receptor is known to be activated by trypsin (Kawabata and Kuroda, 2000). Further, sperm motility was not activated by thrombin (5 - 1000 U/mL, data not shown) which activates PAR1, 3 and 4 (Kawabata and Kuroda, 2000), suggesting that a different isoform, PAR2, may be involved in motility activation. To test this hypothesis, we determined if there was a molecule that cross reacts with an anti-PAR2 antibody in *A. remigis* sperm. Using a monoclonal antibody against amino acids 37-50 of human PAR2 we detected a PAR2-like protein that is localized in the tail but not the acrosome (Figure 3.8A). No signal was detected when the sperm were stained with only a secondary antibody (data not shown). This result suggests that there is a PAR2-like protein on the flagellum that may be involved in motility activation.

## DISCUSSION

Our characterization of the *A. remigis* sperm tail reveals an unusual structure that contains a helical axoneme and two helical mitochondrial derivatives. Although this helical structure is rare in insect sperm (Phillips, 1969; Jamieson *et al.*, 1999), a similar structure has been observed previously in the cat flea *Ctenocephalides felis* (Siphonaptera) (Phillips, 1969) and the stag beetle *Prosopocoilus inclinatus* (Coleoptera) (Irie *et al.*, 2007). The *P. inclinatus* sperm also exhibits a three-dimensional helical waveform (Irie *et al.*, 2007), as is observed in the *A. remigis* sperm. However, the zippering motion that was observed in the *A. remigis* sperm has not been reported in this species, suggesting that the unique zippering motion is not simply due to the helical configuration of either the axoneme or the mitochondrial derivatives.

A clue about the mechanism of the zippering motion may come from our observation that a segment of the flagellum can generate a helical waveform, while other adjacent regions are quiescent. Because of the helical waveform, the motile segment is forced to rotate along its long axis (Ishijima *et al.*, 1992; Woolley and Vernon, 2001). However, the adjacent quiescent regions are not rotating along its long axis. This rotation of a partial segment of the axoneme would generate the zippering motion (Figure 3.9). The zippering configuration may then be loosened when other parts of the axoneme start zippering. In addition, since the two large mitochondrial derivatives are helical, there may not be a strong elastic force to counter balance the zippering flagellum and restore a straight configuration. This model is supported by our observations that some immotile

flagella are fixed in a zippered configuration. A detailed analysis of this motion remains to be performed to test this hypothesis.

In contrast to insect sperm motility exhibited *in vitro*, little is known about sperm motility *in vivo* because of limited knowledge concerning the properties of insect seminal and spermathecal fluids or the restrictions imposed by the often very small architecture of the female reproductive tracts (Werner and Simmons, 2008). In this study, the zippering motion was observed only *in vitro*. However, we did detect an immotile *A. remigis* flagellum in the zippered configuration in the spermathecal tube and in the fertilized egg, suggesting that the zippering motion also occurs *in vivo*. It was surprising that we observed the flagellum in a zippered configuration inside a fertilized egg because the micropyle of the *A. remigis* egg seems too narrow ( $\approx 1.9 \mu\text{m}$ , Figure 3.10) for the loop end of the flagellum to pass through. Therefore, sperm may exhibit a zippering motion after entry into the egg. The entry of a long flagellum into an egg has also been reported in the fruit fly *Drosophila* (Order Diptera) (Karr and Pitnick, 1996; Pitnick and Karr, 1998). In *Drosophila*, the sperm flagellum exhibits a consistent coiling configuration in the anterior end of the egg, suggesting that there is an intracellular sperm-egg interaction to position the male pronucleus in the proper region of the egg (Karr, 1991).

In addition to these unusual motility patterns, we report that *A. remigis* sperm motility is activated by proteases such as trypsin and papain. Since both enzymes cleave the carboxyl side of the amino acids lysine and arginine (Keil, 1992), proteolysis of a particular cleavage site may be involved in motility activation in *A. remigis*. In *Bombyx*

*mori*, cleavage of the carboxyl side of arginine is implicated in sperm motility activation (Aigaki *et al.*, 1987). In contrast to *B. mori*, *A. remigis* does not form a spermatophore and therefore trypsin activation of insect sperm motility may represent a common and evolutionary conserved mechanism in insects. Whether a trypsin-like protease is an endogenous activator *in vivo* and where it comes from in *A. remigis* have yet to be determined. In analogy with *B. mori*, it is possible that the activator is secreted from males when the sperm are ejaculated into females. However, we could not find accessory glands in *A. remigis* males. Alternatively, a protease could be produced by the female in order to activate sperm in the female reproductive tract. In the boll weevil, *Anthonomus grandis* (Order Coleoptera) (Villavaso, 1975), spermathecal gland secretions were shown to contribute to the activation and maintenance of sperm motility. However, nothing is known about the specific molecules that are involved in the motility activation of *A. grandis* sperm in females.

Sperm motility was activated not only by trypsin but also by phosphatase inhibitors such as calyculin A and okadaic acid. It is unlikely that these phosphatase inhibitors degrade proteins to supply an energy source for sperm motility or glycoproteins in the sperm plasma membrane (Kasuga *et al.*, 1987; Osanai *et al.*, 1987; Osanai and Kasuga, 1990), suggesting that there is a downstream signaling pathway that regulates sperm motility in the *A. remigis* sperm. This idea is further supported by our result that sperm motility is inhibited by the broad spectrum kinase inhibitor staurosporine. Since nearly all of the sperm are immotile in the seminal vesicle, there may be an inhibitory mechanism that maintains sperm quiescence, and a highly active endogenous

phosphatase may be a key player in this inhibition. Both calyculin A and okadaic acid are potent inhibitors of protein phosphatase1 (PP1) and protein phosphatase 2A (PP2A), suggesting that these phosphatases may be involved in the maintenance of sperm quiescence in the seminal vesicle. In mammals, the PP1 isoform PP1 $\gamma$ 2 is expressed in sperm and prevents immature sperm from initiating motility (Vijayaraghavan, 1996; Chakrabarti, 2007). No reagents that were tested altered the way that the *A. remigis* sperm move (flagellar zippering).

In addition to phosphatases, our results suggest that there is a kinase that phosphorylates proteins that are involved in sperm motility. By testing various kinase inhibitors, we found that U0126 blocked trypsin activation of sperm motility. Although U0126 is known to inhibit a MEK/ERK signaling pathway, we could not detect ERK1/2 in Western blots of whole seminal vesicle sperm. However, ERK1/2 was detected in testis samples, suggesting that levels of ERK1/2 in sperm may be so low that enrichment by immunoprecipitation may be required to detect the protein by Western blot. Alternatively, an ERK-like protein that is not recognized by this anti-ERK1/2 antibody, or a non-ERK kinase downstream of U0126 may be involved in motility regulation. In human sperm, ERK1/2 is localized to the tail of mature sperm and stimulates forward and hyperactivated motility (Almog *et al.*, 2008). Further, we identified one potential target of the U0126-sensitive kinase, a 46kDa protein that is localized in the axoneme. However, the phosphorylation level was not increased by the presence of trypsin. These results suggest that the 46kDa protein is present in mature sperm but that its activity is blocked in quiescent sperm by the activity of a phosphatase. We have also shown that there is a

PAR2-like protein on the flagellum by immunofluorescence. This PAR2-like protein may be a target of trypsin to activate *A. remigis* sperm motility. In contrast, PAR2 is involved in tryptase-induced reduction of sperm motility in human sperm (Zitta *et al.*, 2007). A current model for *A. remigis* sperm motility activation by trypsin based on our results is illustrated in Figure 3.11.

In summary, we reveal that *A. remigis* sperm are activated by trypsin and exhibit a novel zippering motility. A detailed analysis of this unique motility may shed light on the relationship between flagellar morphology and the motility. Further, we show that there is a signaling pathway that regulates *A. remigis* sperm motility. Trypsin activation of insect sperm motility may be a common mechanism of activation in insects as it can be found both in insects that produce spermatophores and in *A. remigis*, which does not produce a spermatophore.

### CHAPTER 3: REFERENCES

Aigaki T., Kasuga H. and Osanai M. (1987): A specific endopeptidase, BAE esterase, in the glandula prostatica of the male reproductive system of the silkworm, *Bombyx mori*. *Insect Biochem.* 17, 323-28.

Aigaki T., Kasuga H., Nagaoka S. and Osanai M. (1994): Purification and partial amino acid sequence of initiatorin, a prostatic endopeptidase of the silkworm, *Bombyx mori*. *Insect Biochem Molec Biol.* 24, 969-75.

Ao X. and Lehrer S.S. (1995): Phalloidin unzips nebulin from thin filaments in skeletal myofibrils. *J Cell Sci.* 108, 3397-403.

Almog T., Lazar S., Reiss N., Etkovitz N., Milch E., Rahamim N., Dobkin-Bekman M., Rotem R., Kalina M., Ramon J., Raziel A., Brietbart H., Seger R. and Naor Z. (2008): Identification of extracellular signal-regulated kinase 1/2 and p38 MAPK as regulators of human sperm motility and acrosome reaction and as predictors of poor spermatozoan quality. *J Biol Chem.* 283, 14479-89.

Arnqvist G. (1997): The evolution of water strider mating systems: causes and consequences of sexual conflicts. In: Choe J.C. and Crespi B.J., editors. *The evolution of mating systems in insects and arachnids.* Cambridge University Press. pp.146-163.

Brokaw C.J. (1979): Calcium-induced asymmetrical beating of triton-demembrated sea urchin sperm flagella. *J Cell Biol.* 82, 401-11.

Campbell V. and Fairbairn D.J. (2001): Prolonged copulation and the internal dynamics of sperm transfer in the water strider *Aquarius remigis*. *Can J Zool.* 79, 1801-12.

Chakrabarti R., Cheng L., Puri., Soler D. and Vijayaraghavan S. (2007): Protein phosphatase PP1 gamma2 in sperm morphogenesis and epididymal initiation of sperm motility. *Asian J Andol.* 9, 445-52.

Darszon A., Labarca P., Nishigaki T. and Espinosa F. (1999): Ion channels in sperm physiology. *Physiol Rev.* 79, 481-510.

English J., Pearson G., Wilsbacher J., Swantek J., Karandikar M., Xu s. and Cob M.H. (1999): New insights into the control of MAP kinase pathways. *Exp Cell Res.* 253, 255-70.



- Friedländer M., Jeshtadi A. and Reynolds S.E. (2001): The structural mechanism of trypsin-induced intrinsic motility in *Manduca sexta* spermatozoa in vitro. *J Insect Physiol.* 47, 245-55.
- Ho H.C., Granish K.A. and Suarez S.S. (2002): Hyperactivated motility of bull sperm is triggered at the axoneme by  $Ca^{2+}$  and not cAMP. *Dev Biol.* 250, 208-17.
- Irie M., Kubo-Irie M. and Mohri H. (2007): The first observation of 3-dimensional motion and twist in sperm flagella of the stag beetle *Prosopocoilus inclinatus*. *Plasma Fusion Research.* 2, S1028-1-4.
- Ishijima S., Miyako S.H., Naruse M., Ishijima S.A. and Hamaguchi Y. (1992): Rotational movement of a spermatozoon around its long axis. *J Exp Biol.* 163, 15-31.
- Jamieson B.G.M., Dallai R. and Afzerius B.A. (1999): *Insects: Their spermatozoa and phylogeny.* USA: Science Publishers. p 1-23.
- Karr T.L. (1991): Intracellular sperm/egg interactions in *Drosophila*: A three-dimensional structural analysis of a paternal product in the developing egg. *Mech Dev.* 34, 101-11.
- Karr T.L. and Pitnick S. (1996): The ins and outs of fertilization. *Nature.* 379,405-6.
- Kasuga H., Aigaki T. and Osanai M. (1987): System for supply of free arginine in the spermatophore of *Bombyx mori*. *Insect Biochem.* 17, 317-22.
- Katsuno S. (1977): Studies on eupyrene and apyrene spermatozoa in the silkworm, *Bombyx mori* L. (Lepidoptera: Bombycidae) V. The factor related to the separation of eupyrene sperm bundles. *Appy Ent Zool.* 12, 370-1.
- Kawabata A. and Kuroda R. (2000): Protease-activated receptor (PAR), a novel family of G protein-coupled seven trans-membrane domain receptors: activation mechanisms and physiological roles. *Jpn J Pharmacol.* 82, 171-4.
- Keil B. (1992): *Specificity of proteolysis.* New York: Springer.
- Miyata H., Noda N., Fairbairn D.J., Oldenbourg R., Cardullo R.A. (2010): Assembly of the fluorescent acrosomal matrix and its fate in fertilization in the water strider, *Aquarius remigis*. *J Cell Physiol.* In press.

- Neill A.T. and Vacquier V.D. (2004): Ligands and receptors mediating signal transduction in sea urchin spermatozoa. *Reproduction*. 127, 141-9.
- Nishida E., Iida K., Yonezawa N., Koyasu S., Yahara I. and Sakai H. (1987): Cofilin is a component of intranuclear and cytoplasmic actin rods induced in cultured cells. *Proc Natl Acad Sci USA*. 84, 5262-6.
- Osanai M., Aigaki T., Kasuga H. and Yonezawa Y. (1986): Role of arginase transferred from the vesicular seminalis during mating and changes in amino acid pools of the spermatophore after ejaculation in the silkworm, *Bombyx mori*. *Insect Biochem*. 16, 879-85.
- Osanai M., Aigaki T. and Kasuga H. (1987): Energy metabolism in the spermatophore of the silkworm, *Bombyx mori*, associated with accumulation of alanine derived from arginine. *Insect Biochem*. 17, 71-5.
- Osanai M., Kasuga H. and Aigaki T. (1989): Isolation of eupyrene sperm bundles and apyrene spermatozoa from seminal fluid of the silkworm, *Bombyx mori*. *J Insect Physiol*. 35, 401-8.
- Osanai M. and Kasuga H. (1990): Role of endopeptidase in motility induction in apyrene silkworm spermatozoa; micropore formation in the flagellar membrane. *Experientia*. 46, 261-4.
- Osanai M. and Baccetti B. (1993): Two-step acquisition of motility by insect spermatozoa. *Experientia*. 49, 593-5.
- Phillips D.M. (1969): Exceptions to the prevailing pattern of tubules (9+9+2) in the sperm flagella of certain insect species. *J Cell Biol*. 40, 28-43.
- Pisano C., Bonaccorsi S. and Gatti M. (1993): The *kl-3* loop of the *Y* chromosome of *Drosophila melanogaster* binds a tektin-like protein. *Genetics*. 133, 569-79.
- Pitnick S. and Karr T.L. (1998): Pternal products and by-products in *Drosophila* development. *Proc R Soc Lond B*. 265, 821-6.
- Pollister A.W. (1930): Cytoplasmic phenomena in the spermatogenesis of *Gerris*. *J Morphol*. 49, 455-507.

- Preziosi R.F. and Fairbairn D.J. (1992): Genetic population structure and levels of gene flow in the stream-dwelling waterstrider, *Aquarius* (= *Gerris*) *remigis* (Hemiptera: Gerridae). *Evolution*. 44, 430–40.
- Rubenstein D.I. (1989): sperm competition in the water strider, *Gerris remigis*. *Anim Behav*. 38, 631-6.
- Tandler B. and Moriber L.G. (1966): Microtubular structures associated with the acrosome during spermiogenesis in the Water-strider, *Gerris remigis* (Say). *J Ultrastruct Res*. 14, 391-404.
- Urner F. and Sakkas D. (2003): Protein phosphorylation in mammalian spermatozoa. *Reproduction*. 125, 17-26.
- Vijayaraghavan S., Stephens D.T., Trautman K., Smith G.D., Khatra B., da Cruz e Silva E.F. and Greengard P. (1996): Sperm motility development in the epididymis is associated with decreased glycogen synthase kinase-3 and protein phosphatase 1 activity. *Biol Reprod*. 54, 709-18.
- Villavaso E. J. (1975): The role of the spermathecal gland of the boll weevil, *Anthonomus grandis*. *J Insect Physiol*. 21, 1457-62.
- Visconti P.E. and Kopf G.S. (1998): Regulation of protein phosphorylation during sperm capacitation. *Biol Reprod*. 59, 1-6.
- Weigensberg I. and Fairbairn D.J. (1994): Conflicts of interest between the sexes: a study of mating interactions in a semiaquatic bug. *Anim Behav*. 48, 893-901.
- Werner M. and Simmons L.W. (2008): Insect sperm motility. *Biol Rev*. 83, 191-208.
- Woolley D.M. and Vernon G.G. (2001): A study of helical and planar waves on sea urchin sperm flagella, with a theory of how they are generated. *J Exp Biol*. 204, 1333-45.
- Wu C.F., Wang R., Liang Q., Liang J., Li W., Jung S.Y., Qin J., Lin S. and Kuang J. (2010): Dissecting the M phase-specific phosphorylation of serine-proline or threonine-proline motifs. *Mol Biol Cell*. 21, 1470-81.
- Yoshida M., Ishikawa M., Izumi H., De Santis R. and Morisawa M. (2003): Store-operated calcium channel regulated the chemotactic behavior of ascidian sperm. *Proc Natl Acad Sci USA*. 100, 149-54.

Yoshida M., Kawano M. and Yoshida K. (2008): Control of sperm motility and fertility: Diverse factors and common mechanisms. *Cell Mol Life Sci.* 65, 3446-57.

Zitta K., Albrecht M., Weidinger S., Mayerhofer A. and Kohn F. (2007): Protease activated receptor 2 and epidermal growth factor receptor are involved in the regulation of human sperm motility. *Asian J Androl.* 9, 690-6.

## FIGURE LEGENDS

**Figure 3.1** Morphology of the water strider sperm flagellum. The water strider sperm axoneme has a helical twist, as indicated by anti-tubulin immunofluorescence and DIC images (A). The mitochondrial derivatives also follow a helical path along the axoneme, as shown by the fluorescence Mitotracker Red CMXRos and DIC image (B). Anti-tubulin and anti-actin double staining show that the two structures alternate (C). Antibodies used in panels A and C recognize bands of the appropriate molecular mass on Western blots (D). Mr, Molecular mass. Scale bars = 2  $\mu\text{m}$ .

**Figure 3.2** Lag time in response to proteases. Protease-treated sperm slowly become motile. The average time to reach fully active motility was 2.1 min for trypsin (n=8) and 9.5 min for papain (n=3). In contrast, sperm motility was not activated by PNGase F. The average time to reach fully active motility was 1.1 min when sperm that were pretreated with PNGase F were switched to trypsin (n=5). Means  $\pm$  SEM are presented (a,b,  $p < 0.05$ , ANOVA with post-hoc tests).

**Figure 3.3** Water strider sperm waveforms. Sperm can beat with a typical helical wave (A). The flagellum can also fold back upon itself and form a coiled segment (B1-B3). The coiled structure can then undergo forward progressive motility with the loop acting as the anterior end (C1-C3). The loop end is indicated by arrows. Scale bars = 20  $\mu\text{m}$ .

**Figure 3.4** Sperm in the female reproductive tract exhibit a zippered configuration. Sperm axonemes in the zippered configuration were observed in a female spermathecal

tube (A) and a fertilized egg (B). The fertilized egg was squashed prior to observation.

Scale bars = 10  $\mu\text{m}$ .

**Figure 3.5** Motility level in response to activators. (A) Sperm were treated with 20  $\mu\text{g/mL}$  Trypsin (n=5), PBS (n=5), 3 mM 8-bromo-cAMP (n=3), 3 mM 8-bromo-cGMP (n=4), 10  $\mu\text{M}$  A23187 in the presence of 100  $\mu\text{M}$   $\text{Ca}^{2+}$  (n=5), 20  $\mu\text{M}$  thapsigargin (no added  $\text{Ca}^{2+}$ ) (n=6), 10  $\mu\text{M}$  Calyculin A (n=6), or 10  $\mu\text{M}$  okadaic acid (n=5). Motility was observed for 10 min and the highest level of motility was scored. Means  $\pm$  SEM are presented (a,b,c,  $p < 0.05$ , ANOVA with post-hoc tests). (B) The time to attain full motility with okadaic acid (OA) and calyculin A (Caly) was much longer than that with trypsin (Tryp) (10  $\mu\text{M}$  Caly ( $\circ$ ), n=6; 10  $\mu\text{M}$  OA ( $\blacktriangledown$ ), n=5, 20  $\mu\text{g/mL}$  Trypsin ( $\bullet$ ), n=14). Means of the indicated numbers of independent experiments are plotted.

**Figure 3.6** Motility level in response to inhibitors. (A) When sperm were pre-incubated with various concentrations of BAPTA-AM for 30 min and then stimulated with trypsin, the greatest extent of motility was significantly reduced by 10  $\mu\text{M}$  and 20  $\mu\text{M}$  BAPTA-AM. Means  $\pm$  SEM are presented (\*\*,  $p < 0.005$ , ANOVA with Dunnett's test; trypsin as a reference; 1, 5, 10  $\mu\text{M}$ , n=3; 20  $\mu\text{M}$ , n=4). (B) When sperm were pre-incubated with various concentrations of staurosporine for 10 min and then stimulated with trypsin, the greatest extent of motility was reduced in a concentration dependent manner. Means  $\pm$  SEM are presented (\*,  $p < 0.01$ ; \*\*,  $p < 0.001$ , ANOVA with Dunnett's test; trypsin as a reference; 1, 10, 20  $\mu\text{M}$ , n=3; 5  $\mu\text{M}$ , n=4). (C) The half-time of inhibition by staurosporine is shown. Sperm were incubated with trypsin for 5 min to fully activate

motility and the buffer was then exchanged for one containing staurosporine in the presence of trypsin. Motility declined rapidly in inhibitor treated sperm, compared to sperm treated with trypsin alone (more than 45 min) (n = 3 for each concentration). (D) Sperm were pre-incubated for 30 min with H8 (50  $\mu$ M, n=2), H89 (50  $\mu$ M, n=2), bisindolylmaleimide I (BIM, 10  $\mu$ M, n=2), Go 6983 (20  $\mu$ M, n=2), KN-62 (10  $\mu$ M, n=2) or U0126 (50  $\mu$ M, n=3) and then stimulated with trypsin. The greatest extent of motility was significantly reduced by U0126. Means  $\pm$  SEM are presented (a,b,  $p < 0.05$ , ANOVA with post-hoc tests).

**Figure 3.7** MPM-2 is localized in the axoneme and displays less phosphorylation in the presence of U0126. (A) A 46 kDa protein possesses an MPM-2 epitope. Mr, molecular mass. (B) MPM-2 staining is colocalized with tubulin. Scale bar = 5  $\mu$ m. (C) A 46 kDa protein is less phosphorylated in the presence of U0126 (relative density; untreated/U0126 = 1/0.57), while the phosphorylation level of the protein is similar between untreated sperm and trypsin-treated sperm (relative density; untreated/U0126 = 1/0.95). Sperm were either untreated or incubated with U0126 (50  $\mu$ M, 30 min) or trypsin (20  $\mu$ g/mL, 5 min) before SDS-PAGE. (D). ERK1/2 was detected in the testis but not in mature sperm.

**Figure 3.8** A PAR2-like protein is present in the tail. An antibody against human PAR2 cross reacted with a component on the surface of the water strider sperm flagellum (red, PAR2; green, acrosomal matrix intrinsic fluorescence (Miyata *et al.*, 2010)). Scale bar = 5  $\mu$ m.

**Figure 3.9** Consecutive images showing a possible model for the formation of the flagellar zippering motion in *A. remigis* sperm using a string. While the left edge was fixed, the right edge was forced to rotate. The string begins to zipper, the structure formed is similar to that of the *A. remigis* sperm when zippering.

**Figure 3.10** A micropyle of the *A. remigis* egg. The egg was frozen by liquid nitrogen and observed with a Hitachi TM-1000 Tabletop Scanning Electron Microscope. One micropyle was observed at the end of the egg. Scale bar = 10  $\mu\text{m}$ .

**Figure 3.11** A current model for the signaling pathways involved in motility activation of *A. remigis* sperm. Trypsin activates a PAR2-like protein in the membrane, leading to an increase in intracellular  $\text{Ca}^{2+}$  and a decrease in phosphatase activity, thereby phosphorylating proteins involved in motility activation. Moreover, a U0126-sensitive kinase phosphorylates a 46kDa protein constitutively, which is necessary for the initiation of sperm motility.



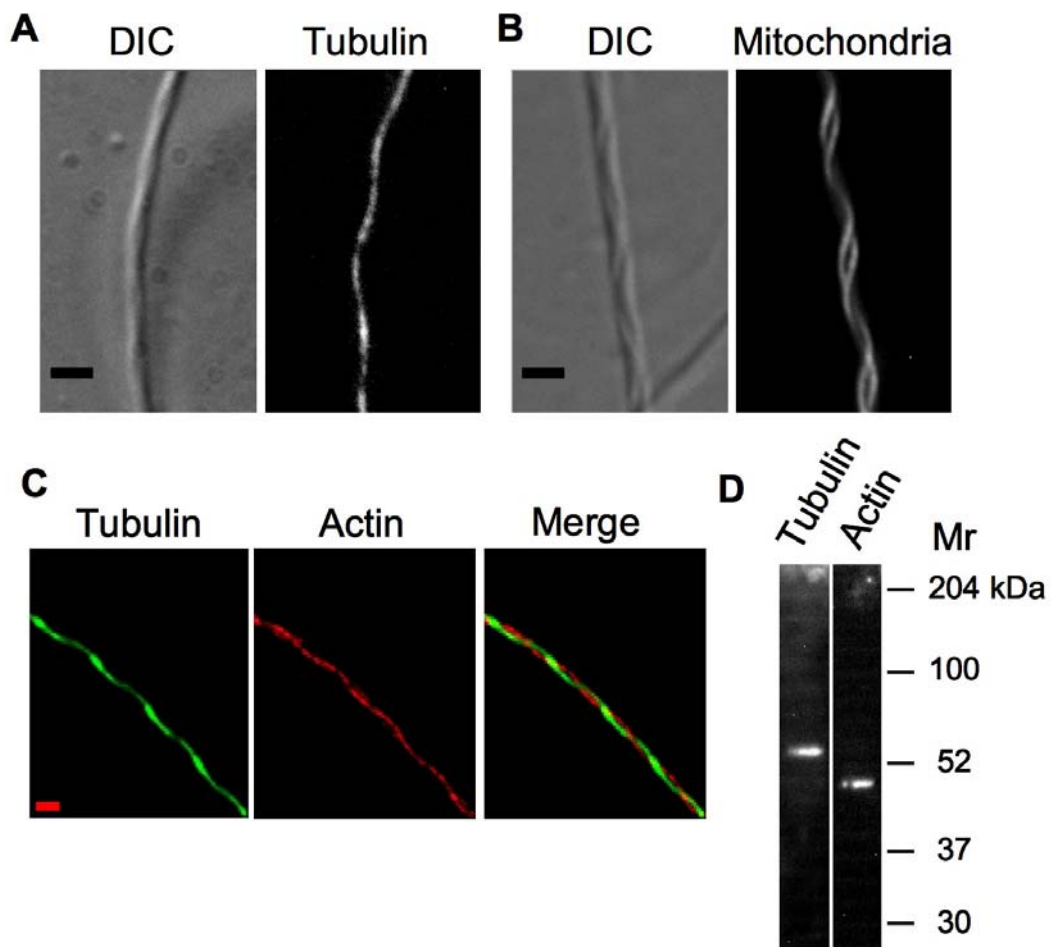


Figure 3.1 Morphology of the water strider sperm flagellum.

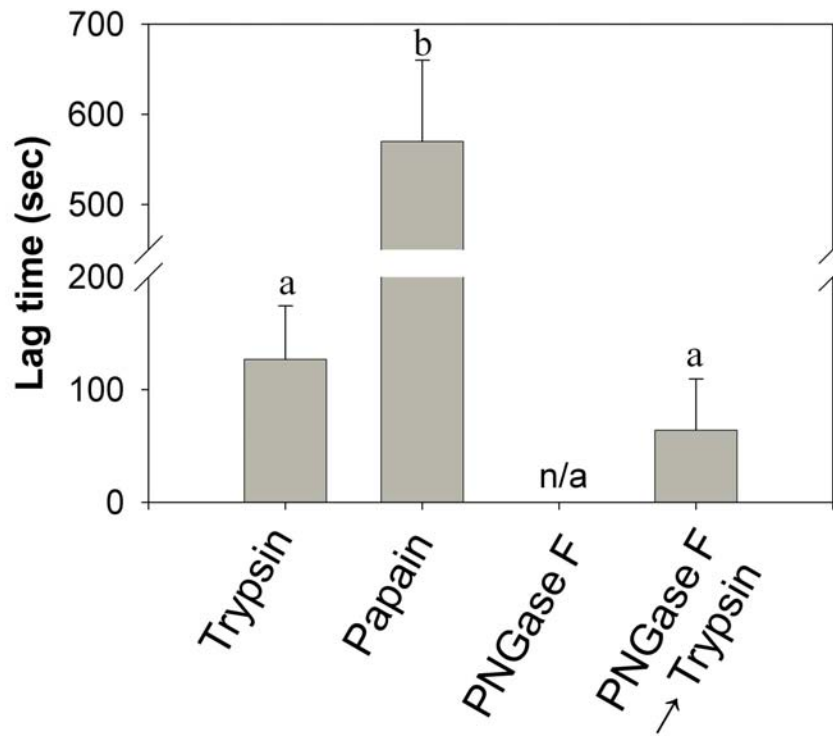


Figure 3.2 Lag time in response to proteases.

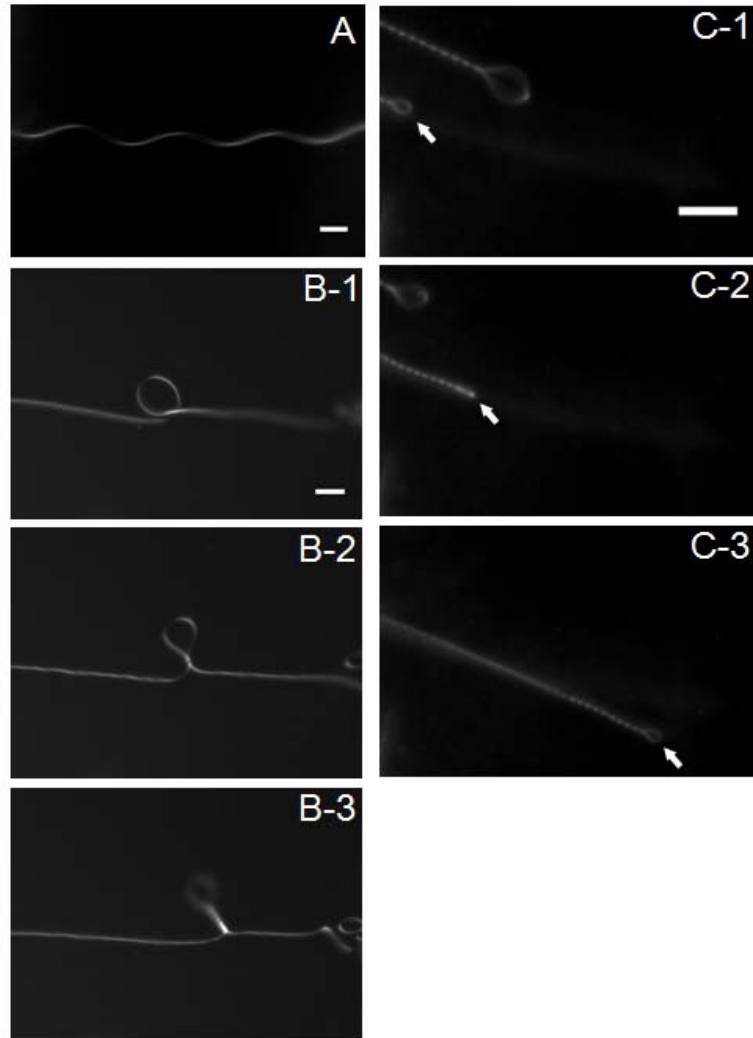


Figure 3.3 Water strider sperm waveforms.

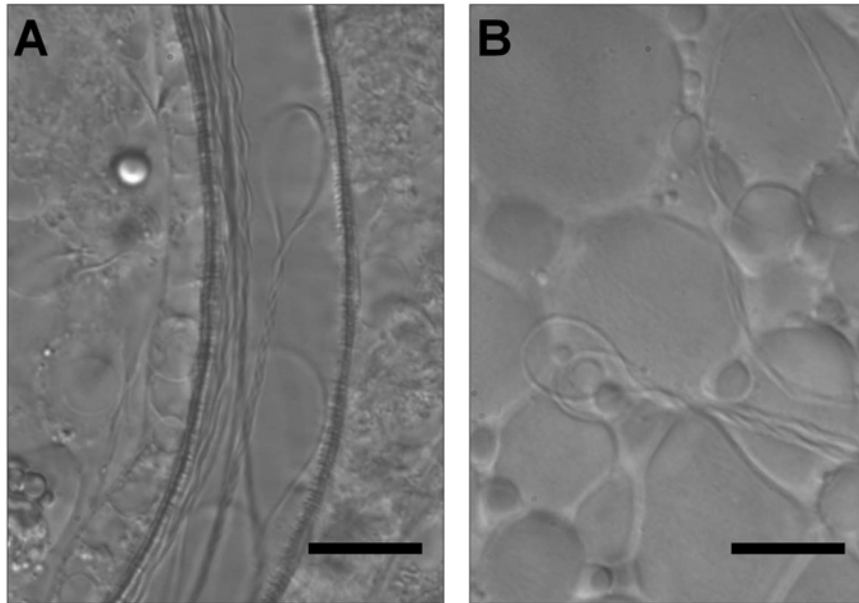


Figure 3.4 Sperm in the female reproductive tract exhibit a zippered configuration.

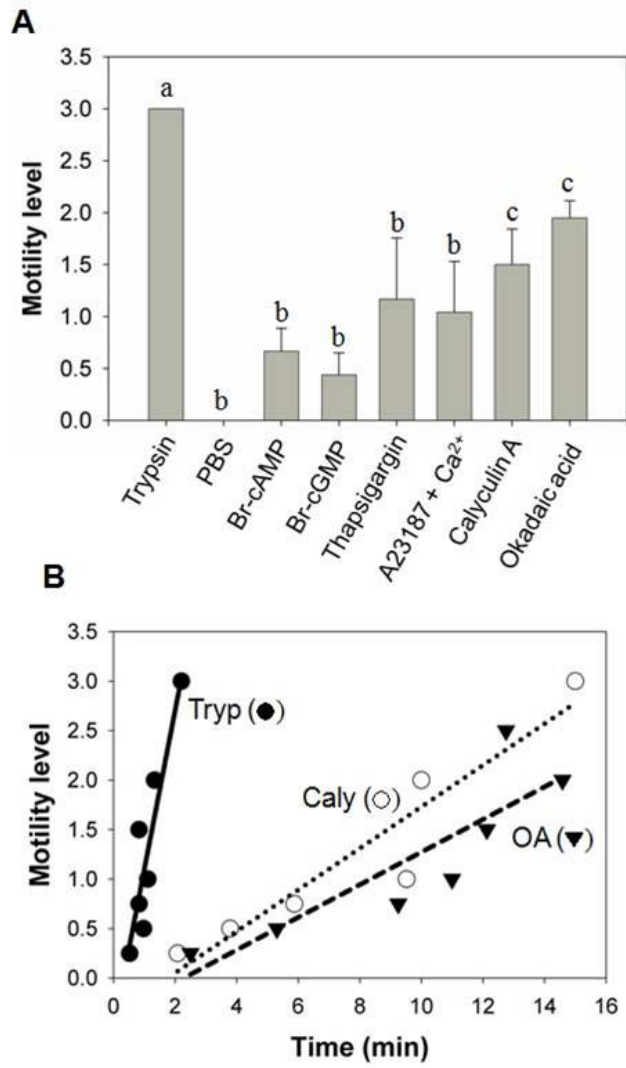


Figure 3.5 Motility level in response to activators.

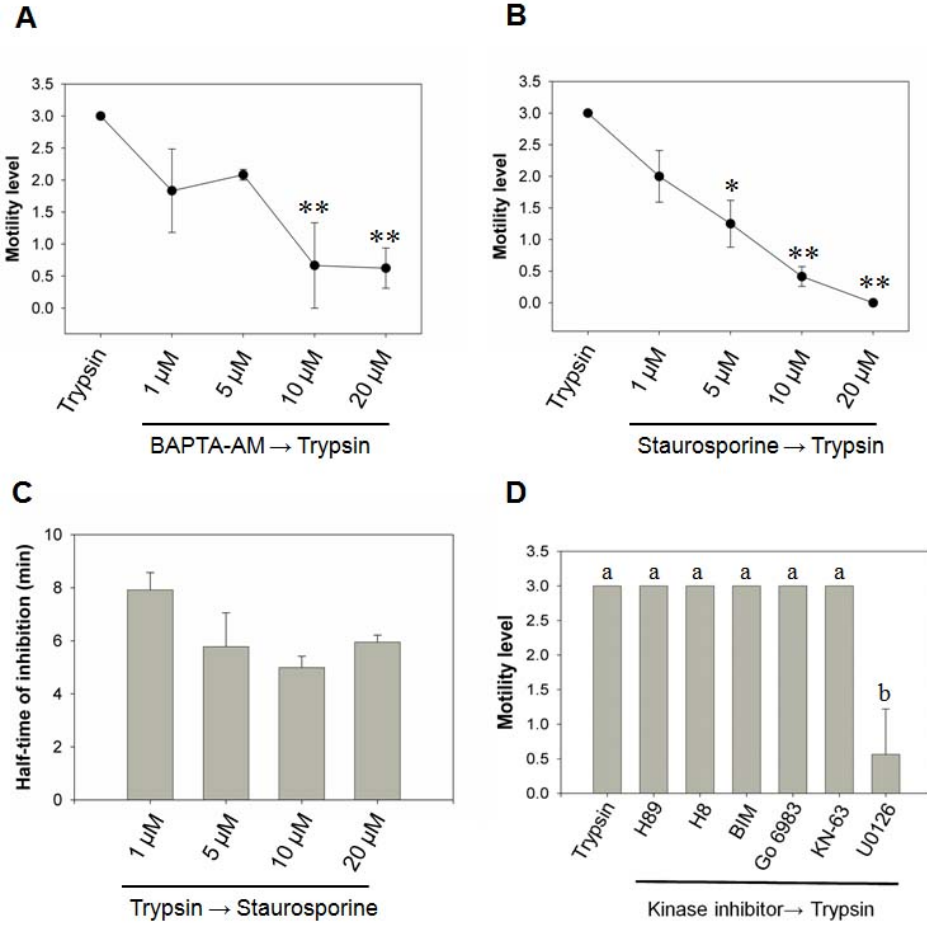


Figure 3.6 Motility level in response to inhibitors.

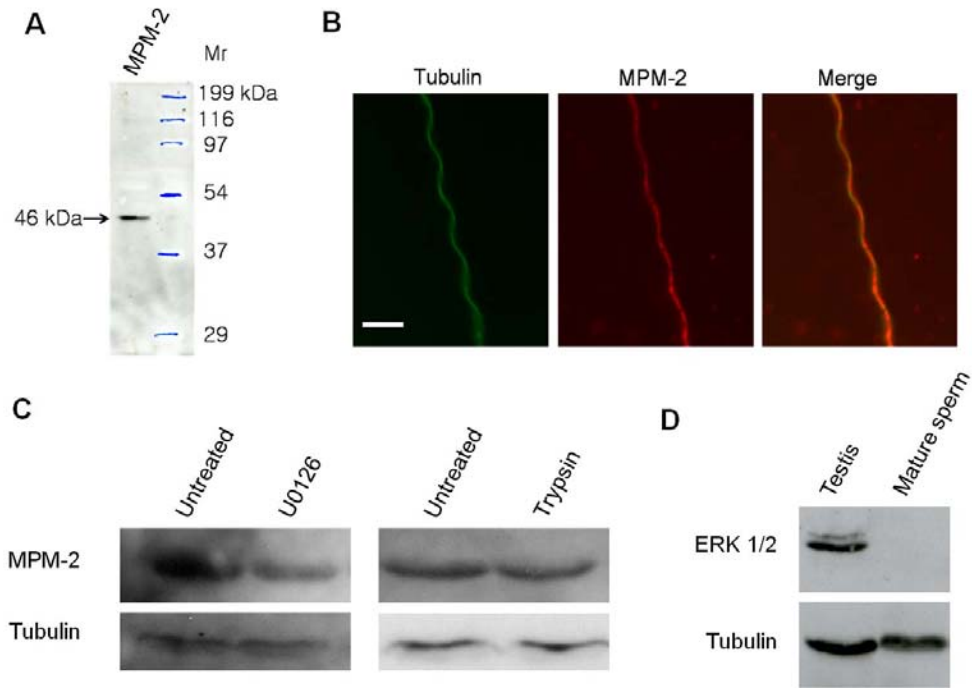


Figure 3.7 MPM-2 is localized in the axoneme and displays less phosphorylation in the presence of U0126.

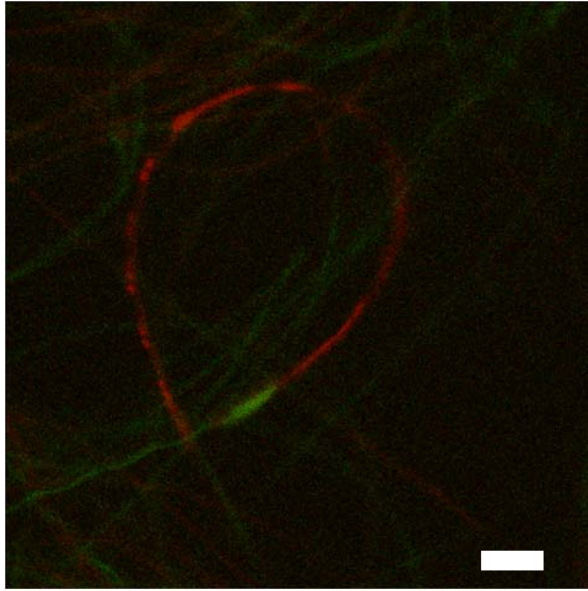


Figure 3.8 A PAR2-like protein is present in the tail.



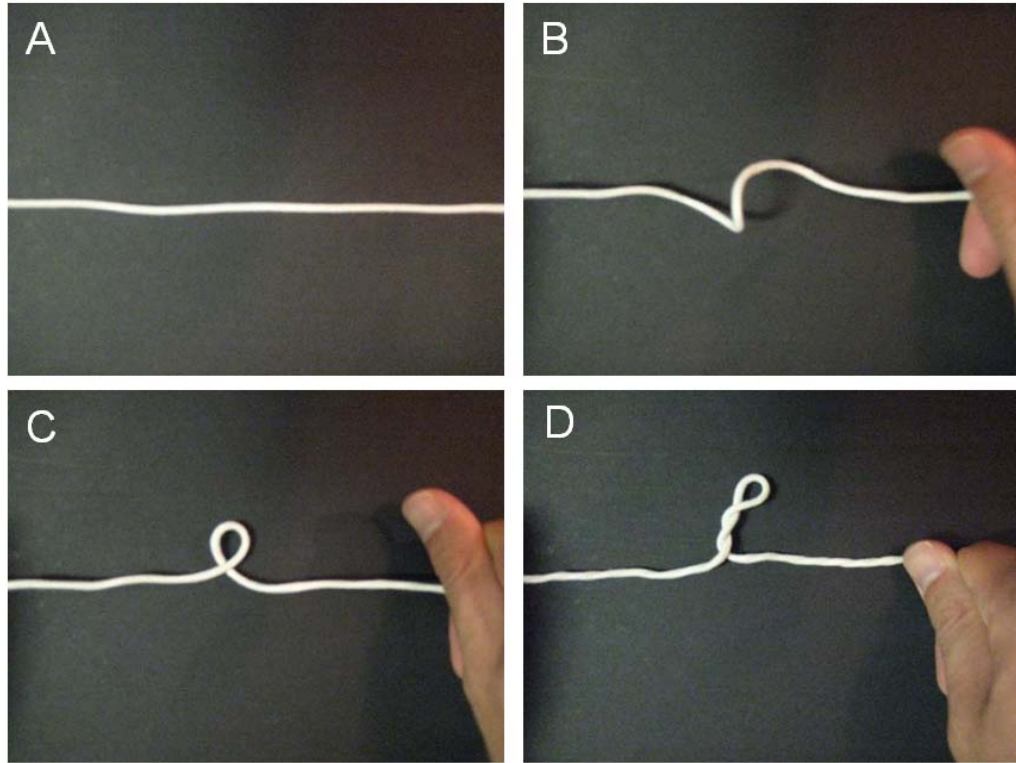


Figure 3.9 Consecutive images showing a possible model for the formation of the flagellar zippering motion in *A. remigis* sperm using a string.

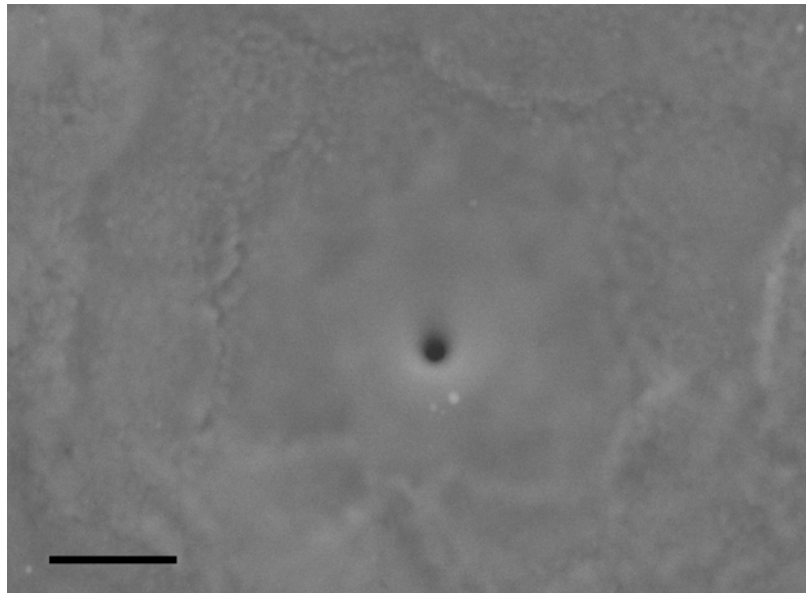


Figure 3.10 A micropyle of the *A. remigis* egg.

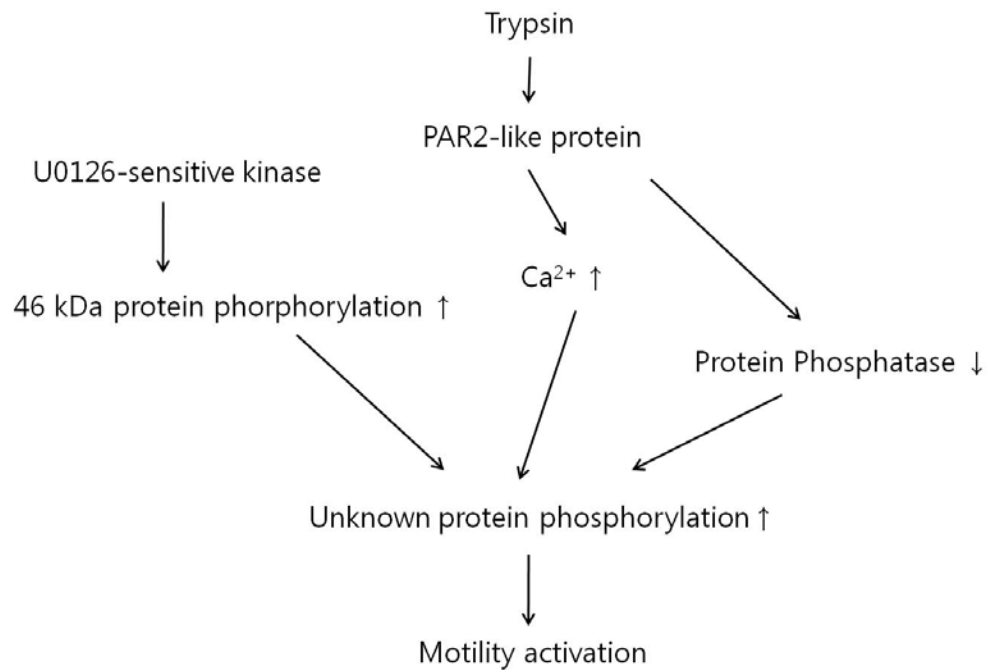


Figure 3.11 A current model for the signaling pathways involved in motility activation of *A. remigis* sperm.

Table 3.1 Motility scale

<b><u>Rank</u></b>	<b><u>Level of Motility</u></b>
0	non-motile
0.5	5 - 10% of sperm twitching or slow waves
0.75	~ 25% of sperm twitching or slow waves
1	~ 50% of sperm exhibiting partial motility
2	> 75% of sperm exhibiting partial and/or full of motility
3	> 90% of sperm fully motile

CHAPTER 4

DICSUSSION

THE CONSEQUENCES OF MAKING A LONG SPERM: POTENTIAL ROLES FOR  
THE ACROSOMAL MATRIX, THE INITIATION OF SPERM MOTILITY, AND  
COMPARISONS WITH OTHER ANIMALS

The biogenesis of a mature gamete from its stem cell is a complex process that is under genetic and environmental regulation. In the case of sperm, the development of a functional cell is initiated in the testis but its full potential is not realized until it encounters the egg. Following meiosis, a round spermatid is incapable of fertilizing an egg and must undergo several highly regulated developmental steps such as acrosome formation, the acrosome reaction and motility regulation in both the male and female reproductive tracts. In contrast to mammals and echinoderms that have long been studied, little is known about these events in insects (Wilson *et al.*, 2006; Werner and Simmons, 2008). Insect sperm exhibit considerable variation in morphology and ultrastructure while they possess typical structures such as a microtubule-based flagellum and a specialized organelle known as the acrosome that is positioned anterior to the nucleus (Jamieson *et al.*, 1999). It has been suggested that this diversity reflects sperm competition (Simmons, 2001), a situation that occurs when sperm from two or more males competes for successful fertilization of the ova in a single female (Parker, 1970). Although there is evidence for sperm competition in some insect taxa (Simmons, 2001; Snook, 2005), an understanding of the post-meiotic events that lead to unusual morphological features or behaviors of insect sperm would help elucidate the mechanisms of sperm competition. The overall goal of this dissertation was to describe the post-meiotic events of sperm in a semi-aquatic insect, the water strider *Aquarius remigis*, and follow their life history from spermatogenesis to fertilization and early development thereby obtaining insights into reproductive strategies. Both microscopical and biochemical methods were utilized to investigate these events. In this chapter, I will discuss the acrosome formation, the

acrosome reaction, and sperm motility regulation in *A. remigis*, focusing on my experiments that have not been described in the previous chapters.

### **Acrosome formation in *A. remigis***

Following meiosis, a round spermatid differentiates into a highly specialized cell that possesses both an acrosome and a flagellum. The *A. remigis* acrosome, at approximately 2.5  $\mu\text{m}$  in length, is unusually long (Tandler and Moriber, 1966; Miyata *et al.*, 2010) and therefore presented a good system to study its formation at both microscopical and biochemical levels. As was reported previously using a transmission electron microscope (Tandler and Moriber, 1966), the round acrosomal vesicle (referred to as the acroblast) was formed next to the nucleus in the early stage of spermiogenesis in *A. remigis*. The round acrosome then began to elongate to its final shape that was both long and complex. Further investigations suggest that there appear to be two critical mechanisms involved in the formation of this unique structure, the assembly of the acrosomal matrix and the establishment of microtubules that surround the developing acrosome.

#### Assembly of the acrosomal matrix

Utilizing an intrinsically fluorescent molecule that is localized in the acrosome, I investigated the formation of the acrosomal matrix in living spermatogenic cells. Before this investigation, no measurements on the mobility or the dynamic assembly of acrosomal molecules have been reported in any species. This may be due to the small size

of acrosomes in most other species (acrosomes are typically a few microns in length) which would preclude the kinds of microscopical and biophysical studies that were done here. My analysis on the *A. remigis* acrosome revealed that the fluorescent molecule first appears as two distinct populations in the acroblast and exhibits unrestricted mobility in the acrosomal vesicle of round spermatids. The fluorescent molecule becomes progressively more immobilized in condensing spermatids and is completely embedded in a rigid matrix in the acrosome of mature sperm. Taken together, these results suggest that the fluorescent molecule and associated proteins are up-regulated post-meiotically in the developing *A. remigis* sperm resulting in the formation of a rigid matrix consisting of monomeric units possessing a uniform polarization. Further, my investigations revealed that the fluorescent molecule is flavin adenine dinucleotide (FAD) and that the acrosomal matrix is stabilized by disulfide bonds. These studies support a hypothesis in which FAD is involved in the assembly of the acrosomal matrix by mediating the formation of disulfide bonds during spermiogenesis.

In order to test this hypothesis, it will be important to identify a protein that binds to FAD. Since FAD is not known to polymerize on its own, there should be a protein that binds to FAD and assembles into the acrosomal matrix. FAD can exist in cells as a cofactor of proteins (Massey, 2000; Joosten and Berkel, 2007). In order to verify this prediction, I attempted to purify this protein using ion-exchange column chromatography (Bio-Rad, Q2) using the intrinsic fluorescence as a marker. I used proteins from the *A. remigis* testis for fractionation rather than mature sperm since the fluorescent molecule is likely soluble in the round acrosome. Indeed, I obtained a distinct fluorescent fraction



with this method. However, there were many proteins ( $\geq 10$  proteins) in this fraction probably because different proteins aggregate in a non-specific manner during the purification. It is not surprising that this protein aggregation occurs since acrosomal proteins may form disulfide bonds. Careful adjustments of sample and elution buffers will be necessary to purify the molecule that binds to FAD and therefore test my hypothesis. My research represents the first time that an acrosome has been found to contain FAD. Since an acrosomal matrix is also stabilized by disulfide bonds in mammalian sperm (Mate *et al.*, 1994; Westbrook-Case *et al.*, 1995, Kim *et al.*, 2001), it is possible that FAD may exist in the acrosome of these species and may be involved in the formation of the acrosomal matrix during spermiogenesis

#### Establishment of microtubules that surround the developing acrosome

Tandler and Moriber (1966) used transmission electron microscopy to study the sperm of *A. remigis* and reported that the elongating acrosome was surrounded by structures that they referred to as cytoplasmic microtubules. Using an antibody against  $\beta$ -tubulin, I confirmed that the elongating acrosome was surrounded by microtubules (Figure 4.1A). In contrast, I could not observe microtubules that surround the acrosome in the mature sperm (Figure 4.1B), suggesting that the microtubules are transient structures that are lost during spermiogenesis. These temporal microtubules may be involved in the formation of the long acrosome by stabilizing the developing acrosome and transporting molecules intracellularly. Since the microtubule-containing structure is helical, this structure may be especially involved in the formation of the helical region of

the acrosome. In mammals, the dramatic change in nuclear and acrosomal morphology at the acrosome-phase and maturation-phase is assisted by an ephemeral structure called the manchette that consists of a parallel array of microtubules and intermediate filaments (Kierszenbaum and Tres, 2004). Further, in birds, the nucleus is helical and its formation is assisted by the manchette that surrounds the nucleus in a helical fashion (Fawcett *et al.*, 1971). Microtubules that surround the elongating acrosome have also been reported in another species of water strider, *Gerris paludum*, using a transmission electron microscope (Lee, 1985).

#### The fluorescent molecule is FAD

My investigations using *in vitro* and *in vivo* spectrophotometry, fluorimetry, and electrophoresis strongly suggest that the fluorescent molecule in the acrosome is FAD. Further analysis of the fluorescent band on an SDS gel (Chapter 2) using mass spectrometry would confirm this idea. FAD exists in cells in isolation or as a prosthetic group of flavoproteins that are capable of catalyzing various oxidation-reduction reactions (Massey, 2000; Joosten and Berkel, 2007). FAD is formed from riboflavin (Vitamin B2) (Massey, 2000; Joosten and Berkel, 2007) and insects are incapable of synthesizing the isoalloxazine skeleton of riboflavin (Miller and Silhacek, 1995). Considering the unusually long structure of the acrosomal matrix, mature *A. remigis* males would require a significant amount of riboflavin in their diet. Proteins that are involved in the storage and transport of riboflavin may be up-regulated in mature *A. remigis* males. I observed some old males whose internal structures were yellow. These

males may stop producing sperm resulting in an accumulation of riboflavin in their internal structures. It would be interesting to study flavin assimilation in *A. remigis*, especially in regards to its role in spermatogenesis and reproduction.

### **Acrosome reaction in *A. remigis***

#### Acrosome reaction

Following spermiogenesis, sperm need to go through several maturational steps. In some animal taxa, one of these steps is the acrosome reaction that has been studied extensively in echinoderms and mammals (Patrat *et al.*, 2000; Neill and Vacquier, 2004). In contrast, studies on the *Drosophila* acrosome suggest that the insect acrosome enters the egg without the necessity of the acrosome reaction (Perotti, 1975; Wilson *et al.*, 2006). In *A. remigis*, however, I initially hypothesized that the acrosome is discarded prior to its entry into the egg since the unusually long acrosome of *A. remigis* sperm ( $\approx 2.5$   $\mu\text{m}$ ) is much longer than the diameter of the egg ( $\approx 1.0$   $\mu\text{m}$ ) (Pollister, 1930). Further, this unusually long acrosome is remarkably rigid (Tandler and Moriber, 2006) and therefore would hinder sperm motility in the female reproductive tract. To test this hypothesis, I used the intrinsic fluorescence of the acrosomal matrix to follow its fate from spermatogenesis to fertilization. Surprisingly, the fluorescent acrosomal matrix was observed inside fertilized eggs and remained intact through gastrulation. To the best of my knowledge, this represents the first study that follows the fate of the acrosomal matrix until gastrulation. These observations reveal that the unusually long acrosomal matrix

remains associated with the sperm throughout its long, tortuous route through the female reproductive tract, and the entire fertilization process.

The persistence of the acrosomal matrix through fertilization does not, *per se*, mean that the *A. remigis* acrosome does not undergo a regulated exocytotic event (an acrosome reaction) prior to successful syngamy. Since successful fertilization requires the fusion of both sperm and egg pronuclei, the separation of the acrosome and the flagella from the sperm's haploid nucleus, must occur soon after sperm entry into the egg. It is possible that the acrosome undergoes an acrosome reaction without discarding the complex matrix. One strategy to investigate if the acrosome undergoes an acrosome reaction is to observe if the acrosomal membrane is intact in fertilized eggs. I followed this strategy using the lipophilic carbocyanine dye (DiI C16) that is routinely used to stain the outer leaflets of plasma membranes and has been used with limited success to label some organelle membranes following intracellular injection of the dye (Honig and Hume, 1986). However, this did not work because the lipophilic dye also bound to the components of the acrosomal matrix and did not serve as a specific marker for the membrane that surrounds it. Therefore a specific dye that binds to the membrane but not the acrosomal matrix is needed to investigate the fate of the acrosomal membrane. It may also be possible to use transmission electron microscopy in fertilized eggs to look for the presence of the membrane that surrounds the acrosomal matrix. Alternatively, if a technique that genetically engineers *A. remigis* is developed, it may be possible to express a soluble green fluorescent protein (GFP), in particular one with fluorescent properties that are distinct from FAD, in the acrosome and investigate its fate. This

approach was used successfully to study the fate of the acrosome in *D. melanogaster* (Wilson *et al.*, 2006). If the *A. remigis* acrosomal membrane is intact in a fertilized egg, I predict that the soluble fluorescent protein in the acrosome will be observed in a fertilized egg.

#### Biological relevance of the unusually long acrosome in *A. remigis* sperm

The function of this unusually long acrosome is still largely unknown. However, its complex structure and its persistence through fertilization and early development may offer some clues. Since the matrix is not discarded, or disassembled, prior to its entry into an egg, it is possible that the acrosome plays a structural role during the passage of the sperm through the female reproductive tract. There are two narrow regions in a female reproductive tract where the acrosome may serve this function. First, a part of the *A. remigis* female reproductive tract is narrow ( $\approx 12 \mu\text{m}$  in diameter) and tightly wound with the linear stretches of the looping regions shorter than the length of the sperm (Figure 1.4) (Campbell and Fairbairn, 2001). It would seem unlikely for the long, relatively rigid acrosome to pass through this tightly wound region of the female reproductive tract. It may be that this structure is stretched and straightened during passage of eggs through the female oviduct and that this facilitates movement of sperm as well. Second, the spermathecal tube is also extremely narrow (Figure 1.4) ( $\approx 23 \mu\text{m}$  in diameter, Campbell and Fairbairn, 2001). It would seem difficult for a sperm possessing a long rigid acrosome to change direction inside the spermathecal tube although it is possible that the sperm may not need to change direction to achieve successful fertilization. The unique

zippering motion may be important for the sperm to emerge from the spermathecal tube without changing direction. To test whether the sperm do not change direction in the spermathecal tube, a detailed analysis to determine whether all of the sperm are aligned in the same direction in the spermathecal tube would be necessary.

In addition to the fate of the acrosomal matrix, I used the intrinsic fluorescence along with advanced microscopical and imaging methodologies to investigate the structure of the acrosomal matrix in intact, fully formed, *A. remigis* sperm. A deconvolution microscope identified two distinct domains of the 2500  $\mu\text{m}$  acrosome that contains two distinct morphological regions. The first is a 300  $\mu\text{m}$  long helix, with a 7  $\mu\text{m}$  repeat that is proximate to the nucleus. The second, which is an extension of the helix, is much longer (~2200  $\mu\text{m}$ ) and possesses a smaller diameter than the helix. The function of these two structures is unknown although it is interesting to speculate that the long linear region may facilitate sperm navigation through the male and female reproductive tracts while the helical domain, which interestingly mirrors the periodic structures in the tail and the helical motility patterns, may play a role in sperm penetration through the micropyle and the egg.

The eventual fate of the acrosomal matrix after gastrulation remains unknown although two possibilities are readily apparent. First, the acrosomal matrix may be expelled into a midgut and may be discarded by hatched nymphs. In *Drosophila* sperm, their mitochondrial derivatives follow a similar fate and are discarded by nymphs (Pitnick and Karr, 1998). Alternatively, it is possible that the acrosomal matrix is digested after

gastrulation and its components are utilized by the embryo. Since *A. remigis* cannot synthesize riboflavin (Miller and Silhacek, 1995), it may be important for the embryo to acquire sufficient amounts of riboflavin to ensure proper development. Therefore, FAD from the acrosomal matrix may be a useful source of riboflavin for the embryo.

### **Sperm motility regulation in *A. remigis***

#### Sperm motility activation by trypsin may be common in insects

Another maturational step that sperm undergo after spermiogenesis is the activation of sperm motility. In many animals, including many vertebrates and echinoderms (Acott and Carr, 1984; Darszon *et al.*, 1999; Neill and Vacquier, 2004), mature sperm are immotile during storage in the male reproductive tract. The initiation of sperm motility is generally achieved through various extracellular cues including, but not restricted to, changes in pH or viscosity (Yoshida *et al.*, 2008). In insects, motility initiation requiring proteases such as trypsin appears to be common and has been observed in both holometabola (Lepidoptera) and hemimetabola (Orthoptera) (Osanai and Baccetti, 1993; Friedländer *et al.*, 2001). Support for this general mechanism of activation is provided by my results presented in this dissertation for sperm from *A. remigis* (Hemiptera, hemimetabola) that became vigorously motile following the addition of trypsin. In addition, I have also found that the motility of the sperm from the mosquito, *Culex quinquefasciatus* (Diptera, holometabola) was spontaneously initiated when both seminal vesicles and accessory glands were mechanically squashed (Figure 4.1A and B). This spontaneous activation was effectively blocked by the addition of a protease

inhibitor (Figure 4.2C and D), strongly suggesting that a protease is also involved in the initiation of sperm motility in this species.

#### Signaling pathways involved in trypsin activation

To identify a specific kinase involved in sperm motility initiation, I tested a wide range of kinase inhibitors (protein kinase A inhibitors: H8 or H89; protein kinase C inhibitors: bisindolylmaleimide I or Go 6983; a Ca<sup>2+</sup>/calmodulin-dependent protein kinase inhibitor: KN-62; a casein kinase inhibitor: IC261; a glycogen synthase kinase 3 inhibitor: AR A014418; phosphoinositide 3-kinase: LY 294002; a p38 kinase inhibitor: SB 203580; a tyrosine kinase inhibitor: genistein). However, none of these inhibitors blocked the motility activation by trypsin. In contrast to these inhibitors, an ERK kinase inhibitor U0126 partially blocked sperm motility. U0126 also blocked the sperm motility rapidly in the mosquito, *C. quinquefasciatus* (Figure 4.2C and D). However, ERK was not detected in the *A. remigis* sperm using indirect immunofluorescence or immunoblotting with an antibody against ERK. It is possible that the tools that are currently available for detecting ERK may not allow for its detection in *A. remigis* sperm or that it is expressed in levels that do not allow for its detection. Alternatively, these results suggest that the kinase that is involved in the *A. remigis* sperm motility activation may be a novel kinase. To test if ERK is localized in the sperm, concentrating ERK with immunoprecipitation may be necessary. Further, searching an ERK-like protein in *C. quinquefasciatus* with its known genome sequence and determining its expression in the



testis with RT-PCR may offer an alternative approach to see if there is a novel ERK-like protein in the sperm.

Since my results demonstrate that protein phosphorylation is involved in trypsin activation, there would be a molecule that conveys a trypsin signal into an intracellular signal. I hypothesized that a protease activated receptor 2 (PAR2) is involved in trypsin activation since this receptor is known to be activated by trypsin (Kawabata and Kuroda, 2000). PAR2 belongs to the large superfamily of G-protein-coupled seven trans-membrane domain receptors and is involved in inflammatory responses in mammals (Kawabata and Kuroda, 2000; Fiorucci and Distrutti, 2002). Trypsin cleaves the extracellular N-terminal peptide of PAR2 and the exposed new N-terminal peptide binds to the body of PAR2, resulting in receptor activation (Kawabata and Kuroda, 2000). To date, PARs have yet to be definitively identified in invertebrates. I showed that there was a PAR2-like protein on the *A. remigis* flagellum by immunofluorescence. This receptor may initiate a signaling cascade in the cell in response to trypsin. To confirm this hypothesis, it will be important to determine the amino acid sequence of a PAR2-like protein in *A. remigis* sperm using tandem mass spectrometry. A detailed analysis is now being performed in the Cardullo lab.

#### Sperm motility in a female reproductive tract

It is still unknown if a trypsin-like protease is the actual activator *in vivo* and what its origin is in *A. remigis*. As is suggested in the silkworm, *Bombyx mori*, the activator may be secreted from males when the sperm are ejaculated into females. Campbell and

Fairbairn (2001) observed sperm movement in the gynatrial sac, vermiform appendix, spermathecal tube, and fecundation canal when females were dissected as soon as a male disengaged, suggesting that the sperm motility is activated as the sperm are ejaculated. Although I could not observe accessory glands in *A. remigis* males, it is possible that a trypsin-like protease is secreted by cells within the male reproductive tract. In this regard it would be interesting to see if there is a trypsin-like protease activity that is associated with the male reproductive tract.

Previous reports have shown that sperm can then be stored in the female spermathecal tube for at least 3 weeks (Rubenstein, 1989, Campbell and Fairbairn, 2001). It is still unknown if the motility of the *A. remigis* sperm is activated again by secretions from the female reproductive tract prior to fertilization. In the boll weevil, *Anthonomus grandis* (Order Coleoptera) (Villavaso, 1975), spermathecal gland secretions were shown to contribute to the activation and maintenance of sperm motility. However, nothing is known about the specific molecules that are involved in the motility activation of *A. grandis* sperm in females. *A. remigis* females possess two gynatrial glands in their female reproductive tracts (Figure 1.4) (Campbell and Fairbairn, 2001). It is possible that these gynatrial glands may be involved in the activation and maintenance of sperm motility following an extended quiescent period prior to fertilization. The timing of these events, especially in regards to successful reproductive strategies, including mechanisms of sperm competition, is of particular interest for future studies.

Since the flagellum of insect sperm seems to enter the egg with the membrane intact (Perotti, 1975), it raises the question as to whether they are still capable of motility following egg entry. Interestingly, I observed a flagellum in its "zippered" state in the egg suggesting that motility continues for at least some time following fertilization. In *Drosophila*, the sperm flagellum exhibits a consistent coiling configuration in the anterior end of the egg (Karr, 1991), suggesting that the *Drosophila* sperm still move inside an egg. In all insects, the importance of this behavior, and the fate of a potentially rich source of material (including tubulin, actin, and the components that make up the acrosomal matrix) for the zygote will be the subject of future studies.

### **Comparison with other animals**

While there are significant differences in post-meiotic events when comparing sperm of *A. remigis* with other animals, important similarities do exist (Table 4.1). Although the morphology of the acrosome is markedly different between *A. remigis* and all described mammalian sperm, some mechanisms such as the formation of the acrosomal matrix that is stabilized by disulfide bonds and the establishment of a microtubule-containing structure are similar (Kierszenbaum and Tres, 2004; Tachibana *et al.*, 2005; Buffone *et al.*, 2008). The *Drosophila* acrosome is much smaller in size ( $\approx 3.5 \mu\text{m}$ ) than the *A. remigis* acrosome (Pitnick *et al.*, 1995; Perotti *et al.*, 2001). However, a manchette-like structure is also formed during spermiogenesis in *Drosophila* (Mermall *et al.*, 2005). It is still unknown if the *Drosophila* acrosome contains the acrosomal matrix and if it is stabilized by disulfide bonds. In many species such as human, mouse, frog and

sea urchin, the acrosome undergoes an acrosome reaction (Yoshizaki and Katagiri, 1982; Darszon *et al.*, 1999; Neill and Vacquier, 2004). In contrast, the *Drosophila* acrosome does not undergo an acrosome reaction (Wilson *et al.*, 2006). Further, some species such as teleosts and *Caenorhabditis elegans* (nematodes) do not possess acrosomes (Baccetti, 1985; Singson, 2001). These comparisons suggest that the function of the acrosome is not universal. In *A. remigis*, the function of the long acrosome is still unknown. But, my studies suggest that the acrosome may play a structural role during the passage of a female reproductive tract and ultimately into the egg itself. A structural role for the acrosome has not been reported in many species such as human, mouse and frog although, in sea urchins, the appearance of an actin-based acrosomal process after the acrosome reaction plays an important role in sperm-egg recognition (Neill and Vacquier, 2004). The *Drosophila* acrosome enters the egg and persists in the cytoplasm at least as late as prometaphase of the first embryonic cycle (Wilson *et al.*, 2006). The unusually long acrosomal matrix of *A. remigis* also enters an egg and persists at least as late as gastrulation. The fate of the acrosomal components after gastrulation will be the subject of future studies.  $\text{Ca}^{2+}$ , cAMP and protein phosphorylation are involved in sperm motility regulation in many species (Visconti and Kopf, 1998; Darszon *et al.*, 1999; Urner and Sakkas, 2003; Neill and Vacquier, 2004; Krapf *et al.*, 2007; Krapf *et al.*, 2009). Similarly, I found that  $\text{Ca}^{2+}$  and protein phosphorylation, but not cAMP, are important regulators of sperm motility regulation in *A. remigis*. It appears that the sperm flagellum in many species, including those from *A. remigis*, enters the egg during the fertilization process

(Karr., 1997; Fechter *et al.*, 1996; Simerly *et al.*, 1993; Sutovsky *et al.*, 1996; Hiraoka and Hirao, 2005).

## **Summary**

The structure and function of the acrosome and the motility apparatus of *A. remigis* sperm were the basis for this dissertation. While I found some common structures and functions in the *A. remigis* sperm as mentioned above, I also found several structures and functions that have not been previously reported in any other taxa. In regard to the acrosome, I reported that an acrosome contains a fluorescent molecule with properties consistent with those of FAD. Since an acrosomal matrix is also stabilized by disulfide bonds in mammals (Mate *et al.*, 1994; Westbrook-Case *et al.*, 1995, Kim *et al.*, 2001), FAD may also exist in the acrosome of these species. In addition, I described the mobility of acrosomal molecules (FAD) in live sperm and spermatids and showed that there is a dynamic change in the mobility of the acrosomal molecules during acrosome formation. Further, I showed that the acrosomal matrix enters the egg and persists at least as late as gastrulation. In regard to the motility apparatus, I described a unique structure in which tubulin and actin are twisted each other. This structure can be a unique system to study the interaction of microtubules and microfilaments. I also described a unique zippering motion that may interest investigators who study flagellar motility. Further, this is the first report to demonstrate that protein phosphorylation is involved in motility regulation in insect sperm and that PAR2 may exist in invertebrates. To date, studies that follow sperm life history from spermatogenesis to fertilization in one insect species have been

rare (Werner and Simmons 2008). Increased knowledge about these events in insects may give us insights about the functional significance of the diversity that exists in insect sperm morphology.

## CHAPTER 4: REFERENCES

- Acott T.S. and Carr D.W. (1984): Inhibition of bovine spermatozoa by caudal epididymal fluid: II. Interaction of pH and a quiescence factor. *Biol Reprod.* 30, 926-35.
- Bacetti B. (1985): Evolution of the sperm cell. In: Metz C.B. and Monroy A., editors. *Biology of fertilization Vol 2.* Academic Press, Inc. pp.3-47.
- Bernardini G., Stipani R. and Melone G. (1986): The ultrastructure of *Xenopus* spermatozoon. *J Ultrastruct Mol Struct Res.* 94, 188-94.
- Buffone M.G., Foster J.A. and Gerton G.L. (2008): The role of the acrosomal matrix in fertilization. *Int J Dev Biol.* 52, 511-22.
- Campbell V. and Fairbairn D.J. (2001): Prolonged copulation and the internal dynamics of sperm transfer in the water strider *Aquarius remigis*. *Can J Zool.* 79, 1801-12.
- Chakrabarti R., Cheng L., Puri., Soler D. and Vijayaraghavan S. (2007): Protein phosphatase PP1 gamma2 in sperm morphogenesis and epididymal initiation of sperm motility. *Asian J Andol.* 9, 445-52.
- Darszon A., Labarca P., Nishigaki T. and Espinosa F. (1999): Ion channels in sperm physiology. *Physiol Rev.* 79, 481-510.
- Fawcett D.W., Anderson W.A. and Phillips D.M. (1971): Morphogenetic factors influencing the shape of the sperm head. *Dev Biol,* 26, 220-51.
- Fechter J., Schöneberg A. and Schatten G. (1996): Excision and disassembly of sperm tail microtubules during sea urchin fertilization: requirements for microtubule dynamics. *Cell Motil Cytoskeleton.* 35, 281-8.
- Fiorucci S. and Distrutti E. (2002): Role of PAR2 in pain and inflammation. *Trends Pharmacol Sci.* 23, 153-5.
- Fraire-Zamora J.J. and Cardullo R.A. (2010): The physiological acquisition of amoeboid motility in nematode sperm: is the tail the only thing the sperm lost? *Mol Reprod Dev.* 9, 739-50.
- Friedländer M., Jeshtadi A. and Reynolds S.E. (2001): The structural mechanism of trypsin-induced intrinsic motility in *Manduca sexta* spermatozoa in vitro. *J Insect Physiol.* 47, 245-55.

- Hiraoka J. and Hirao Y. (2005): Fate of sperm tail components after incorporation into the hamster egg. *Gamete Res.* 19, 368-80.
- Honig M.G. and Hume R.I. (1986): Fluorescent carbocyanine dyes allow living neurons of identified origin to be studied in long-term cultures. *J Cell Biol.* 103, 171-87.
- Jamieson B.G.M., Dallai R. and Afzerius B.A. (1999): *Insects: Their Spermatozoa and Phylogeny*, USA: Science Publishers.
- Joosten V. and van Berkel W.J. (2007): Flavoenzymes. *Curr Opin Chem Biol.* 11, 195-202.
- Karr T.L. (1991): Intracellular sperm/egg interactions in *Drosophila*: A three-dimensional structural analysis of a paternal product in the developing egg. *Mech Dev.* 34, 101-11.
- Kawabata A. and Kuroda R. (2000): Protease-activated receptor (PAR), a novel family of G protein-coupled seven trans-membrane domain receptors: activation mechanisms and physiological roles. *Jpn J Pharmacol.* 82, 171-4.
- Kierszenbaum A.L. and Tres L.L. (2004): The acrosome-acroplaxome-manchette complex and the shaping of the spermatid head. *Arch Histol Cytol.* 67, 271-84.
- Kim K., Cha M.C. and Gerton G.L. (2001): Mouse sperm protein sp56 is a component of the acrosomal matrix. *Biol Reprod.* 64, 36-43.
- Krapf D., Visconti P.E., Arranz S.E. and Cabada M.O. (2007): Egg water from the amphibian *Bufo arenarum* induces capacitation-like changes in homologous spermatozoa. *Dev Biol.* 306, 516-24.
- Krapf D., O'Brien E.D., Cabada M.O., Visconti P.E. and Arranz S.E. (2009): Egg water from the amphibian *Bufo arenarum* modulates the ability of homologous sperm to undergo the acrosome reaction in the presence of the vitelline envelope. *Biol Reprod.* 80, 311-19.
- Lee Y.H. (1985): Spermatogenesis of the water strider, *Gerris paludum* (Heteroptera, Gerridae). *J Ultrastruct Res.* 90, 235-50.
- Massey V. (2000): The chemical and biological versatility of riboflavin. *Biochem Soc Trans.* 28, 283-96.



- Mate K., Kosower N.S., White I.G. and Rodger J.C. (1994): Fluorescent localization of thiols and disulfides in marsupial spermatozoa by bromobimane labelling. *Mol Reprod Dev.* 37, 318–25.
- Mermall V., Bonafé N., Jones L., Sellers J.R., Cooley L. and Mooseker M.S. (2005): *Drosophila* myosin V is required for larval development and spermatid individualization. *Dev Biol.* 286, 238-55.
- Miller S.G., Silhacek D.L. (1995): Riboflavin binding proteins and flavin assimilation in insects. *Comp Biochem Phyiol.* 110, 467-75.
- Miyata H., Noda N., Fairbairn D.J., Oldenbourg R., Cardullo R.A. (2010): Assembly of the fluorescent acrosomal matrix and its fate in fertilization in the water strider, *Aquarius remigis*. *J Cell Physiol.* In press.
- Mohammad S., Alavi H. and Cosson J. (2006): Sperm motility in fishes. (II) Effects of ions and osmolality: A review. *Cell Biol Int.* 30, 1-14.
- Neill A.T. and Vacquier V.D. (2004): Ligands and receptors mediating signal transduction in sea urchin spermatozoa. *Reproduction.* 127, 141-9.
- Osanai M. and Baccetti B. (1993): Two-step acquisition of motility by insect spermatozoa. *Experientia.* 49, 593-5.
- Parker G.A. (1970): Sperm competition and its evolutionary consequences in the insects. *Biol Rev.* 45, 525-67.
- Patrat C., Serres C. and Jouannet P. (2000): The acrosome reaction in human spermatozoa. *Bio Cell.* 92, 255-66.
- Perotti M.E. (1975): Ultrastructural aspects of fertilization in *Drosophila*. pp. 57-68. In: Afzelius B.A. (ed). *The functional anatomy of the spermatozoon*. Pergamon Press, New York.
- Perotti M.E., Cattaneo F., Pasini M.E., Verni F. and Hackstein J. H. (2001): Male sterile mutant *casanova* gives clues to mechanisms of sperm-egg interactions in *Drosophila melanogaster*. *Mol Reprod Dev.* 60, 248-59.
- Pitnick S., Markow T.A. and Spicer G.S. (1995): Delayed male maturity is a cost of producing large sperm in *Drosophila*. *Proc Natl Acad Sci U S A.* 92, 10614-8.

- Pitnick S. and Karr T.L. (1998): Pteral products and by-products in *Drosophila* development. Proc R Soc Lond B. 265, 821-6.
- Pollister A.W. (1930): Cytoplasmic phenomena in the spermatogenesis of *Gerris*. J Morphol. 49, 455-507.
- Rubenstein D.I. (1989): sperm competition in the water strider, *Gerris remigis*. Anim Behav. 38, 631-6.
- Simerly C.R., Hecht N.B., Goldberg E. and Schatten G. (1993): Tracing the incorporation of the sperm tail in the mouse zygote and early embryo using an anti-testicular alpha-tubulin antibody. Dev Biol. 158, 536-48.
- Simmons L.W. (2001): Sperm in competition II: sperm morphology. In: Krebs J.R. and Clutton-Brock T., editors. Sperm competition and its evolutionary consequences in the insects. Princeton University Press. pp.250-276.
- Singson A. (2001): Every sperm is sacred: fertilization in *Caenorhabditis elegans*. Dev Biol. 230, 101-9.
- Snook R.R. (2005): Sperm in competition: not playing by the numbers. Trends Ecol Evol. 20, 46-53.
- Sousa M. and Azevedo C. (1988): Ultrastructure and silver-staining analysis of spermatogenesis in the sea urchin *Paracentrotus lividus* (Echinodermata, Echinoidea). J Morphol. 195, 177-88.
- Sutovsky P., Navara C.S. and Schatten G. (1996): Fate of the sperm mitochondria, and the incorporation, conversion, and disassembly of the sperm tail structures during bovine fertilization. Biol Reprod. 55, 1195-205.
- Tachibana M., Terada Y., Murakawa H., Murakami T., Yaegashi N. and Okamura K. (2005): Dynamic changes in the cytoskeleton during human spermiogenesis. Fertil Steril. 84, 1241- 8.
- Tandler B. and Moriber L.G. (1966): Microtubular structures associated with the acrosome during spermiogenesis in the Water-strider, *Gerris remigis* (Say). J Ultrastruct Res. 14, 391-404.
- Toshimori K. and Ōura C. (1982): An ultrastructural observation of mouse fertilization *in vivo* as revealed by 200 kV electron microscopy. J Electron Microsc. 31, 35-43.

- Urner F. and Sakkas D. (2003): Protein phosphorylation in mammalian spermatozoa. *Reproduction*. 125, 17-26.
- Vijayaraghavan S., Stephens D.T., Trautman K., Smith G.D., Khatra B., da Cruz e Silva E.F. and Greengard P. (1996): Sperm motility development in the epididymis is associated with decreased glycogen synthase kinase-3 and protein phosphatase 1 activity. *Biol Reprod*. 54, 709-18.
- Villavaso E. J. (1975): The role of the spermathecal gland of the boll weevil, *Anthonomus grandis*. *J Insect Physiol*. 21, 1457-62.
- Visconti P.E. and Kopf G.S. (1998): Regulation of protein phosphorylation during sperm capacitation. *Biol Reprod*. 59, 1-6.
- Werner M. and Simmons L.W. (2008): Insect sperm motility. *Biol Rev*. 83, 191-208.
- Westbrook-Case V.A., Winfrey V.P. and Olson G.E. (1995): Sorting of the domain-specific acrosomal matrix protein AM50 during spermiogenesis in the guinea pig. *Dev Biol*. 167, 338-49.
- Wilson K.L., Fitch K.R., Bafus B.T. and Wakimoto B.T. (2006): Sperm plasma membrane breakdown during *Drosophila* fertilization requires Sneaky, an acrosomal membrane protein. *Development*. 133, 4871-9.
- Yoshida M., Kawano M. and Yoshida K. (2008): Control of sperm motility and fertility: Diverse factors and common mechanisms. *Cell Mol Life Sci*. 65, 3446-57.
- Yoshizaki N. and Katagiri C. (1982): Acrosome reaction in sperm of the toad, *Bufo bufo japonicas*. *Gamete Res*. 6, 343-52.

## FIGURE LEGENDS

Figure 4.1 Microtubules surround the acrosome during spermatogenesis but do not persist in the mature acrosome. Immunofluorescence images of developing spermatids **(A)** and mature sperm **(B)** that were stained with an antibody against  $\beta$ -tubulin and viewed using fluorescence microscopy. **(A)** The panel on the left shows the intrinsic fluorescence of the acrosome with a corresponding image (tubulin) on the right. Scale bar = 10  $\mu$ m. **(B)** A panel on the left is a DIC image with a corresponding fluorescence image ( $\beta$ -tubulin) in the right panel. Tubulin was not detected in the mature acrosome. h<sub>p</sub>, periodic region of the head; n, nucleus; t, tail. Scale bar = 10  $\mu$ m.

Figure 4.2 The motility activation of the *C. quinquefasciatus* sperm is inhibited by both a protease inhibitor and the ERK kinase inhibitor U0126. **(A)** A partially activated *C. quinquefasciatus* sperm. Three images, taken 0.33 seconds apart (blue, green and red), were superimposed. Scale bar = 40  $\mu$ m. **(B)** A fully activated *C. quinquefasciatus* sperm. Three images, taken 0.33 seconds apart (blue, green and red), were superimposed. Scale bar = 20  $\mu$ m. **(C)** Partial activation of *C. quinquefasciatus* sperm was inhibited by a protease inhibitor cocktail (1:50 dilution, Sigma-Aldrich, n = 4) but not by U0126 (20  $\mu$ M, n = 3). Seminal vesicles and accessory glands were squashed in a buffer containing either the protease inhibitor cocktail or U0126. The y-axis shows the percentage of partially activated sperm following squash after 6 minutes. Means  $\pm$  SEM are presented (a,b, p < 0.05, ANOVA with post-hoc tests). **(D)** The full activation of *C. quinquefasciatus* sperm was inhibited by a protease inhibitor cocktail (1:50 dilution,

Sigma-Aldrich, n = 4) and U0126 (20  $\mu$ M, n = 3). Seminal vesicles and accessory glands were squashed in a buffer containing either a protease inhibitor cocktail or U0126. The y-axis shows the percentage of fully activated sperm following squash after 6 minutes. Means  $\pm$  SEM are presented (a,b,  $p < 0.05$ , ANOVA with post-hoc tests).

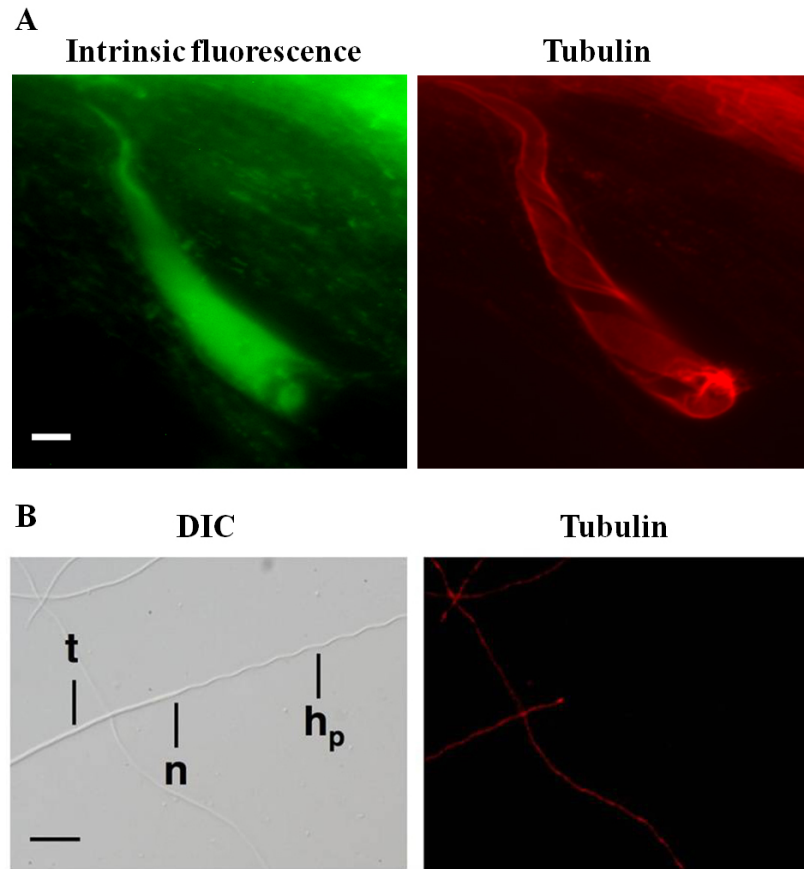


Figure 4.1 Microtubules surround the acrosome during spermatogenesis but do not persist in the mature acrosome.

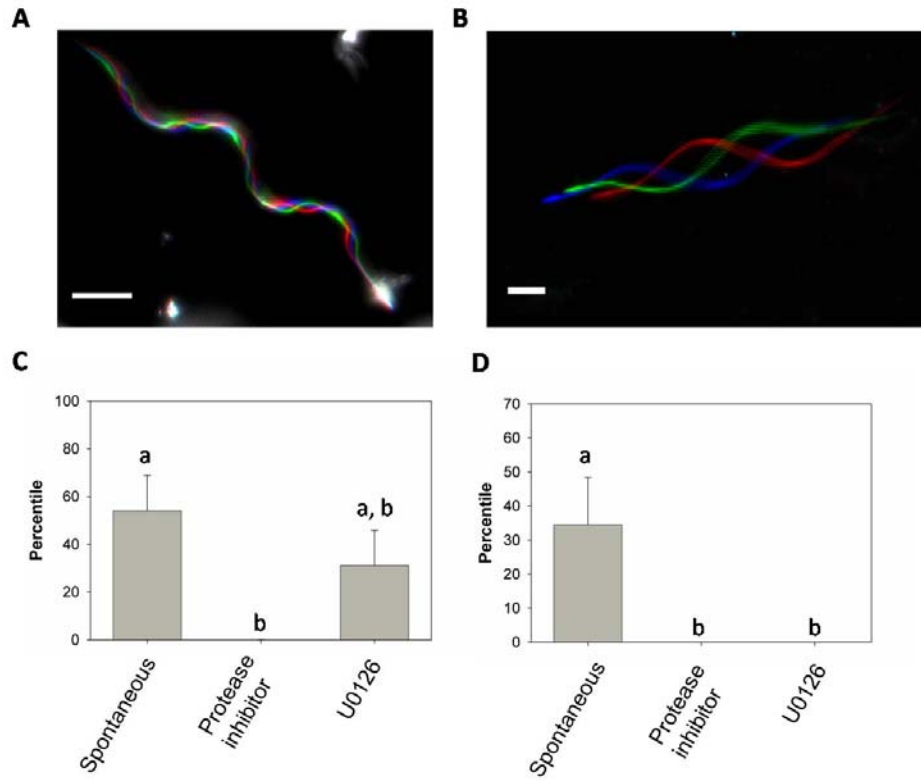


Figure 4.2 The motility activation of the *C. quinquefasciatus* sperm is inhibited by both a protease inhibitor and the ERK kinase inhibitor U0126.

Table 4.1 Summary of post-meiotic events in animal sperm.

Post-meiotic event	Water strider	Fruit fly	Human	Mouse	Teleosts	Frog	Sea urchin	C. elegans
Formation of acrosomal matrix	Yes	Unknown	Yes <sup>1</sup>	Yes <sup>1</sup>	n/a	No <sup>2</sup>	No <sup>3</sup>	n/a
A manchette-like structure	Yes	Yes <sup>4</sup>	Yes <sup>5</sup>	Yes <sup>6</sup>	n/a	Yes <sup>7</sup>	No <sup>8</sup>	n/a
Acrosome reaction	Unknown	No <sup>9</sup>	Yes <sup>10</sup>	Yes <sup>10</sup>	n/a	Yes <sup>2</sup>	Yes <sup>3</sup>	n/a
Entry of an acrosomal matrix into an egg	Yes	Yes <sup>9</sup> (acrosome)	Unknown	No <sup>11</sup>	n/a	n/a	n/a	n/a
Sperm motility regulation by cAMP	No	Unknown	Yes <sup>10</sup>	Yes <sup>10</sup>	Yes <sup>12</sup>	Yes <sup>13</sup>	Yes <sup>10</sup>	Unknown
Sperm motility regulation by Ca <sup>2+</sup>	Yes	Unknown	Yes <sup>10</sup>	Yes <sup>10</sup>	Yes <sup>12</sup>	Yes <sup>14</sup>	Yes <sup>10</sup>	Yes <sup>15</sup>
Sperm motility regulation by protein phosphorylation	Yes	Unknown	Yes <sup>10</sup>	Yes <sup>10</sup>	Yes <sup>12</sup>	Yes <sup>13</sup>	Yes <sup>10</sup>	Yes <sup>15</sup>
Entry of a flagellum into an egg	Yes	Yes <sup>16</sup>	Unknown	Yes <sup>17</sup>	Unknown	Unknown	Yes <sup>18</sup>	n/a

1, Buffone *et al.*, 2008; 2, Yoshizaki and Katagiri, 1982; 3, Neill and Vacquier, 2004; 4, Mermall *et al.*, 2005; 5, Tachibana *et al.*, 2005; 6, Kierszenbaum and Tres, 2004; 7, Bernardini *et al.*, 1986; 8, Sousa and Azevedo, 1988; 9, Wilson *et al.*, 2006; 10, Darszon *et al.*, 1999; 11, Toshimori and Ōura, 1982; 12, Mohammad *et al.*, 2006; 13, Krapf *et al.*, 2007; 14, Krapf *et al.*, 2009; 15, Fraire-Zamora and Cardullo, 2010; 16, Karr, 1991; 17, Simerly *et al.*, 1993; 18, Fechter *et al.*, 1996.